UNIVERSITY OF SOUTHAMPTON

Fabrication and characterisation of fabric supercapacitor

By Sheng Yong

A thesis submitted in partial fulfilment for the degree of Doctor of Philosophy

In the

Faculty of Physical and Applied Science

Department of Electronics and Computer Science

University of Southampton

21 October 2016

Abstract

Fabric supercapacitor is a flexible electrochemical device for energy storage application. It is designed to power up flexible electronic systems used for, for example, information sensing, data computation and communication. The development of a flexible supercapacitor is important for e-textiles since supercapacitor can achieve higher energy density than a standard parallel plate capacitor and a larger power density compared with a battery. This research area is currently facing barriers on improve the device fabrication performance/cost efficiency, electrode throughput and reduce the device packaging difficulty.

This work presents research into fabric supercapacitor, including the basic theory of supercapacitors, review of previous fabric supercapacitor designs based on different materials and frication method and a description of the characterisation methods used to evaluate supercapacitors. The objective of this thesis is to propose the design, fabrication and characterization of prototype fabric supercapacitors with cost efficient electrode material, fast and reliable fabrication method and improved device structure.

Within the thesis four prototype flexible supercapacitors with fabric electrode has been achieved: the multilayer layer supercapacitor with dip coated fabric electrode and aqueous electrolyte achieved a specific capacitance of 14.1 $F.g^{-1}$ a low normalized equivalent series resistance (ESR) (Ω.cm) of 22 Ω.cm, the multilayer layer supercapacitor with spray coated fabric electrode and aqueous electrolyte achieved a specific capacitance of 15.3 $F.g^{-1}$ a low normalized ESR of 20.8 Ω.cm, the two layer solid-state supercapacitor with spray coated fabric electrode and gel electrolyte achieved a specific capacitance of 15.4 $F.g^{-1}$ a normalized ESR of 61.2 Ω.cm, the single layer solid-state supercapacitor with spray coated fabric electrode and gel electrolyte achieved a specific capacitance of 14.9 $F.g^{-1}$ a normalized ESR of 183 Ω.cm. All of the supercapacitor presented in this thesis achieves an excellent cycling stability over 15000 cycles. At the end of the thesis several areas improvements will be discussed for further development.

Acknowledgements

I would like to thank Prof Steve Beeby, Prof John Owen and Dr John Tudor for all their guidance and support over the course of my PhD. Thesis would never have been possible without all the effort they teaching me how to research and write professionally. I would also like to thank Proof Steve Beeby again for his help and advice during my postgraduate education, and for introducing me on broad to this field of research.

Thanks to the research staffs and students in Prof John Owen's group, Dr Kai Yang and Dr Ruessel Torah for their time, and for providing expertise on electrochemistry, chemistry and electronics in this work respectively. Also thanks to Linlu Li, Yunhui Zhao, BeiBei Wang and Shengkai Wang for assisting in the fabrication and testing of the devices respectively.

I would like to also thank the EPSRC for supporting this research with grant reference EP/1005323/1.

Thanks students in Bay 4 and 5 for their friendliness and companionship. Thanks to Junjie, Zhao, Zihao, and everyone else who made the lab a happy and comfort place to work.

Thanks also go to the people closest to me. My wife, my parents and my friends for everything they have done for me.

Table of Contents

List of Figures

List of Tables

List of Acronyms

Electrical double-layer capacitance - EDLC

Double-layer capacitance - C_{dl}

Electrical double layers - EDL

diffusion capacitance - C_{diff}

Total double-layer capacitance - C_{edl}

Sodium carboxymethyl cellulose - CMC

Reduced graphene oxide - RGO

Single-walled carbon nanotubes - SWN

Area double-layer capacitance - CA

Specific capacitance - C_g

Farads per unit price - $C_\$$

Polyaniline - PANI

Sulphuric acid - H_2SO_4

Poly (ethylene-vinyl acetate) - EVA

Carbon nanotube - CNT

Poly (ethylene terephthalate) - PET

Manganese dioxide - MnO2

Polypyrrole - PPY

Potassium hydroxide - KOH

Polyvinyl alcohol - PVA

Polytetrafluoroethylene - PTFE

Nitric acid - HNO_3

Poly-pyrrole - Ppy

Ruthenium oxide - RuO_2

Galvanostatic cycling - GC

Cyclic voltammetry - CV

lithium sulphate- Li_2SO_4

Polystyrene - PS

Silk fabrics - S

cotton sheet - C_{ot}

Thick poly-cotton fabrics - B_{thick}

Thin poly-cotton fabrics - W_{thin}

Supercapacitor - SC

Ammonium dihydrogen phosphate - $NH_4H_2PO_4$, ADP

Diammonium phosphate - $(NH_4)_2HPO_4$, DAP

N-Methyl-2-pyrrolidone - NMP

1 Introduction

Electrochemical capacitors, also known as supercapacitors consist of two electrodes composed of a high surface area material, positioned either side of a very thin charge separator layer that contain the electrolyte[1]. Supercapacitors can achieve high specific capacitance while maintain a fast charge/discharge rate comparable to conventional capacitors.

1.1 Project motivation

Wearable electronics is the implementation of electronic systems on clothing and accessories. These electronic systems typically require an energy storage device with high energy and power density. The research and development of an energy storage system is important for the powering of such electronic systems. Efficient energy storage devices have attracted interest from both the scientific communities and the commercial sector [1]. One such device, the supercapacitor, originated in 1957 [2] is one potential energy storage [3].

Electronic fabrics, also known as e-textiles or smart fabrics, can achieve both the function of normal garments, such as protection from the outside environment, and electronic functions such as sensing, data processing, energy harvesting and energy storage [4]. Potential applications of e-textiles include medical monitoring and personal electronics [1]. Conventional energy storage devices such as the electrochemical secondary battery are not compatible with fabrics and limited in several areas like poor cycling stability and low power density. Therefore new light weight and flexible energy storage devices such as supercapacitors are desirable for e-textiles, but these have not yet been fully developed [5] [6].

A supercapacitor can be used in many applications with different energy and power requirements. By using a high energy density supercapacitor as a power source, an electronic device can achieve a long operation time. Supercapacitors are also used as a power source in applications that need high power density and reliability like power back-up systems [5] [7].

1.2 Project aims and objectives

This research will provide a solution for energy storage in wearable devices by implementing a flexible supercapacitor into a fabric substrate. The proposed fabric supercapacitor should meet the following objectives:

1. The device need to be lightweight (less than few grams in weight).
2. The device should be inexpensive using low cost materials and manufacturing processes (e.g. based on commercial available low-cost materials like Norit SXU activated carbon powder (10 pence.g^{-1}))
3. The device needs to be flexible and built upon a fabric material with multi and single textile layer architectures.
4. The device should achieve a specific capacitance of 10 F.g^{-1}, and a power density of 5 kW.kg^{-1},
5. The device needs to has excellent stability (e g. less than 10% capacitance loss after cycling for more than 15000 cycles).

1.3 Novelty

The novelty in this work come from the electrode ink formulation, electrode fabrication and post treatment methods and supercapacitor cell architecture. Dipping and spray-coating are common procedures in textile industry, with the use of the proposed low cost carbon ink and specified post treatments, these enable a fast way to produce large area of fabric electrode used in the supercapacitor architecture. Although examples of high performance fabric supercapacitor exist in the literature, they use very expensive and hazardous materials that are not the best option for wearable systems. This thesis presents the first time of a flexible solid-state supercapacitor based on only one layer of spray-coated fabric electrode with non-hazardous materials. The specific novelty claims in this thesis are listed below

- A material formulation of carbon ink for spray-coting that adheres to the yarns of fabrics for durable, dry electrodes.
- An optimised method of dipping and spray-coating process for turning four different types of fabric into non-hazardous carbon fabric electrode.
- The application of vacuum impregnation process to optimise the wettability between the electrode and the gel electrolyte.
- A multilayer supercapacitor based on dip-coated fabric electrode with aqueous electrolyte.

- A multilayer supercapacitor based on spray-coated fabric electrode with aqueous electrolyte.
- An improved material formulation of non-hazardous gel-electrolyte for solid state supercapacitor design.
- A two-layer solid-state supercapacitor based on spray-coated fabric electrode with gel electrolyte.
- A single layer solid-state supercapacitor based on spray-coated fabric electrode with gel electrolyte.
- An analysis of the electrochemical performance of different types of the supercapacitor based on the fabric electrode.

1.4 Publications arising from this work

Four publications have arisen from this work. The published articles are a poster session and three conference paper. The publications are listed here in chronological order

- S Yong, J R Owen, M J Tudor, S P Beeby, "Fabric based supercapacitor" Journal of Physics: Conference Series, 476, 012114, and in poster session at Powermems, London, 2013
- S Yong, J R Owen, M J Tudor, S P Beeby, "Aqueous supercapacitor on textiles with carbon electrode" in poster session at Carbon in Electrochemistry, Faraday Disscussion 172, Sheffield, 2014.
- S Yong, J R Owen, M J Tudor, S P Beeby, "Flexible solid-state fabric based supercapacitor" Journal of Physics: Conference Series, 660, 12074, and in poster session at Powermems, Boston, 2015.
- S Yong, J R Owen, M J Tudor, S P Beeby, "Integrated flexible solid-state supercapacitor fabricated in a single fabric layer" at poster session at Powermems, Paris, 2016.

1.5 Report structure

The introduction to this research is given in chapter 1. The literature review of supercapacitors is given in chapter 2, which includes a description of the development of capacitive devices from parallel plate capacitors to supercapacitors. The electrochemical measurements for supercapacitors that are applied in this project are summarized in chapter 3. In chapter 4 the fabrication and performance evaluation of a supercapacitor made using a dip coated fabric carbon electrode will be presented. Chapter 5 presents the fabrication and performance evaluation of a supercapacitor made using a spray coated fabric carbon electrode. In chapter 6

the fabrication and performance analysis of a supercapacitor made using a spray-coated fabric carbon electrode will be presented. Finally, chapter 7 concludes the contents of the previous chapters and details the future work required to improve the performance of the supercapacitor.

2 Literature Review

The performance of an electrical energy storage device can be characterised by its energy density and power density. Energy density indicates how much energy can be stored in the device per unit weight of device or the active material used in the device. Power density describes the rate of energy that can be derived from the device per unit weight of device or active material [7]. In the past, electrochemical secondary batteries were the most appropriate electrical energy storage devices for most applications since they have a larger energy density than capacitive devices. However, an electrochemical secondary battery has three disadvantages. First, its power density is less than non-faradic energy storage devices like the supercapacitor. Second, in comparison with non-faradic devices such as a supercapacitor, a standard secondary battery suck as lead-acid battery has a shorter lifetime. Third, faradic energy storage devices like batteries contain hazardous waste substances which impose extra difficulties to device recycling. Parallel plate capacitors exhibit high power density, but their low energy density limits their performance as energy storage devices [8]. The performance of a range of energy storage devices is shown in figure 2.1.

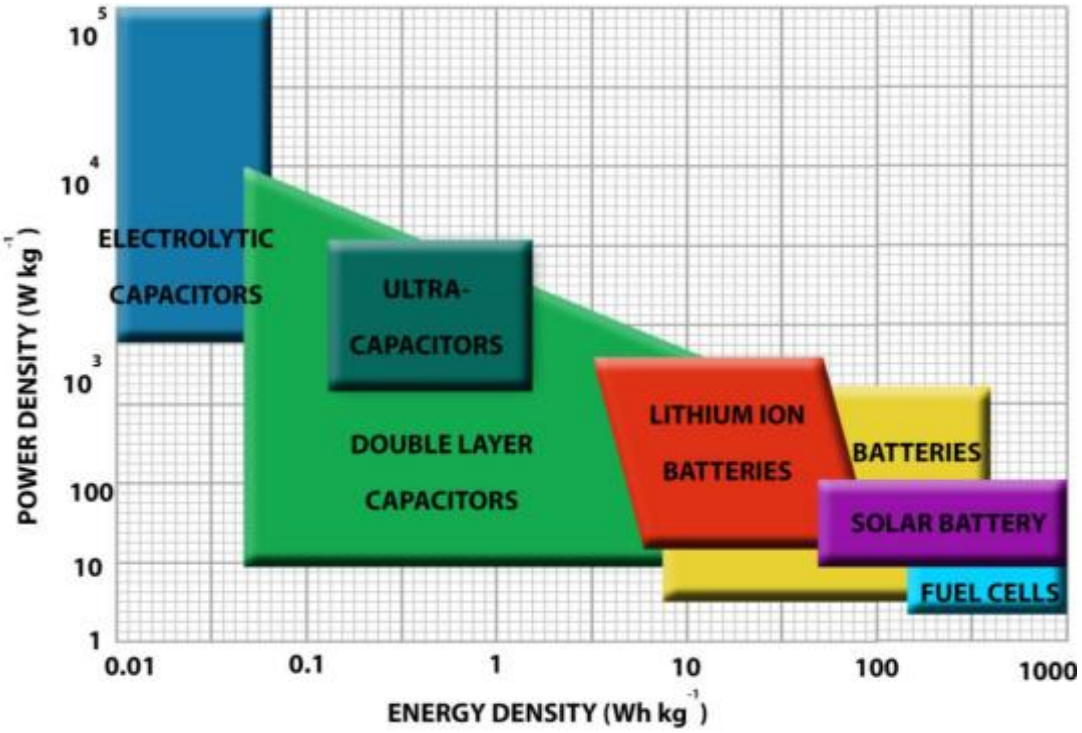

Figure 2.1: Ragone plot of common energy storage devices based on total device weight [9].

In comparison with conventional parallel plate capacitors, the supercapacitor can achieve much higher energy density than its predecessor, while providing relatively high power density [10].

Supercapacitors are constructed of material with a high surface area as its electrode, a thin and porous separator layer, high mobility and ionic conductivity electrolyte and non-corroding current collector with respect to the electrolyte. These technical advancements give supercapacitors the potential to achieve necessary properties to overcome the shortcomings of both capacitors and batteries and become the ubiquitous energy storage device in the future.

2.1 From capacitor to supercapacitor

A capacitor is one of the most basic elements in an electrical circuit; it tracks the electrical signal electrostatically. The capacitor was designed to realise electrical signal filtering functions, using its frequency selective properties. It can also be used in a buffer circuit to store electrical energy [11].

2.1.1 Parallel plate capacitor

The parallel plate capacitor shown in figure 2.2 was the first capacitive device, invented by Leiden Jar in the eighteenth century [11]. It was fabricated with two plates that formed metallic electrodes, separated by a solid dielectric layer. When a voltage difference occurs between the top and bottom electrodes, an internal electrostatic field will exist across the dielectric with opposite polarity to that of the external electrical field. It will effectively separate the charge existing in the dielectric to block the flow of electrical energy driven by the external field. In order to increase the capacitance beyond the level of the parallel plate capacitor, the surface area of the electrodes has to be increased, the dielectric constant of the material between the two electrodes has to be increased and the distance between electrodes has to be decreased.

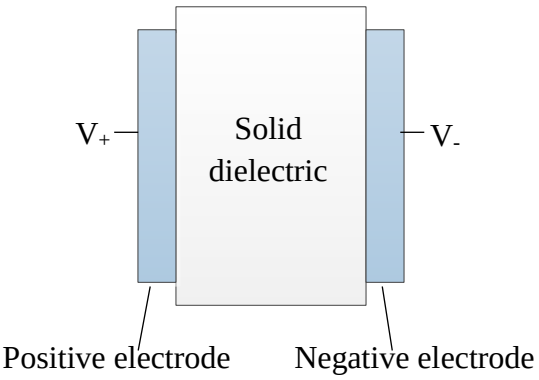

Figure 2.2: The basic structure of the parallel plate capacitor.

2.1.2 Electrolytic capacitors

The next stage in the development of capacitive devices was the electrolytic capacitor, in particular the aluminium electrolytic capacitor. It shares the basic principles of cell structure

with electrochemical batteries but uses the same material as the anode and cathode [12]. Generally an electrolytic capacitor consists of an electrolytic paper, containing a boric acid solution, and two pieces of aluminium foil. One of the aluminium foil electrodes is then etched and oxidised to form a thin layer of aluminium oxide which acts as the dielectric of the device [12]. The detailed cross-sectional view of an aluminium foil-based electrolytic capacitor can be seen in figure 2.3.

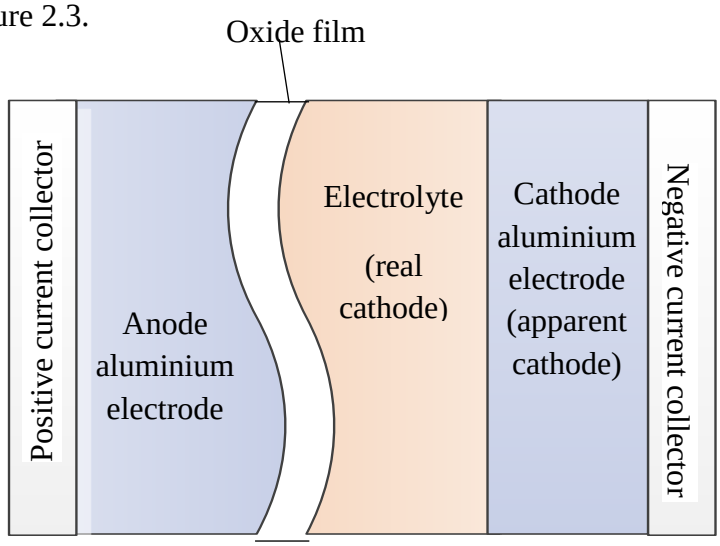

Figure 2.3: Cross-sectional view of an electrolytic capacitor.

In aluminium electrolytic capacitors, the etching process significantly increases the effective surface area of the anode aluminium electrode. This layer has a thickness of between 1.3 nm and 1.5 nm and has a single-direction insulation property when in contact with the real cathode material (the liquid electrolyte). As a result, electrolytic capacitors are able to generate a large series capacitance in comparison with parallel plate capacitors [12]. However, the thickness of etched oxide layer is not a fully controllable value, it is difficult to achieve an oxide layer thickness below 1 nm; as a result the series capacitance of electrolytic capacitors is consequently still limited [11]. Before the invention of the supercapacitor, aluminium electrolytic capacitors were used in the majority of applications which required large capacitors, and they have been widely adopted in many electronic circuits as well as some electrical applications.

2.2 Supercapacitor

The supercapacitor is the third generation of capacitive devices. It has the potential to achieve a higher energy density than conventional parallel plate capacitors, and to deliver higher power density. In comparison with batteries, a supercapacitor has relatively simple operating

principles and construction methods. It can be made with cheap porous materials like carbon and aqueous electrolytes such as Li_2SO_4 salty water. In the recent development of energy storage devices, the combination of supercapacitors and electrochemical secondary batteries has led to hybrid batteries that represent the most advanced energy storage devices to date.

Supercapacitors store energy based on two types of capacitive mechanism: the electrical double-layer capacitance (EDLC) and the pseudo-capacitance. The EDLC is based on the capture and release of electrostatic charge that occurs at the interfaces between the electrode and the electrolyte. This is discussed in more detail in section 2.2.1. Pseudo-capacitance arises from the fast reversible Faradaic redox reactions mechanism [13]; this is discussed in more detail in section 2.2.2. Generally, these capacitive mechanisms occur simultaneously in a supercapacitor.

A supercapacitor is constructed using two electrical double-layer interfaces, each having opposite polarity with respect to the electrolyte solution. To utilise these properties a charge separator containing an electrolytic solution will be placed in between the top and bottom supercapacitor electrodes. A diagrammatic representation of the electric potential profile in a charged supercapacitor is shown in figure 2.4.

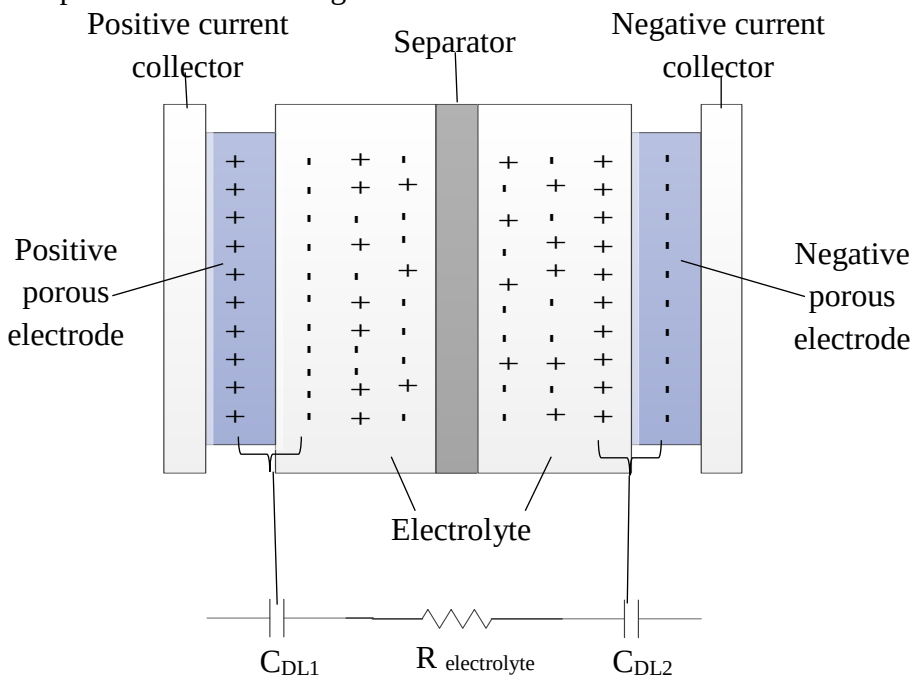

Figure 2.4: Diagram of electric potential profile in a charged EDLC at open circuit, where C_{DL1} and C_{DL2} represent the double-layer capacitance at the interfaces.

In a supercapacitor the exchange of electrostatic charge occurs via the balance of ions at the electrode and electrolyte interface; it introduces an internal potential difference across the

electrolytic dielectric similar to the p-n junction in a semiconductor. Charge on the inner surface of electrodes will be balanced by the accumulation of counter-ions in the electrolyte. This process forms a pair of electrical double layers (EDL) on the inner surfaces of the electrodes that provide a very thin dielectric layer of a few nanometres or less. The electric double-layer pair structure causes charge separation and thereby introduces capacitance between the electrodes [14]. The maximum potential difference between the top and bottom electrodes is restricted by the thermodynamic stability of the electrolyte material [14]. High-performance EDLC requires its electrode material to have a highly conductive surface area, uniform pore size distribution and high surface wettability with respect to the electrolyte [15]. In high-performance EDL capacitors, the electrolyte needs to have a high ionic conductivity and low viscosity, and should not chemically attack the current collector material [13].

In comparison with energy storage devices like a battery, a supercapacitor has some disadvantages [2]: low volume energy density and low operating voltage for supercapacitor with aqueous electrolytes, and it requires expensive materials for supercapacitor encapsulation. A potential solution to overcome these disadvantages is to stack multiple numbers of supercapacitor in series for higher energy density and operating voltage limit. However this complicates device packaging and increases device cost.

2.2.1 Electric double layer mechanism

The EDL mechanism allows supercapacitors to have a significantly higher capacity than a conventional capacitor. The double layer arises between the electrode and the electrolyte interface which acts as the dielectric layer which is only a few nanometres thick. Secondly the supercapacitor based on the EDL mechanism uses a high surface-area material such as carbon as its electrodes material which can have a large effective surface area [13].

The term ‘electric double layer’ refers to two arrays of opposite-charged ions separated by a very small distance. As Von Helmholtz [15] proposed, when a conductive solid is immersed into the electrolyte solution, the double-layer structure will arise either from the acid-based ionisation or the absorption of ions at the electrode/electrolyte interface - this model is illustrated in figure 2.5(a). As a result, ions in the electrolyte with the opposite charge to that of the electrode will be attracted by the charged solid surface and form an oppositely charged layer [16]. The EDL will remain electrostatic until the charged solid reverses its polarity. In Von Helmholtz’s model the electrical double layer has been treated as a static layer; however, according to the Boltzmann principle, the electrical double layer would be influenced by the

effects of the thermal fluctuation of the electrolyte solution and will not remain static in the compact array shown in figure 2.5(a). This model tends to underestimate the effect of EDL on ion polarisation at the electrode/electrolytic interface.

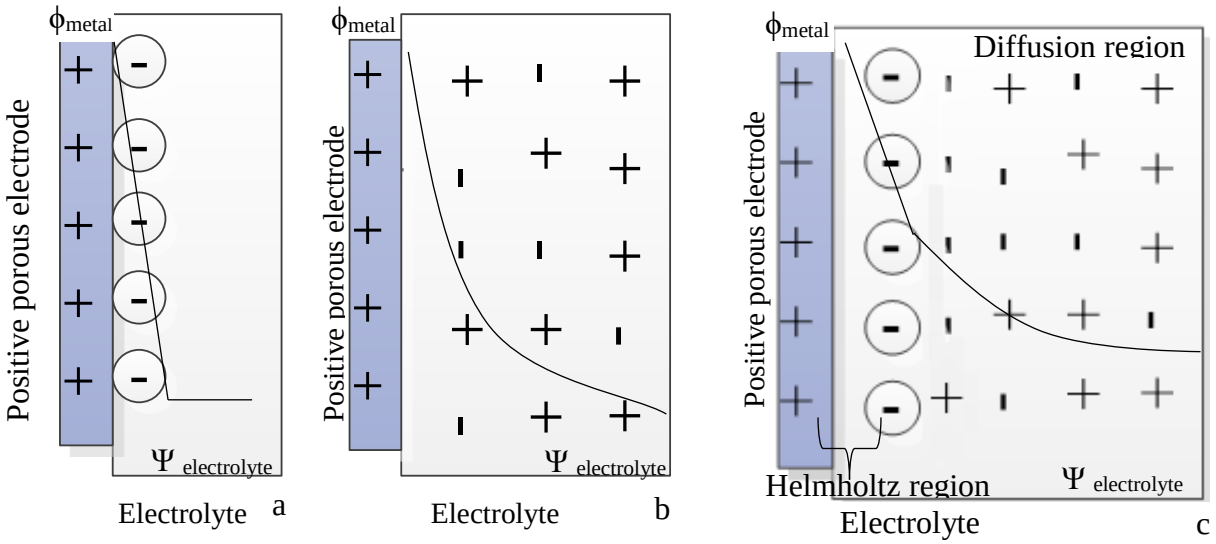

Figure 2.5: Models of the electric double-layer mechanism; (a) Helmholtz model, (b) Gouy and Chapman model, (c) Stern model for finite ion size with thermal distribution..

Gouy and Chapman [17] improved the modelling of the EDL by including the factors of continuous distribution of the ions in the electrolyte and thermal fluctuations. In this model the EDL in response to the metal surface charge was imagined as a three-dimensional diffuse distribution of cations and anions, as shown in figure 2.5(b). However in Gouy and Chapman's model the ions were assumed to be point charges, an assumption which is only valid at typical potential ranges and overestimates the energy that can be stored in the diffusion layer.

Later, Stern further improved the accuracy of the EDL model as shown in figure 2.5(c). This model suggests that the ion distribution at the inner region close to the electrode surface could be treated as the ions absorption process, the inner region is called the Helmholtz region and this corresponds and to Von Helmholtz's model that gives a capacitance C_H. In this model, the region beyond the Helmholtz region could be treated as a diffuse region similar to Gouy and Chapman's model of the EDL, and having a capacitance C_{diff}. Based on the Stern model, the capacitance of EDL structure can be assumed as two types of capacitance connected in series. The first type of capacitance is the C_{DL}, and the second type of capacitance is called the diffusion capacitance ($C_{diff)}$. This diffusion capacitance is defined by the surface charge and electric surface potential. Therefore the total electrical double-layer capacitance (C_{edl}) can be expressed as [13]:

$$\frac{1}{C_{edl}} = \frac{1}{C_{diff}} + \frac{1}{C_{DL}} \qquad \text{(Equation 2.1)}$$

2.2.2 Pseudo-capacitance mechanism

Pseudo-capacitance is another type of energy storage mechanism which can occur at the same time as the electrical double-layer capacitance. It involves fast reversible Faradaic reactions like electrosorption, redox reactions and intercalation processes at the electrode/electrolytic interface [15]. The most commonly known electrode materials for pseudo-capacitors include ruthenium oxide, manganese oxide and electrically conducting polymers such as polyaniline [14].

In a specifically designed supercapacitor, pseudo-capacitance can be made much higher than EDL capacitance. However, supercapacitors based on the pseudo-capacitance mechanism have some of the same drawbacks as batteries do, such as low power density and poor cycling stability.

2.3 The structure of fabric supercapacitors

Fabric supercapacitors share the same structure as other parallel plate energy storage devices like electrostatic capacitors, rigid supercapacitors and batteries. A supercapacitor or fabric supercapacitors cell is constructed with multiple parallel layers; these layers are fabric electrodes, current collectors' layer, (encapsulation) protection layer and the charge separator layer. The charge separator layer contains electrolyte; these material layers are compressed layer by layer, sealed in an encapsulation set-up, and form a fabric supercapacitor as shown in figure 2.6. This type of structure has been demonstrated in many reports about fabric supercapacitor design in the previous years [18], [19], [20],[21], [22].

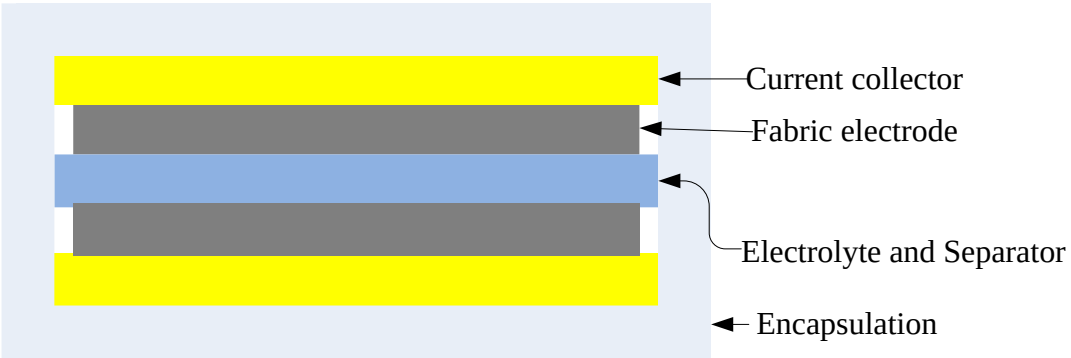

Figure 2.6: Cross-sectional view of parallel plate fabric supercapacitor.

Fibre supercapacitor is another type of fabric supercapacitor which has been demonstrated in many papers [23], [24], [25]. In fibre supercapacitors, two pieces of fabric fibre are coated with conductive coating (equivalent to the current collector in parallel plate fabric supercapacitor), electrode materials and gel electrolyte. Then these two pieces of processed fibre are twisted and squeezed to form a fibre supercapacitor and covered in a flexible protection tube; the cross-sectional view of this structure is shown in figure 2.7 (a). Figure 2.7(b) shows the cross-sectional view of another type of fibre supercapacitor; this one is achieved with a coaxial set-up. |Kou et al. [26] implemented a fibre supercapacitor via the coaxial wet-spinning technique; the wet spun fibres contains reduced graphene oxide (RGO) and CNT materials with sodium carboxymethyl cellulose (CMC) sheath and additional cold particle coating. The twist-type supercapacitor achieved an area capacitance of 0.269 $F.cm^{-2}$. In this case the supercapacitors are coated on the surface of the fabric fibre layer by layer forming a coaxial device as shown in figure 2.8. In comparison with twist supercapacitor devices this method increases the surface area of the electrode materials that make contact with the gel electrolyte that improves its electrochemical performance; however, the fabrication difficulty of coaxial supercapacitor devices is greater than that of the twist supercapacitor devices since it is required to coat many material layers, one on top of the other. Finally, these fibre supercapacitors will be woven together with the correct electrical connections to form an energy-storage fabric.

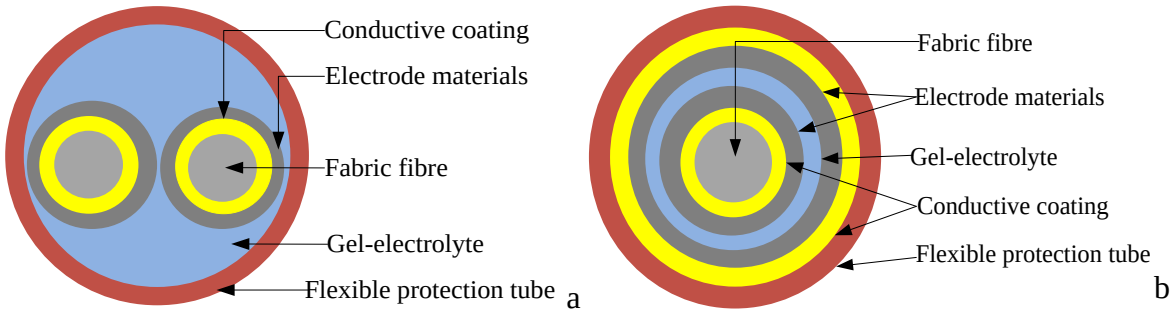

Figure 2.7: Structured view of fibre supercapacitor, (a) twist supercapacitor device and (b) coaxial supercapacitor devices.

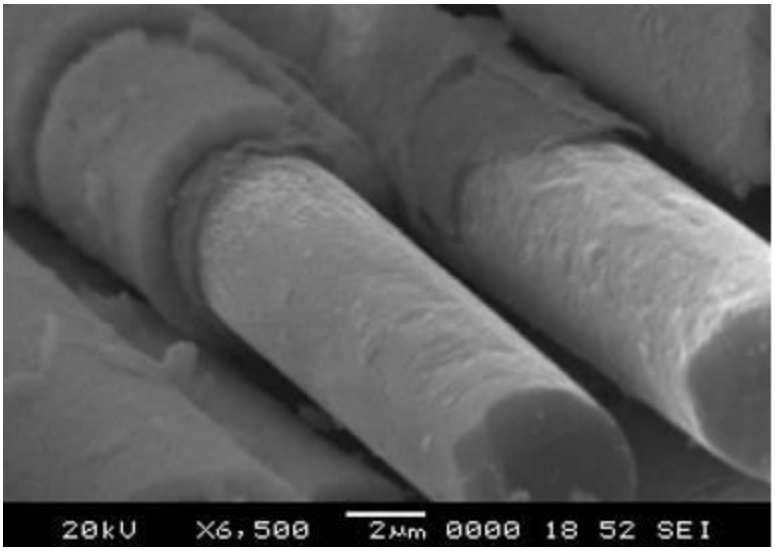

Figure 2.8: SEM image showing zirconium oxide/hafnium oxide/zirconium nitride multi-layered interface coatings on carbon fibres [27].

In comparison with parallel plate fabric supercapacitors the fabric supercapacitors made by fibre supercapacitors offer two advantages: first, fibre supercapacitors are encapsulated during fabrication; they do not require extra encapsulation set-up as is the case with the parallel plate fabric supercapacitors. Secondly, unlike the parallel plate fabric supercapacitors, the fabric supercapacitors made from woven supercapacitor fibres forms a standard textile structure that allows the flow of air through them. Therefore, in smart textile applications, this type of supercapacitor is more comfortable than parallel plate fabric supercapacitors. However, the lack of standardised metrics and experimental details (e.g. fibre dimensions and ESR per unit length) makes interpretation of results difficult [28]. A fundamental challenge for this approach is the trade-off between the fibre diameter and electrode conductivity. For fibre supercapacitors, increasing capacitance by lengthening the fibre results in an increase in ESR. In the case of the multi-layer fabric supercapacitors the capacitance is proportional to area and increasing the area reduces the ESR. In addition, the fibre supercapacitors are relatively harder to fabricate than parallel plate fabric supercapacitors.

2.4 Supercapacitor material selection

The supercapacitor is a multi-layered device, and several materials are required for its construction. Two carbon-based electrodes are required, as well as a porous separator layer that contains the electrolyte and prevents short-circuiting between the electrodes. There also needs to be an inert metal layer that prevents oxidation and chemical corrosion at the current collector.

2.4.1 Supercapacitor electrode materials

In the fabric supercapacitor the electrode materials will influence its electrochemical behaviours, while in the electrical double-layer (EDL) type supercapacitor, the carbon materials on the fabric electrode which are in contact with the electrolyte will determine the double-layer capacitance and the device maximum capacitance. In the pseudo-capacitive supercapacitor the oxide materials or conductive polymer will determine the pseudo-capacitance capacitance that is caused by the redox reaction between the electrode materials and the electrolyte.

Carbon and its derivatives are the most appropriate materials for an EDL supercapacitor electrode, because of several properties. First, carbon can be modified to have a low electrical resistivity. Second, carbon achieves a high specific surface area over 1000 $m^2.g^{-1}$ after the activation process. Third, a carbon particle has controllable pore size and distribution, and different types of carbon materials can be mixed together.

Carbon has a unique position in the periodic table; it has some semiconducting properties and band structures that can be further processed into different forms like activated carbon, carbon black, graphite and carbon nanotube. Depending upon different activation and pre-treatment processes, carbon materials will have a different area double-layer capacitance C_A ($\mu F.cm^{-2}$). Carbon blacks have C_A between 4.5 and 10 $\mu F.cm^{-2}$[29], C_A for activated carbons is around 10 to 15 $\mu F.cm^{-2}$[30], fine graphite powers have C_A values of 20 to 35 $\mu F.cm^{-2}$[2] and single-walled carbon nanotubes (SWNT) will have C_A values from 7.39 to 22.8 $\mu F.cm^{-2}$ [31].In supercapacitors the theoretical maximum specific capacitance C_g (farads per unit grams) and farads per unit price ($C_\$$) is another important factor: the terms C_g and $C_\$$ can be expressed as

$$C_g = C_A \times A_g \qquad \text{(Equation 2.2)}$$

$$C_\$ = C_A \times A_g \div \$_g \qquad \text{(Equation 2.3)}$$

Where C_A is the theoretical area double-layer capacitance, A_g is the area per unit gram ($m^2.g^{-1}$) of the carbon material, $\$_g$ ($\$.g^{-1}$) is the unit prize of the carbon material. For electrodes using carbon material, from equation 2.2 its theoretical maximum area capacitance C_a of selected electrode can be calculated by

$$C_a = C_g \times m \quad . \qquad \text{(Equation 2.4)}$$

In equation 2.4, m is the mass of carbon material of selected electrode per unit area. Table 1 list the theoretical maximum farads per dollar in $F.\$^{-1}$ of carbon electrodes using the various commercially available carbon powers as EDL supercapacitor electrode materials.

Table 2.1: Theoretical double layer capacitance per unit prize of various carbon and carbon-based materials.

Material's name	Carbon type	Specific area A_g ($m^2.g^{-1}$)	Theoretical specific capacitance C_g ($F.g^{-1}$)	Unit price $\$_g$ ($\$.g^{-1}$)	Farads per dollar $C_\$$ ($F.\$^{-1}$)
Timcal ENSACO 350G [32]	Carbon black	70	7	0.019	368
Norit SXU [33]	Activated carbon	1200	180	0.14	1286
Kuraray Yp-50F [34]	Activated carbon	1600	240	1.14	210
Norit CA1 [33]	Activated carbon	1100	165	0.09	1833
GS-2299 nano-Graphite Powder [35]	Graphite	400	140	0.15	933
GS-4827 nano-Graphite Powder [35]	Graphite	250	87.5	0.06	1458
HiPco carbon nanotube [36]	SWNT	1315	300	460	0.65

Table 2.1 lists the theoretical maximum specific double-layer capacitance and farads per gram of different commercially available carbon powders. Activated carbon powders and some fine graphite powders like GS-4827 can obtain a high figure of merit over 1200 $F.\$^{-1}$. These materials can achieve much higher farads per dollar than SWNT although SWNT has the potential to achieve very high specific double-layer capacitance of about 300 $F.g^{-1}$. Carbon black has a low unit price but is unable to provide a high specific capacitance due to its relative low surface area. Some specially treated activated carbon powders, e. g. Kuraray Yp-50F, have a very high theoretical double-layer specific capacitance of about 210 $F.g^{-1}$, but its high commercial unit price reduces its farads per dollar.

For a complete supercapacitor cell, as shown in figure 2.4, its specific capacitance will be about four times smaller than the specific capacitance of its electrode. This is because a complete supercapacitor consists of two double-layer interface capacitors connected in a series. The total capacitance of a complete supercapacitor will be half of the single electrode double-layer capacitance. A complete supercapacitor cell also contains twice the active material compared with an individual electrode. Hence, the specific capacitance of a supercapacitor electrode is four times higher than a complete supercapacitor cell [37]. For example, the theoretical specific capacitance of a supercapacitor cell made with YP-50f activated carbon electrode is 82.5 $F.g^{-1}$.

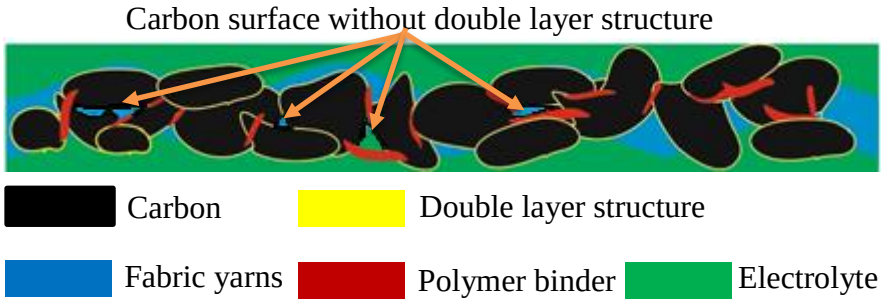

Figure 2.9: Schematic of the materials in the fabric yarns (fabric, carbon, binder, electrolyte)

Theoretically, the specific surface area of the porous material like carbon can be obtained with nitrogen gas absorption test and Brunauer–Emmett–Teller theory. Figure 2.9 shows a schematic of the materials in a fabric carbon electrode yarns, the rough mass percentage value for each materials are 2:13:35:50 (binder: carbon: fabric: electrolyte). In a real carbon based fabric supercapacitor, some of the electrode materials are not exposed to the electrolyte solution, the polymer binder, carbon material stacking and the surface oxidation is preventing the carbon material surface get in contract with the electrolyte, it result in no double layer capacitance arise on its surface and hence reduce the device specific capacitance.

The experimental specific capacitance of a supercapacitor is much lower than its electrode material's theoretical specific capacitance. Kim et al. [38] demonstrated the electrochemical performances of a supercapacitor with activated carbon electrode. The electrodes were made using the YP-50f activated carbon powder from Kuraray Chemical (Japan), polymer binder, and carbon black. The supercapacitor achieved a specific capacitance of 24.3 F.g-1; that is much lower than its theoretical maximum value (82.5 $F.g^{-1}$). This is because most of the surface area of the activated carbon particles is not in contract with the electrolyte solution due to the. associated polymer binder and issues of wettability.

It is essential to use carbon for the electrodes for a supercapacitor on a flexible substrate to achieve a performance that is comparable to that of rigid supercapacitors. Most supercapacitors tend to use expensive materials as the active material in supercapacitor, such as CNT [39] together with an additive pseudo-capacitance material such as ruthenium oxide [40] or polyaniline. These methods permit the fabrication of supercapacitors with high storage capacity and power/energy efficiency; however, they also keep the cost of flexible supercapacitors high and have a high fabrication complexity that limits the commercial potential of flexible supercapacitors.

Activated carbon (AC), also known as engineered carbon, is another potential material for supercapacitor electrodes due to its large specific surface area, low electric resistivity and relatively low cost in comparison with other materials such as CNT. Traditionally carbonaceous materials like wood, coal and nut shells can be used to make activated carbon via a process called activation. The activation process involves thermal and/or chemical treatment that removes the 'disorganised' carbon in the interstices of the original carbonaceous material; these processes create additional pores in the carbon material to increase its surface area [15]. Subramanian et al. [41] proposed a supercapacitor based on AC made from natural fruit fibres. In their work the chemically treated activated carbon electrode achieved a specific capacitance of 74 $F.g^{-1}$. Jost et al. [42] implemented a supercapacitor based on a blend of activated carbon (Yp-17F) and carbon black powder. The supercapacitor was constructed in a cell with a PTFE separator. The fabric-based carbon electrode was achieved by a combination of dipping and screen-printing processes. The resulting fabric-based supercapacitor electrode achieved a specific capacitance of 65 $F.g^{-1}$.

The invention of carbon nanotubes was an important breakthrough in the research and development of the carbon industry [43]. Supercapacitor electrodes made with carbon nanotubes benefit from unique properties such as the porous structure, excellent electrical conductivity, high specific surface area, and good thermal and mechanical stability. Both single-walled and multi-walled carbon nanotubes have attracted a large amount of research interest to investigate their suitability for supercapacitor electrodes. Chen et al. [19] made a supercapacitor electrode via inkjet printing and single-walled carbon nanotube. Their supercapacitor electrode achieves a specific capacitance of 138 $F.g^{-1}$ with high power and energy density. Hu et al. [6] presented a supercapacitor design based on carbon-conductive fabrics. In their work the electrode is a piece of conductive fabric material which has a coating

of single-walled nanotubes applied with a dipping process. This fabric supercapacitor electrode achieves a specific capacitance of 80 $F.g^{-1}$ at current density 20 $mA.cm^{-2}$.

In the pseudo-capacitive supercapacitor, oxides (MnO_2, ZnO_2) and conductive polymer (PANI) are the most appropriate materials; unlike the primary cell (battery), the supercapacitor based on these materials can be recharged and supports higher capacitance in comparison with the EDL-type supercapacitor. After many recharge cycles the capacitance of the pseudo-capacitive supercapacitor will reduce due to irreversible material transform in the redox reaction.

Previous reports of flexible supercapacitors using carbon nanotube (CNT), graphene and/or pseudo-capacitance materials achieve high specific capacitance, but it is essential to note that the specific capacitance or area capacitance of these devices will reduce as the charge/discharge cycling number increases. Wang et al. [44] used a pseudo-capacitance additive polymer, polyaniline (PANI), with CNT flexible electrodes, and found that PANI-CNT-Cotton flexible supercapacitor device had a capacitance which fell to 61% of its original value after 3000 cycles. Some of the previous examples of CNT flexible supercapacitors use an aggressive electrolyte such as sulphuric acid (H_2SO_4); this additional process increases the fabrication cost and complexity and is not ideal for e-textile supercapacitors.

Carbon black itself results in supporting very small double-layer capacitance; however, this carbon powder can provide excellent electrical conductivity to reduce the internal resistive power consumption within a supercapacitor electrode that is used as an additive in a carbon electrode [29].

In supercapacitor design, two types of capacitance (EDL capacitance and pseudo-capacitance) can occur at the same time. Combining the carbon materials, oxide materials and redox conductive polymer together in the same piece of electrode may lead to some version of a supercapacitor with outstanding electrochemical performance. Zang et al. [45] proposed a flexible supercapacitor based on graphene and PANI woven fabric films. The proposed device achieved very high specific capacitance of 771 $F.g^{-1}$ and an area capacitance of 0.023 $F.cm^{-2}$. Yang et al. [46] implemented a fabric supercapacitor using a MnO_2-coated carbon fabric electrode. Their device achieved very high specific capacitance of 1260 $F.g^{-1}$ based on the mass of MnO_2 and an area capacitance of 0.026 $F.cm^{-2}$.

2.4.2 Flexible substrates for a supercapacitor electrode

The substrate used in a supercapacitor includes both rigid and flexible materials. The most commonly used rigid substrate is an inert metal plate such as nickel [47] or gold [48]. Wang et al. [47] built a graphene-based supercapacitor device on top of a nickel metal foam. The rigid coin-shaped supercapacitor demonstrated a maximum specific capacitance of 205 $F.g^{-1}$ with a graphene material coating. The nickel metal piece used as the substrate material of the supercapacitor provides an excellent level of electrical conductivity and chemical resistance to most kinds of electrolyte, but it is a rigid material that is not appropriate for flexible applications.

A flexible supercapacitor requires the use of a lightweight, conductive and flexible substrate to form or support the electrode material. Substrate materials need to be suitable for a flexible supercapacitor include fabric and polymers. Zhang et al. [49] implemented a flexible supercapacitor on conductive membrane made with a polymer poly (ethylene-vinyl acetate) (EVA) polymer, carbon black, CNT as the capacitive material, and ruthenium oxide as a pseudo-capacitance additive material. The composite flexible electrode achieved a specific capacitance of 169 $F.g^{-1}$. Kaempgen et al. [18] implemented a flexible supercapacitor on flexible a poly (ethylene terephthalate) (PET) film. These flexible polymer membranes can be used to fabricate a flexible supercapacitor; however, they raise the cost and require complex fabrication methods for integration with e-textiles.

A fabric supercapacitor requires the use of a lightweight, flexible and possibly a conductive fabric substrate to form or support the electrode material. It is preferable to use fabric substrates, and both woven and nonwoven fabrics can be used. Nonwoven fabrics are made by bonding long fibres from wool or molten plastic film via chemical, mechanical, heat or solvent treatment. Nonwoven fabrics usually have a high thickness and relatively large pore volume in comparison to woven fabrics. This allows them to absorb and hold more active carbon material to achieve high performance. In the past, researchers have used nonwoven substrate (cotton) with a dyeing technique with carbon nanotubes (CNT) [50]. Hu et al. [6] fabricated a flexible supercapacitor based on nonwoven cotton substrate, CNT, dyeing technique and LiPF6 aqueous electrolyte, and their device achieved a specific capacitance of 14 $F.g^{-1}$ with high area-specific capacitance of 0.48 $F.cm^{-2}$. Nonwoven fabrics are, however, not widely used to make garments and are not the best choice for wearable electronics

Woven fabrics are formed by weaving natural or artificial yarns together into a thin sheet or fabrics. Woven fabrics are widely used in garments and have good mechanical strength and

tear resistance. One issue that applies to both woven and nonwoven fabric substrates is that the fabric substrate itself is not conductive. Researchers have attempted to solve this problem in different ways. Liu et al. [51] attempted to grow CNT around a graphene oxide-cotton yarn and then weave these yarns together to make a woven flexible supercapacitor electrode with high conductivity and surface area. Their supercapacitor device achieves a specific capacitance of 81.7 $F.g^{-1}$ with a 6M KOH aqueous electrolyte. Yuksel et al. [52] attempted to dye manganese dioxide (MnO_2)/CNT/ polyaniline (PANI) nanocomposite into the woven bare cotton fabric pieces to make a woven fabric supercapacitor electrode with high conductivity and surface area. Their supercapacitor device achieves a specific capacitance of 246 $F.g^{-1}$ with a gel organic electrolyte.

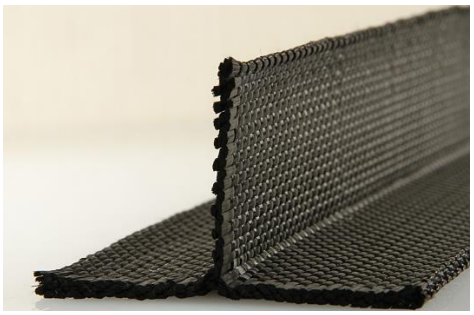

Figure 2.10: Photograph of woven carbon fabrics[53].

As show in figure 2.8, woven fabrics can be improved to to achieve greater conductivity by carbonisation. The carbonised woven fabrics can be functionalised as the fabric supercapacitor electrode. Jin et al. [21] implemented an all-carbon-based supercapacitor with functionalized carbon fabrics; their device achieved a high area-specific capacitance of 0.138 $F.g^{-1}$ with a PVA gel electrolyte. The carbon fabrics can be further modified by coats of conductive polymer and some supercapacitor additive materials like graphene and CNT materials. The conductive polymer includes Polypyrrole, PANI and poly (3,4-ethylenedioxythiophene) polystyrene sulfonate [54][55][56], and the coating process will improve its electrochemical performance as a supercapacitor electrode. In comparison with normal woven fabrics, carbon woven fabrics are expensive and the carbonised materials may be fall off from the fabrics which may require extra encapsulation for a fabric supercapacitor based on carbon woven fabrics.

2.4.3 The electrolyte

The performance of a fabric supercapacitor is not just determined by the fabric electrodes but also by the electrolyte properties. The electrolyte will also define the maximum and optimal operating voltage that influences its energy capacity, device total resistance that can vary power

density, the device life time, and the level of encapsulation required for the fabric supercapacitor cell.

Aqueous electrolytes are the most basic type of electrolyte in supercapacitors. They are made by dissolving inorganic salt or compounds in deionised water. The ionic conductivity of aqueous electrolytes is dependent on the temperature, pressure and molar concentration of the salts in deionized water. Therefore aqueous electrolytes with high molar concentration can have high ionic conductivity, which will significantly reduce the device resistance that enhances the power density of the supercapacitor. In fabric supercapacitors, the most common salts or compounds used in aqueous electrolytes are Potassium hydroxide (KOH) [57], Sulphuric acid (H_2SO_4), [58] and Lithium salts (Li_2SO_4, $LiClO_4$, $LiPF_6$) [59]. However aqueous electrolytes have three disadvantages; first the maximum operating voltage of an aqueous electrolyte-based supercapacitor is limited by the electrolysis of water to 1.23 V [58]. Secondly, the fabric supercapacitor with aqueous electrolytes needs to be encapsulated properly in order to prevent water evaporating from the fabric electrode, otherwise the fabric supercapacitor with aqueous electrolytes will have a very short life time. Finally, a solution holder like filter paper separator is required for aqueous electrolytes supercapacitor design, this material layer contains the aqueous electrolyte and physical separate the top and bottom electrode and prevent electrical short circuits, it increase the total thickness of the supercapacitor and the difficulty for the device encapsulation design.

The gel electrolyte is another type of electrolyte for supercapacitor design - in particular, solid-state supercapacitor design. It is made by dissolving inorganic salt or compounds and polymer in a suitable solvent. In comparison with aqueous electrolytes, gel electrolytes have three significant advantages. First, some gel electrolytes allow a higher operating voltage of up to 3 V, which greatly increases the energy density of the resulting supercapacitor. Second, the dried gel electrolytes at the edge and surface of the fabric supercapacitor will prevent the electrolyte evaporation; it will lead to a solid-state supercapacitor with a longer life time than a similar supercapacitor cell with aqueous electrolyte. Thirdly gel electrolyte can act as the charge separator to prevent short circuits and stick top and bottom electrodes together and reduce the thickness of the supercapacitor device.

The most popular gel electrolyte combination is the water-soluble polymer like polyvinyl alcohol (PVA), water and ionic salts or other compounds; a PVA/water gel solution can dissolve a significant amount of different salts or compounds like (KOH) [60], phosphoric acid

(H3PO4) [61] [62] and Lithium chloride [23]. Senthilkumar et al. [63] implemented an all-solid-state supercapacitor and achieved specific capacitance of 648 $F.g^{-1}$ with energy density of 14.4 $Wh.kg^{-1}$. Their devices were based on polymer electrolyte PVA/H_2PO_4, specially activated carbon from tamarind fruit shell and a redox material Na_2MnO_4. In their device, the Na_2MnO_4 will introduce a redox reaction in the polymer electrolyte PVA/H_2PO_4 to enhance the capacity of the supercapacitor. This work suggested that the improvement of the polymer/gel electrolyte is important for next-generation solid-state supercapacitors.

However, gel electrolytes also have some disadvantages. First, in comparison with an aqueous electrolyte, the effective series resistance of a gel electrolyte is high as it has low ionic conductivity. Second, some gel electrolytes contain corrosive solvent that will be damaging to a fabric electrode as it can dissolve organic fibres and cause the electrode material to become dislodged from the electrode [64]. Third, in comparison with aqueous electrolytes, some organic electrolytes have a higher viscosity, which causes wettability issues resulting in less electrode material being in contact with the organic electrolyte to form the double-layer structure.

2.5 Electrode implementation

Using established techniques for patterning or coating textiles and common fabric materials used in the clothing industry (e.g. woven cotton or polyester), it is possible to produce an inexpensive large-scale fabric carbon electrode. The implementations of a fabric supercapacitor electrode can be concluding in three different ways - dyeing, deposition/coating and spinning - to produce a fibre supercapacitor.

Figure 2.11: fabrication procedure of drying method [39].

Dyeing (dipping, soaking) is the process of bonding materials on the surface of fibre in fabrics. It is achieved by placing fabrics in the material solution and allowing the fabrics to absorb the solution. In the clothing industry the manufacturers normally add some materials into the solution to change the fabric's colour. For the supercapacitor electrode, functional powders or

liquids are added to form the solution; for example, carbon powders, CNT powders, MnO_2 powders, surfactant powders and binders. Dong et al. [56] implemented fabric supercapacitors via the dyeing method shown in figure 2.10. Their carbon fabric electrode contains additive CNT or graphene materials. The supercapacitor using these electrodes achieves a specific capacitance of 141 $F.g^{-1}$ and a very high area capacitance of 3.35 $F.cm^{-2}$. However, the dyeing method has disadvantages: the uniformity of the coating thickness and the amount of carbon that can be absorbed into the fabric depend on the viscosity of the carbon ink used, the wettability of the fabric substrate, and the dyeing process set-up. The fabric supercapacitor made with non-uniformly coated fabric electrode tends to have poor wettability i.e. the electrolyte is unlikely cover the electrode materials. These problems can be minimised by modifying the characteristics of the carbon ink and adding some post-treatment such as dipping the fabric electrodes in an acidic solution to further oxidise the carbon materials in the fabric substrate. These issues can also be solved by changing the implementation method from dipping to spraying. In the spraying method, the carbon solution will be sprayed on to the surface of a fabric uniformly, and the amount of carbon absorbed into the fabric can be controlled by the spraying time and distance from the basic structure of a fabric supercapacitor.

Other techniques include deposition or coating are another paths to fabricate fabric electrodes. It is a process to selectively bond a quantitative amount of supercapacitor electrode materials on to the surface of fabrics or fibres. In some coating processes such as inkjet printing, screen printing and brush coating, the supercapacitor electrode materials like carbon or pseudo-capacitive materials will suspended within a solvent, with or without binder, and forms a thicker solution. Then the mixed solution will be coated on top of the fabric substrate to form a supercapacitor electrode. Electrochemical deposition is another useful coating process used to implement supercapacitor electrodes. In this process electrode materials are transferred on to fabrics without being mixed with solvents or other additive materials. Wang et al. [65] implemented a solid-state fabric supercapacitor; the electrodes were achieved by electrochemically-deposited PANI on top of carbon cloth and metal-organic framework. The electrode itself achieved a very high area specific capacitance of 2.1 $F.cm^{-2}$.

As show in figure 2.11, screen-printed and inkjet-printed thin film on fabrics have been demonstrated previously[66]. These processes enable precise control over the amount of active material coated on to the fabric. In particular, the resolution of inkjet printing is high due to high precision provided by close ink-droplet spacing of the printer. Screen printing methods enable a large area of substrate material to be coated with carbon in a short amount of time.

The quality and stability of a supercapacitor is influenced by the fabrication process used to implement the device [13]. Conedera [48] demonstrated the implementation of a supercapacitor using inkjet printing. In their work, activated carbon powder was mixed with ethylene glycol, as a thinner, and alcoholic Polytetrafluoroethylene (PTFE) binder, to produce a low viscosity, uniform solution that was suitable for inkjet deposition. Kaempgen et al. [18] inkjet-printed single-walled carbon nanotubes on a PET substrate as the bottom electrode of a supercapacitor, then printed a gel electrolyte layer, and then a top electrode of carbon nanotubes. Their printed supercapacitor achieved a specific capacitance of 36 $F.g^{-1}$ with a high power density.

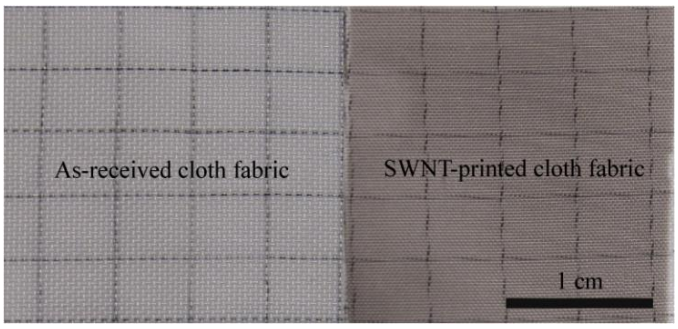

Figure 2.12: photograph of cloth fabric before and after inkjet printing of SWNT films [19].

Spinning (include wet, dry and coaxial spinning shown in figure 2.12) is an another alternative approaches to fabricate supercapacitor, it is a popular method to create fibre supercapacitors. It convert original fibre and electrode material into functional yarns as the electrode of fibre supercapacitor. In this process the polymer or fabric functional yarns are made through precipitation and solidification.

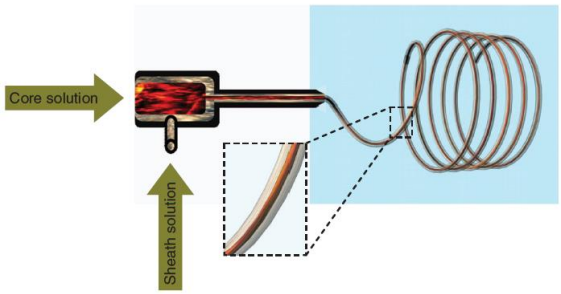

Figure 2 13 fabrication procedure illustration of the coaxial spinning process [26].

As shown in figure 2.6, a complete supercapacitor cell consists of two layers of carbon electrodes with a piece of separator in between. For a fabric electrode the cell needs to be compressed by the top/bottom current collector to minimise the thickness of the fabric

electrodes. This will reduce the electrode resistance and improve the measured specific capacitance, power density and energy density.

2.6 The post-treatment of fabric supercapacitor electrodes

The post treatment of conductive fabric electrodes is another factor that will affect the performance of the fabric supercapacitor. In a fabric supercapacitor, the fabric electrode can be further modified to achieve better capacitance by, for example, boiling or immersing a carbon-based fabric electrode in to an acid or alkali solution [67]. The supercapacitor electrode implemented by Pasta et al. [50] achieves better specific capacitance (70 $F.g^{-1}$) than the supercapacitor electrode implemented by Hu et al. [6] (14 $F.g^{-1}$). These electrodes used the same substrate, similar carbon material (SWNT) and identical fabrication method (dipping). The fabric electrodes made by Pasta et al. [50] were dipped into the 4M nitric acid (HNO_3) solution for a longer time (six hours in comparison with 30 minutes). The acid or alkali compounds in the solution will increase the surface area of the carbon material by oxidising the surface of the carbon particle, and this process will increase the area where the electrolyte comes in contact with the electrode materials to form the double layer structure.

Coating is a process to further modify the electrode by reducing its resistance and introducing additional pseudo-capacitance. The most common coating materials for fabric electrodes are oxide materials [52], metalised nanoparticles [68] and conductive polymers [59]. Zhao et al [59] fabricated a graphene oxide composite fabric electrode with poly-pyrrole (Ppy) coating. Ppy can reduce the resistance of the fabric electrode and provide extra pseudo-capacitance. The fabric supercapacitor made with this electrode and aqueous electrolytes achieved specific capacitance of 114 $F.g^{-1}$.

Vacuum impregnation - also known as porosity sealing - is a potential method for increasing the electrochemical performance of a fabric electrode. This method can improve the infiltration of the electrolyte solution into the porous fabric electrode by extracting air bubbles out of the fabric electrodes. The vacuum impregnation process has been demonstrated previously in solid oxide fuel cell fabrication [69] and some organic products [70], and the fabrication of rigid supercapacitors [71]. In the fabric supercapacitor the fabric substrates will contain a lot of air bubbles that prevent the electrolyte from making contact with the electrode material. Therefore, in comparison with the rigid supercapacitor, vacuum impregnation is more suitable for the flexible electrode of the fabric supercapacitor.

2.7 Fabric supercapacitor designs

A summary of reported flexible supercapacitors and their electrochemical performance in from the past 5 years is presented in table 2.2.

Table 2.2: Fabric supercapacitor design in the past five years.

Author	Year	Active material	Substrate	Electrolyte	Fabrication	Additional treatment	Specific C ($F.g^{-1}$)	Area C ($F.cm^{-2}$)
Pasta et al. [50]	2010	SWNT	Cotton /non-woven	2M LiSO4	Dipping	Dip sample into HNO3	70	N/A
Chen et al. [19]	2010	SWNT+ RuO2	Cloth fabrics /woven	PVA /H3PO4	Inkjet printing	RuO2 CVD coating	138	0.026
Jost et al. [42]	2011	Activated carbon	Polyester fibre/woven	2M LiSO4	Dipping	Additional carbon black in	85	0.00043
Wang et al. [44]	2011	SWNT+ PANI	Wiper /non-woven	1M H2SO4	Dipping	PANI thermal coating	102	N/A
.Lekakou et al. [20]	2011	CNT	Carbon fabric /woven	PEO-LiClO4-EC-THF	Stacking	N/A	2.6	0.000053
Liu et al. [51]	2012	Graphene Oxide	Textile-cotton /woven	6M KOH	Brush coating	Boil Cotton in NAOH	81	N/A
Meng et al. [25]	2013	Graphene fibre	Graphene fibre	1M LiClO4	Electrochemical electrolysation	N/A	40	0.0017
Yang et al. [46]	2013	Carbon fabric/MnO2/ZnO	Carbon cloth	(PVA)/liCl	Dyeing	Dip samples in acid	1260	0.026

Author	Year	Active material	Substrate	Electrolyte	Fabrication	Additional treatment	Specific C ($F.g^{-1}$)	Area C ($F.cm^{-2}$)
Jin et al. [21]	2014	Carbon fabric	Carbon fabric	(PVA)/liCl	Acid etching	Annealing	N/A	0.135
Wang et al. [24]	2014	Co3O4/Graphene	Nickel fibre	6 M KOH	Coating	N/A	N/A	2.1
Zhang et al. [61]	2014	Graphene	Polishing cloth	(PVA)/H3PO4	Deposition	N/A	267	0.008
Su et al. [62]	2014	MnO2/CNT	Yarns	(PVA)/H3PO4	Dyeing	N/A	12.5	N/A
Zhang et al. [73]	2014	CNT	CNT sleeve sponges	KOH	Deposition	N/A	5.3	0.034
Kou et al. [26]	2014	Carbon fabric	Graphene woven fibres	PVA gel electrolyte	Wet spinning	Au CVD coating	N/A	0.269
Hu et al. [72]	2014	Graphene	Graphene fibre	BMM-PF6	Wet spinning	N/A	N/A	0.0024

Author	Year	Active material	Substrate	Electrolyte	Fabrication	Additional treatment	Specific C ($F.g^{-1}$)	Area C ($F.cm^{-2}$)
Liu et al.[23]	2015	Reduced graphene oxide	Cotton fibre	(PVA)/liCl	Deposition	Nickle Coating	311	N/A
Gao et al. [67]	2015	NiCo2O4	Cotton activated carbon	(PVA)/KOH	Growing	Dip samples into NaF	179	N/A
Zhang et al. [45]	2015	PANI /graphene	Graphene woven fabric	(PVA)/H3PO4	Deposition	Dip samples into HCl (1h)	771	0.023
Dong et al. [57]	2015	CNT (Graphene)/ Carbon fabric	Activated carbon fibre	6M KOH	Drying	Dip samples into KOH	141	3.35
Wang et al. [65]	2015	PANI/ Metal−organic frameworks	Carbon cloth	(PVA)/H2SO4	Deposition	N/A	469	0.035
Z|hao et al. [59]	2015	Reduced graphene oxide/Ppy	Nylon fabrics	Li2So4	Dyeing	Ppy coating	114	N/A
Yuksel et al. [52]	2015	PANI/CNT /MnO2	Cotton	PMMA gel electrolyte	Dyeing	PANI coating	246	0.0735
Choi et al. [74]	2015	CNT/MnO2	Nylon fabrics	(PVA)/liCl	Deposition	N/A	N/A	0.0409

Author	Year	Active material	Substrate	Electrolyte	Fabrication	Additional treatment	Specific C ($F.g^{-1}$)	Area C ($F.cm^{-2}$)
Pu et al. [79]	2016	Reduced Graphene oxide/Ni	Polyester yarn	(PVA)/H3PO4	Deposition	Annealing	N/A	72.1
Lam et al. [22]	2016	Calligraphic ink	Silver-coated cotton fabrics	(PVA)/liCl	Drying	N/A	2.9	0.036
Yu et al. [78]	2016	Graphene hydrogel	Stainless steel fabrics	(PVA)/H2SO4	Stacking	Annealing	45	0.184
Huang et al. [77]	2016	CNT	Nickel-coated cotton fabrics	1M Na2SO4	Electro spinning	N/A	N/A	0.973
Zhang et al. [76]	2016	MnO2	Carbon fabrics	Na2SO4	Electrodeposition	N/A	250	0.005
Sun et.al [75]	2016	Reduced Graphene oxide	Polyester textile	(PVA)/H3PO4	Drying	PANI coating	151	0.781

2.8 Discussion

According to table 2.2, the supercapacitor electrode made by MnO_2 and ZnO dip coated carbon fabrics achieved the highest specific capacitance of 1260 $F.g^{-1}$ [46].Similarly Dong et al. [57] implemented a flexible supercapacitor based on PANI coated graphene woven fabric electrode. This device demonstrated the highest area capacitance of 3.35 $F.cm^{-2}$ and a good specific capacitance of 141 $F.g^{-1}$. These are due to the material advantages of pseudo-capacitive materials (MnO2, PANI) in comparison to the rest of the examples (table 2.2) the carbon cloth substrate resulted in a highly electrical conductive fabric substrate which improves the measured capacitance of the supercapacitor.

The supercapacitor implemented by Lekakou et al. [20] has the lowest specific capacitance for the following reasons. Firstly, the weight of substrate was included in the calculation of specific capacitance. Secondly they use an organic/polymer electrolyte PEO-$LiClO_4$-EC-THF that m has a relatively high viscosity in comparison with an aqueous electrolyte which reduces the effective electrode area.

Kou et al. [26] implemented a fibre supercapacitor electrode via a wet spinning method with graphene oxide on a single piece of fibre. Their supercapacitor was constructed by interweaving two individual coaxial fibres together with a polymer electrolyte PVA/H_3PO_4, and achieved a high area capacitance of 0.269 $F.cm^{-2}$. The significant improvement is the structure of the supercapacitor which is different from the traditional multi-layered structured devices that require additional packaging to compress the electrodes for testing purposes.

As shown in table 2.2, in recent years, some people have attempted to build a flexible supercapacitor based on metal-coated woven materials and metal fabrics. Huang et al. [77] implemented a fabric supercapacitor electrode based on nickel-coated cotton fabrics and a spin-coated CNT material layer. Their multi-layer flexible supercapacitor together with an aqueous electrolyte Na_2SO_4 demonstrated a high area capacitance of 0.973 $F.cm^{-2}$. The key advantage of this kind of design is the electrode resistivity which is much lower in comparison with carbon- (carbon black) coated fabrics or some carbonised fabric electrodes. However, the metal coating also shows some other disadvantages: first, it introduces extra weight to the fabric electrode, and second, the process increases the cost of fabric electrodes.

2.9 Conclusion

This chapter reviews supercapacitors and includes a brief history of capacitive devices, the theory and development of double-layer models for supercapacitors, the electrode, electrolyte and substrate material properties with their influence on supercapacitor designs and previous work on flexible supercapacitor electrodes. These examples proved that the performance of supercapacitor with fabric electrode depends on the electrode's material properties, the electrode's wettability with the electrolyte, and the electrical conductivity of the supercapacitor substrate material. These examples also proved that in the past most people have focused on the electrochemical performance of the fabric supercapacitor electrode rather than a full supercapacitor cell, a lot of their supercapacitor electrodes were with pseudo-capacitive materials that suffer from performance reduction over time, non-area selective fabrication methods like dyeing/dipping and brush coating, low throughput method like deposition or glowing, expensive conductive fabric substrates like graphene woven fabrics, very expensive electrode materials such as CNT and graphene and aggressive post treatment method like acid immersing. The supercapacitor electrodes presented in this work shall overcome all these shortages by implements supercapacitor electrode with inexpensive carbon and binder material that will provide excellent stability, inexpensive general proposes woven fabrics, non-hazarded post treatment method (vacuum impregnation) that enhance the electrochemical performance, an area selective and high throughput fabrication method (spray coating). Also in these examples, all of the proposed supercapacitor test were made by at least two layers of fabric electrode and possibly a layer of polymer or paper charge separator, in this work a supercapacitor fabricated in a single layer fabric will be presented with full device evaluation. In conclusion, the fabric supercapacitor is a feasible device but has not yet been fully developed. The performance of a practical supercapacitor not only depends on its electrode and electrolyte but requires more thinking about the device encapsulation and testing set-up.

3 The characterisation of supercapacitor

A supercapacitor is regarded as a symmetrical two-electrode cell. The capacitance, ESR and charge/discharge time constant can be tested by a potentiostat (constant voltage) or galvanostat (constant current) test. This chapter reviews supercapacitor characterisation including the measurement setup, fundamental theories of capacitor and three different test methods.

3.1 Electrochemical characterisation of two-electrode device

Most assembled supercapacitors are two terminal devices [2]. The characterisation of assembled supercapacitors requires two electrodes (counter electrode and working electrode). The testing is conducted by recording the potential difference between the counter and working electrode, and the current flow through the counter and working electrode.

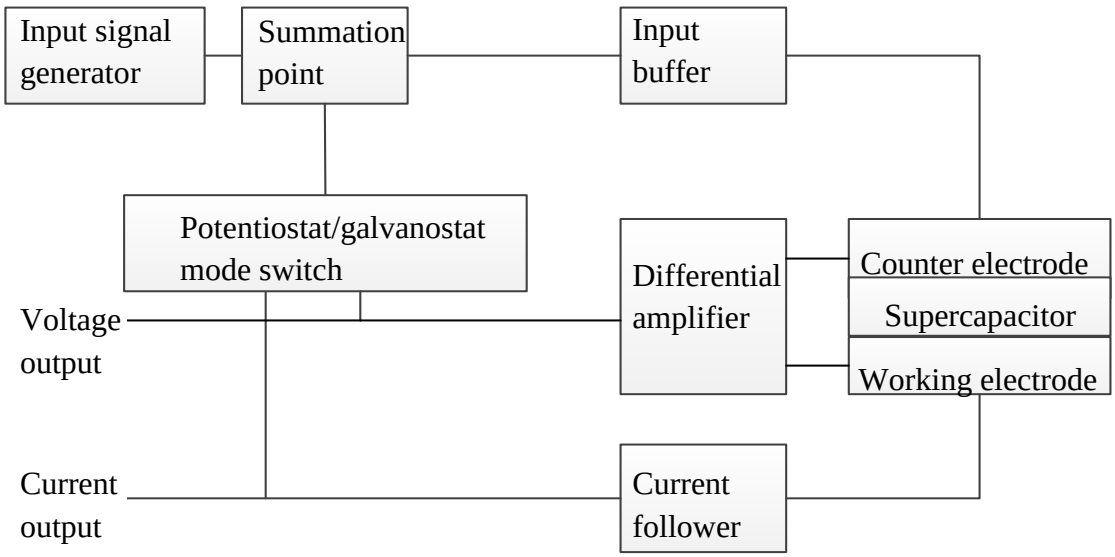

Figure 3.1: block diagram of two-electrode potentiostat/galvanostat test.

Figure 3.1 is the block diagram of a two-electrode test instrument. In the potentiostat operating measurement mode, the input signal generator provides a unit-step voltage signal with controlled current for galvanostatic test, the input signal generator supplies a repeated-ramp signal with controlled potential step for cyclic voltammetry (CV) test and sinusoidal signals at different frequency for the equivalent impedance spectroscopy(EIS) test [80]. In galvanostat operating mode, the input signal generator is required to provide input signal with constant potential for dc charging and discharging test. The summation point is for feedback control of the input current or voltage. The input buffer is to force all input signals into the counter electrode. The output potential is recorded between counter and working electrode using a differential amplifier and the output current is measured using a current follower [81].

When a voltage is applied across the supercapacitor, the polarization of electrons and ionized molecules in the electrolyte will create a current flow in the device. Measuring this current flow will provide values for some of the properties of this capacitive device, including ESR and capacitance.

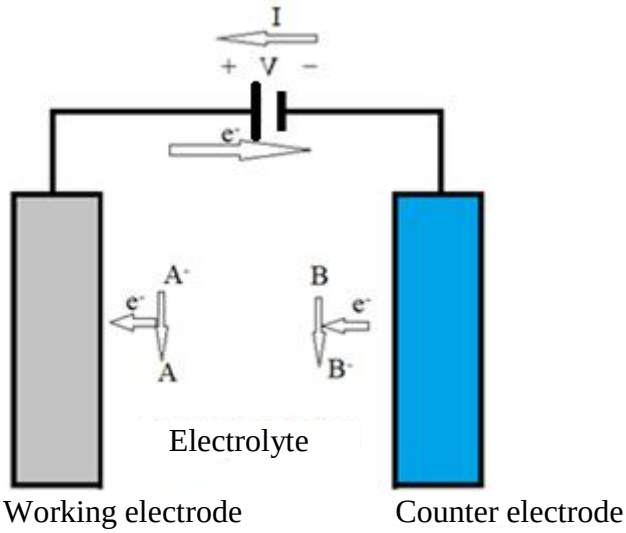

Figure 3.2: An electrochemical reaction at both working and counter electrode.

Figure 3.2 is an example of the reaction occurs in an electrochemical device. When a voltage is applied across the working and counter electrodes, the ion A (A^-) loses an electron and become atom A, on the other side of device atom B gains an electron and turns into ion B (B^-). This will change the electrical dependence of the electrode material and provides a basis for electrochemical measurement to evaluate the capacitance and ESR of the device.

The capacitance C of capacitor defines as the amount of charge of Q with respect with the potential difference V between two oppositely charged plates:

$$C = \frac{Q}{V} \qquad \text{(Equation 3.1)}$$

According to Gauss's law, when the top and bottom electrodes receive a charge of Q, the magnitude of the electric field E in between the parallel electrode plate with area A and can be expressed as:

$$E = \frac{Q}{\varepsilon A} \qquad \text{(Equation 3.2)}$$

In equation (3.2) ε is the dielectric constant of the gap or spacer material between the two electrodes. By integrating equation 3.2 with respect to the distance between the top and bottom electrodes, d, the potential difference across the capacitor can be express as:

$$\mathrm{V} = \int_{-}^{+} E\,dx = Ed = \frac{Qd}{\varepsilon A} \qquad \text{(Equation 3.3)}$$

By combining equations (3.1) and (3.3) the expression that charecterises an ideal parallel plate capacitor becomes:

$$C = \frac{\varepsilon A}{d} \qquad \text{(Equation 3.4)}$$

ε is the dielectric constant of the dielectric layer that equal to the product of the free space dielectric constant ε_0 and the relative dielectric constant ε_r of the dielectric material.

3.1.1 Specific capacitance

In a supercapacitor capacitance is the most important parameter since it indicate how much electronic charge can be stored in the capacitor body. Another important parameter specific capacitance will be use of electrochemical devices like supercapacitor is defined as:

$$C_s = \frac{C}{m} \qquad \text{(Equation 3.5)}$$

Where C is capacitance and m is the weight of the active material of electrodes. Capacitance can be measured by galvanostatic cycling (GC), cyclic voltammetry and equivalent impedance spectroscopy.

3.1.2 Resistance, energy and power density measurement

Power density, P, and energy density, E, are also important factors in supercapacitor design. These are given by:

$$P = \frac{{V_i}^2}{4R_{ESR}} \qquad \text{(Equation 3.6)}$$

$$E = 0.5 \times C{V_i}^2 \qquad \text{(Equation 3.7)}$$

Where V_i is the initial test voltage and $\mathrm{R_{ESR}}$ is the ESR of supercapacitor found by electrochemical test.

3.1.3 Capacitor current-voltage relationship in DC circuit

According to equation 3.2, 3.3 and the current across the capacitor $\mathrm{I(t)} = \frac{\mathrm{dQ}}{\mathrm{dt}}$, the current-voltage relationship of an ideal capacitor In DC condition can be expressed as:

$$\mathrm{I(t)} = \frac{dQ}{dt} = \frac{d}{dt} \times \frac{\varepsilon A}{d} V = \frac{\varepsilon A}{d} \times \frac{dV}{dt} = C \frac{dV}{dt} \qquad \text{(Equation 3.8)}$$

$$C = \mathrm{I(t)} / \frac{dV}{dt} \qquad \text{(Equation 3.9)}$$

By integrating equation 3.8 over time t:

$$\int_0^t Idt = \int_0^t C \frac{dv}{dt} \times dt$$

$$V(t) = \frac{1}{C} \int_0^t Idt + v(0) \qquad \text{(Equation 3.10)}$$

In a DC circuit is assumed the ideal capacitor C is only in series with an ideal resistor R and the capacitor are initially uncharged, and therefore its current-voltage relationship can be express as:

$$V(t) = V_0(1 - e^{-\frac{t}{RC}}) \qquad \text{(Equation 3.11)}$$

$$\mathrm{I\ (t)} = \frac{V_0}{R} e^{-\frac{t}{RC}} \qquad \text{(Equation 3.12)}$$

In equation 3.10 V_0 is the potential step across the capacitor, this equation presents the voltage and current variation when applying a DC step voltage to charge a capacitor, it is also the mathematical representation of capacitor charging with step voltage in galvanostatic cycling test.

3.1.4 Capacitor current-voltage relationship in AC circuit

According to equation 3.8, if the voltage $V(t)$ has the form $V(t) = Acos(2\pi ft)$ where A is the amplitude of $V(t)$ and f is the frequency of $V(t)$, equation 3.8 can be express as:

$$\mathrm{I(t)} = C \frac{dV}{dt} = -C \times 2\pi f \times Asin(2\pi ft)$$

$$\mathrm{I(t)} = C \times 2\pi f \times Acos\left(2\pi ft + \frac{\pi}{2}\right) \qquad \text{(Equation 3.13)}$$

Equation 3.13 indicates that in an AC circuit the current going through a capacitor leads the voltage of capacitor by 90 degrees. Base on equation 3.12 the impedance of a capacitor can be obtained by taking the ratio of the peak voltage to the peak current of the capacitor:

$$Z_c = \frac{|V_{(t)}|}{|I_{(t)}|} = \frac{1}{2\pi f C} \qquad \text{(Equation 3.14)}$$

Equation 3.14 suggest when $f \to +\infty$, Z_C goes to zero that capacitor is act as a short circuit, when $f \to 0$, Z_C goes to infinity that capacitor is act as an open circuit.

3.2 Supercapacitor equivalent circuit and model

A series of electrical components can be used to provide an equivalent circuit that models the behaviour of a supercapacitor. The various models used are examined here.

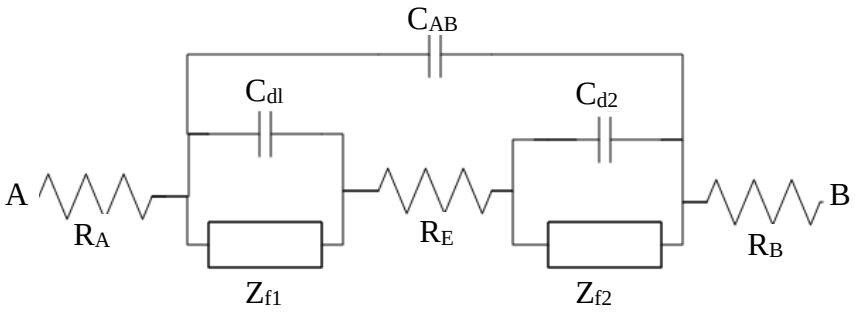

Figure 3.3: The equivalent circuit of a two electrode electrochemical device [2].

In figure 3.3 R_A and R_B represent the resistance of each current collector, R_e is the resistance of the electrolyte, and C_{AB} is the capacitance between the two current collectors. C_{d1}, C_{d2} and Z_{f1}, Z_{f2} are the double layer capacitance and the electrochemical impedance of the counter and working electrodes respectively, these values are defined depending on the electrode material. This equivalent circuit can be simplified for supercapacitors since the current collector is usually a metallic material that has relative very small surface area in comparison with the electrode material like carbon. Therefore, the current collector resistances (R_A and R_B) and the interfacial capacitance between two current collectors, C_{AB} is small that it can be ignored.

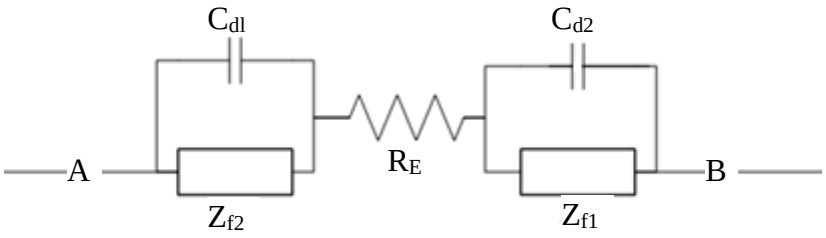

Figure 3.4: Simplified equivalent circuit of two electrodes symmetrical electrochemical device.

Figure 3.4 is the simplified equivalent circuit of a two electrodes electrochemical device. The circuit can be further simplified for symmetrical devices like a double layer supercapacitor, because two electrodes made with same material will have identical response under the EIS test.

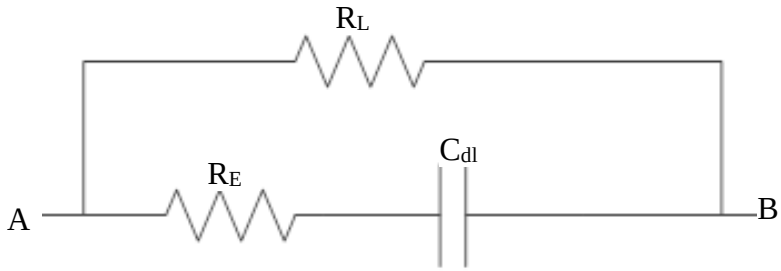

Figure 3.5: The further simplified equivalent circuit of an ideal EDLC.

Figure 3.5 is the equivalent circuit model of an ideal EDLC in voltage or current biased tests like galvanostatic cycling (GC) and cyclic voltammetry (CV) test. In figure 3.5 R_E represents the resistance of the supercapacitor electrode and the electrolyte, R_L replacing the electrochemical impedance Z_{f1} and Z_{f2} of the supercapacitor electrode and represent the leakage resistance of the supercapacitor from top to bottom current collector. In an ideal EDLC the electrode R_E is assumed to be very small and R_L is very large that the device has very small leakage current. This model is valid in GC and CV test at high test frequency [2]

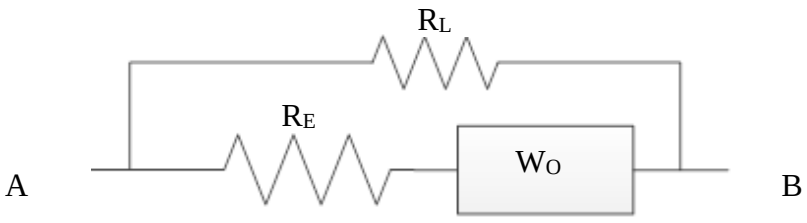

Figure 3.6: The equivalent circuit of an ideal EDLC with Warburg element WO.

In most supercapacitors like EDLC, its electrodes were made with rough and porous materials like carbon, therefore diffusion process occur in the device at very low test frequency. The circuit model 'parallel plate capacitor' (C_{DL}) shown in figure 3.5 is not a suitable model for supercapacitor made with porous electrode materials. Another circuit element is the Warburg element ($W_{O)}$ shown in figure 3.6 replaces C_{DL} and represents the double layer capacitance of the supercapacitor, this circuit is the low frequency equivalent circuit model of an ideal EDLC in the electrochemical impedance spectroscopy (EIS) test. The Warburg element, or Warburg diffusion element is a circuit element used to model one dimensional semi-infinite linear diffusion process; it is a constant phase element with a constant phase of 45 degrees. The impedance of Warburg element can be expressed as:

$$Z_{wo} = \delta(2\pi f)^{0.5} - i\delta(2\pi f)^{0.5} \qquad \text{(Equation 3.15)}$$

In equation 3.15 δ is the Warburg coefficient which relates to the diffusion coefficient and the concentration of the oxide and reduced species in the electrolyte. The Nyquist plot of the Warburg element is a line at 45 degrees when$f \to 0$.

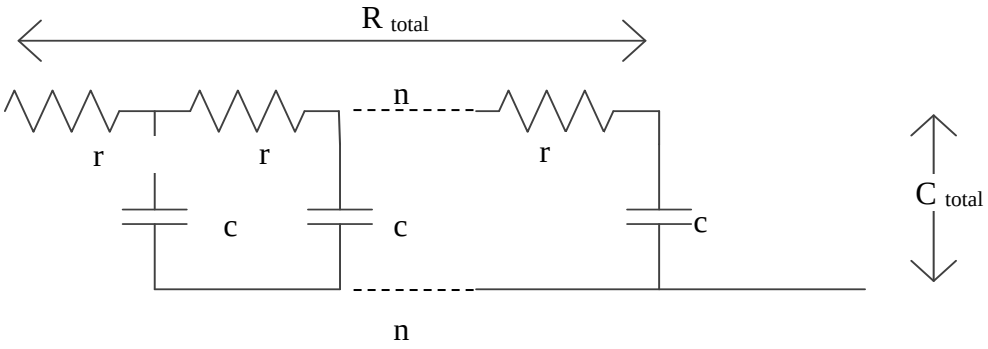

Figure 3.7: Equivalent circuit of Warburg element [1].

The Warburg element can be modelled as transmission line device shown in figure 3.7; n is the number of pores on the electrode (unit electrode length), r is the electrolyte resistance per unit electrode length, c is the capacitance per unit electrode length, R_{total} and C_{total} is the total resistance and capacitance respectively of the porous electrode. When $f \to 0$ the impedance of a Warburg element modelled by transmission line model can be expressed as:

$$Z_{wo} = \frac{R_{total}}{n} - \frac{i}{2\pi f C_{total}} \qquad \text{(Equation 3.16)}$$

According to equation 3.16, the capacitance of an EDLC made with rough and porous electrodes can be obtained from its impedance plot (Nyquist plot), it by test the device with a low frequency AC signal in an equivalent impedance spectroscopy test.

3.3 Galvanostatic cycling test

Galvanostatic cycling, or constant current cycling, determines the charge/discharge or DC characteristics of energy storage devices. It can be used to obtain the capacitance as well as the device's ESR [82]. This test is performed with a constant current source where the voltage is increased by a pre-defined potential step and then returned to 0 V. This is repeated many times. The voltage step used depends on the characteristics of the electrolyte, for example devices based on an aqueous electrolyte can be tested with a voltage step of 1 V whereas organic devices can be tested with a voltage step of up to 2.7 V.

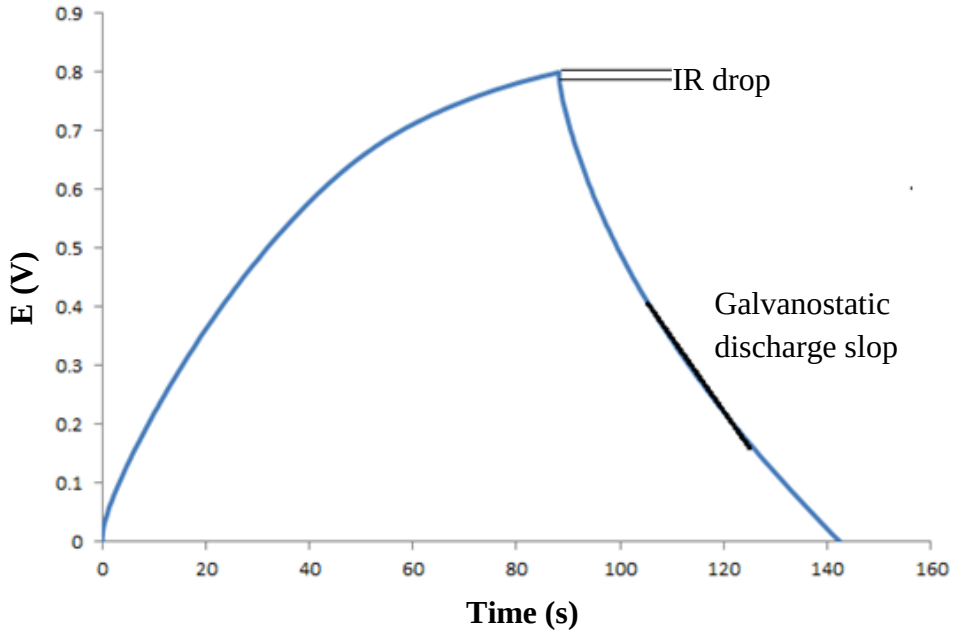

Figure 3.8: A galvanostatic discharge curve of ideal EDLC.

Figure 3.8 is shows an ideal EDLC charge/discharge curve obtained by galvanostatic cycling. The discharge curve for a non-faradic electrode material will typically show a roughly constant rate of voltage change over time after the initial faster potential drop. The potential drop at the beginning of discharge curve is known as the IR drop, and is due to the energy consumption of a device's ESR [37]. Therefore, by extracting the voltage gap created during IR drop from a galvanostatic cycling measurement, the ESR of the device can be expressed via ohms law with predefined test current value.

$$R_{ESR}=\frac{V_{IR\,drop}}{I_i} \qquad \text{(Equation 3.17)}$$

In equation 3.17 $V_{IR\,drop}$ is the voltage gap created during IR drop in volts and I_i is the predefined test current value. Furthermore, the capacitance of the device can be evaluated from

the steady portion of the galvanostatic charge/discharge curve according to equation 3.17 where I_i is the pre-defined current used in galvanostatic cycling test and $\frac{dV}{dt}$ is the slope of galvanostatic discharge curve in the linear region.

ESR can be further explained as area ESR ($\Omega.cm^{-2}$), it can be express as Ω per unit area of the electrode, and normalised ESR ($\Omega.cm$), it can be express as Ω multiply the thickness of the device and divide the device actual area.

3.4 Cyclic voltammetry

A CV measurement is another type of electrochemical measurement. It is performed in a similar way as galvanostatic cycling, however unlike galvanostatic cycling, cyclic voltammetry involves the measurement of the output current and input voltage sweep.

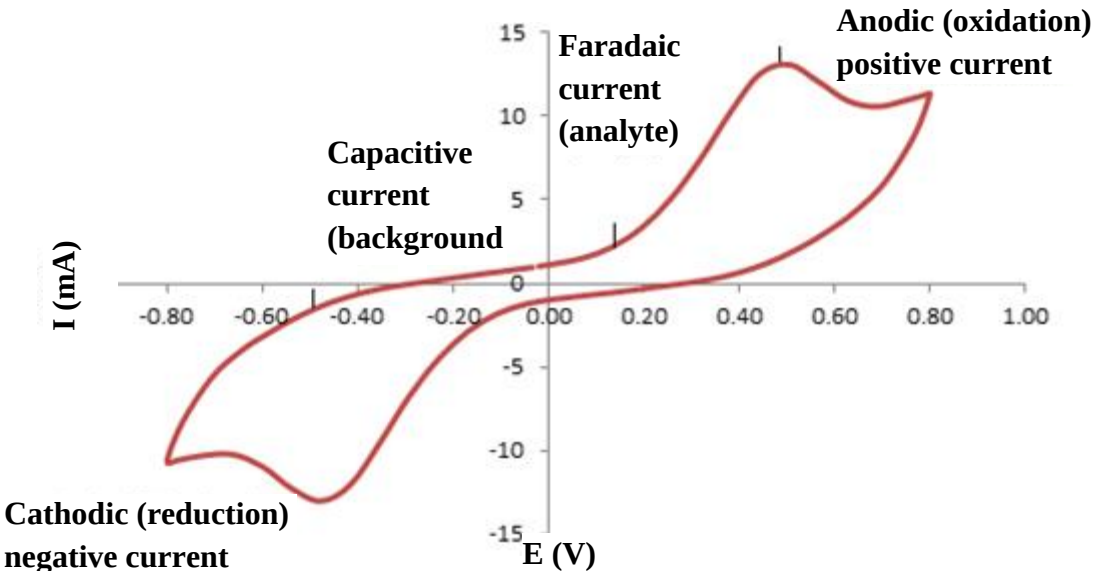

Figure 3.9: Cyclic voltammetry test result of iron electrode.

Figure 3.9 shows the CV test result with a standard faradaic material iron. In CV test the output current of an electrochemical device changes as the with input voltage changes [83]. There are three regions in both the forwards and backwards scanning directions. These regions are capacitive current, faradaic current and oxidation current. When the device is in the capacitive current region, the output current of the device increases as the applied potential increases [37]. This is due to the formation of the electrode double layer and/or the rearrangement of ions from the electrolyte at the electrode/electrolyte interface. The magnitude of the capacitive current is dependent on the effective area of the electrode material, the equivalent resistance of the electrode/electrolyte and the rate of change of the input voltage. In the next stage, a faradaic

reaction will occur that revert the ions to a neutral charge that exist in the electrolyte. At this stage the device current will increase dramatically to the 'anodic peak point' as the input voltage continues to increase. As the input voltage increases up to the maximum, less electrode material can be in contact with electrolytic solution due to material passivation, so the current will drop to a constant value, slightly less than the current at the 'anodic peak point'[83]. Then as the input voltage reduces and then switches its polarity, the current will begin to drop and reverse its direction to the 'negative reduction peak point'. This is due to a reduction reaction occurring at the electrode and electrolytic interface. Finally, as the input voltage returns to the initial value, no reaction will occur and the device will return to capacitive behaviour. These observations indicate the reversibility of the electrochemical reactions with faradaic materials and explain the behaviour of most electrochemical energy storage devices, including batteries and some supercapacitors. However, in pure electrical double layer capacitors, no faradaic reaction occurs in normal operation. Faradaic current will consequently not be present in its cyclic voltammetry result [82].

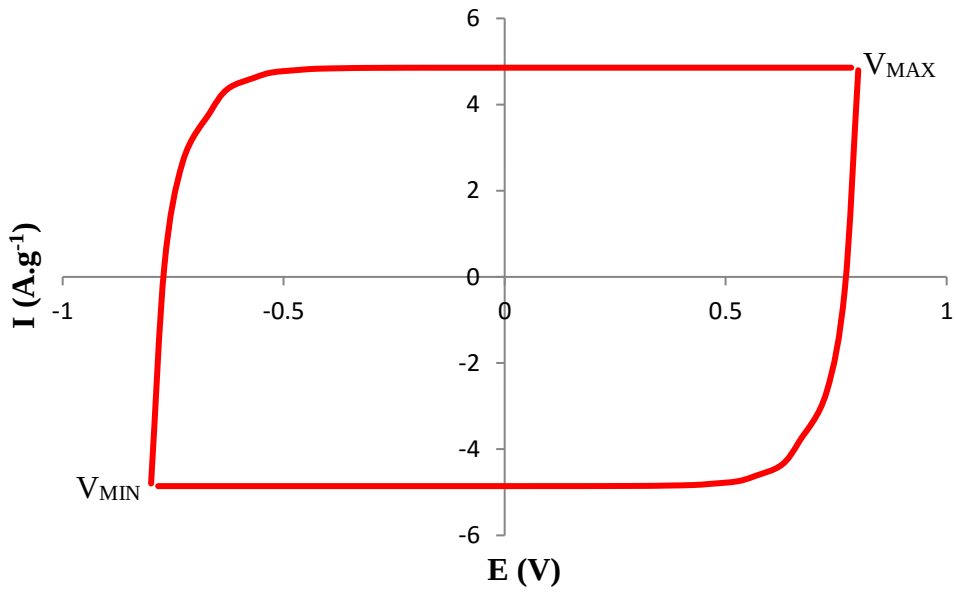

Figure 3.10: Cyclic voltammetry sketch of semi-ideal supercapacitor.

Figure 3.10 shows the CV sketch with a semi-ideal supercapacitor that has equivalent circuit shown in figure 3.5. According to equation 3.8 the result current/voltage sketch curve looks like a rectangular shape plot. The small curvature that appears at the edge of the CV result is associated with the leakage current of the device, theoretically large scan rate will cause increased current leakage and curvature on the result, the shape of CV test result will become a diamond shape plot at very high scan rate.

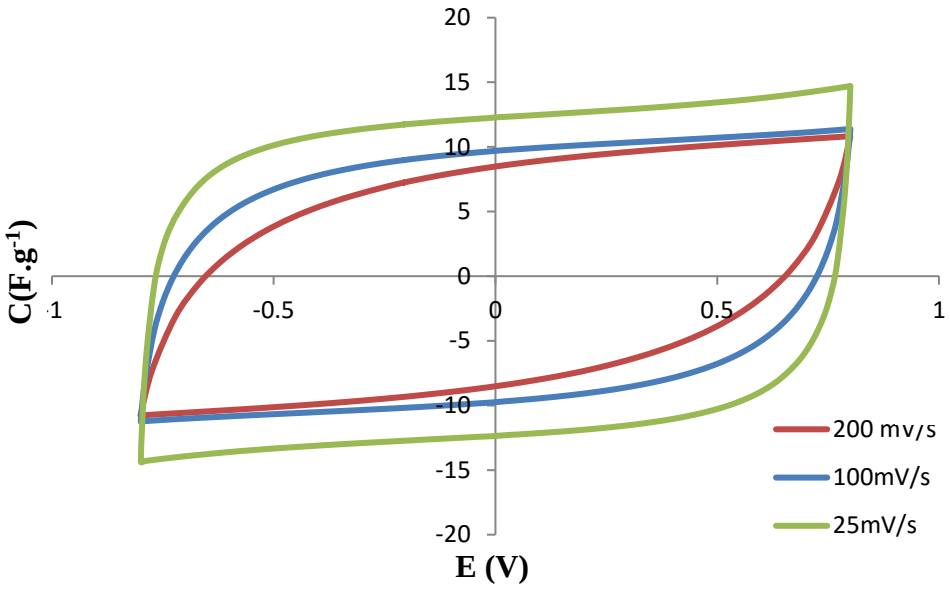

Figure 3.11: Cyclic voltammetry result of IDEAL supercapacitor normalised with scan rate.

In CV test the capacitance of device can also be obtained via equation 3.9, where $\frac{dV}{dt}$ is the rate of voltage change or 'scan rate' of the test and I is the average current in the CV measurement between the maximum voltage V_{MAX} and the minimum voltage V_{MIN} shown in figure 3.10. As shown in figure 3.11 in CV test high voltage scan rate will result in low capacitance. It is due to current leakage of device at high scan rate.

3.5 Electrochemical impedance spectroscopy

EIS is another useful tool to analyse the behaviour of electrochemical devices. This method is uses a bridge calibration circuit and examines the interaction of the tested device with an alternating input. In comparison with other electrochemical tests, an EIS test has three major advantages. First, it is a small perturbation testing technique that is unlikely to modify the characteristics of cell during the measurement and provide the capacitance-voltage relationship without charging the device significantly away from its equilibrium point. Secondly, it provides information regarding the device resistance relative to the power consumption of cell. Third, unlike CV or GC tests, results measured by EIS are time and current independent This method has other advantages including high precision, large frequency range and linearized input characteristics.

An EIS test will not only determine the capacitance of a supercapacitor in respect with test frequency, but also provide the Nyquist impedance plot for a large of frequencies. A Nyquist impedance plot indicates the phase relationship between the real part of the impedance (Z_{re})

and imaginary part of the impedance (Z_{im}) impedance of the device, According to the application note of EC lab software in EIS test the capacitance can be found using simplified circuit model shown in figure 3.12

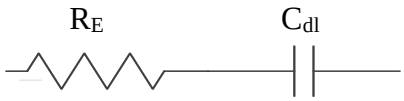

Figure 3.12: The further simplified equivalent circuit of a symmetrical EDLC in EIS test .

In comparison with the circuit model shown in figure 3.5, the circuit model shown in figure 3.12 the further simplified circuit model of EDLC in EIS test, R_E is the resistance of the supercapacitor electrode and the electrolyte C_{DL} is the double layer capacitance of EDLC. This circuit model assumes that there is no leakage in the EDLC. This assumption could only be valid in the low frequency region when the supercapacitor is able to be fully charged and discharged. The characteristic impedance of this mode can be expressed as:

$$Z = Z_{RE} + \frac{1}{i2\pi fC} = Z_{RE} - \frac{i}{2\pi fC} = Z_{re} - iZ_{im} \qquad \text{(Equation 3.17)}$$

$$Z_{re} = Z_{RE},\ Z_{im} = \frac{1}{2\pi fC} \qquad \text{(Equation 3.18)}$$

$$C = \frac{1}{2\pi f Z_{im}} \qquad \text{(Equation 3.19)}$$

In equation 3.18 and 3.19, Z_{RE} is the impedance of the electrode and electrolyte, C is the capacitance and f is the operating frequency when the supercapacitor is able to be fully charged and discharge.

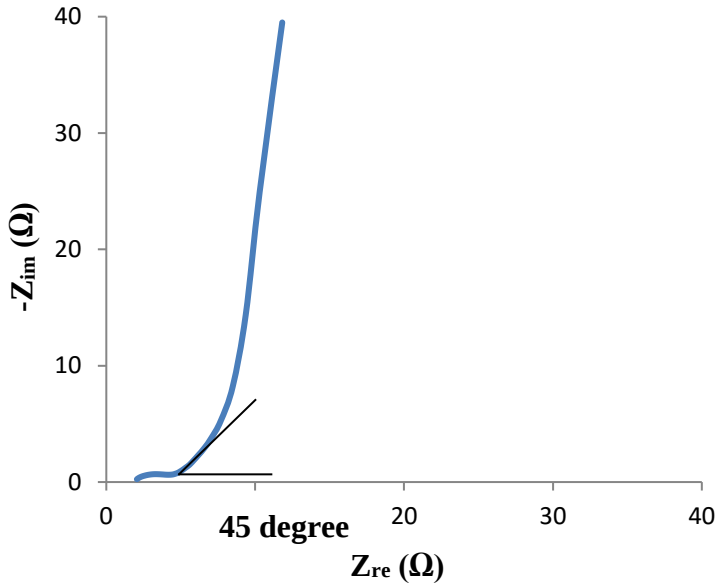

Figure 3.13: Nyquist impedance plot of an ideal EDLC.

Generally, each type of electrochemical device will have a characteristic behaviour in an EIS test. Figure 3.13 is a typical Nyquist impedance plot for a double layer capacitor, from which various properties of the supercapacitor can be extracted. Firstly, the ESR, of the device is the value of the real impedance Z_{re} where Z_{im} close to zero at high frequency region [37]. Secondly, the double layer capacitance of the supercapacitor can be obtained at a very low frequency via equation 3.19. Finally, for a double layer supercapacitor, the vector plotted by the Z_{re} and imaginary Z_{im} impedance of device will have a 45 degrees bend at low frequency in the Nyquist impedance plot. It is at this point where diffusion dominates the behaviour of supercapacitor.

4 Dip-coated fabric electrode for supercapacitors

This chapter presents details of the experimental investigation into fabric supercapacitors fabricated by a dip-coating process. Details of the fabrication process include materials selection, fabric-based electrode dipping/curing process parameters and supercapacitor testing. The last two sections of the chapter present the results, analysis and conclusions.

4.1 Design motivation

The objective of this work is to demonstrate flexible fabric-based electrical double-layer supercapacitors constructed using low-cost conductive carbon fabric electrodes and to examine the performance versus the mass percentages of carbon content. The fabric electrodes presented here use a dipping technique employing commercially available general purpose low-cost activated carbon powders and woven fabrics that are commonly used in clothing applications.

4.2 Material selection

Fabric-based supercapacitors are typically constructed using two pieces of conductive fabric and a paper charge separator layer that contains an aqueous electrolyte. The fabric substrate used in this project are two different woven poly-cotton fabrics with different density; the thickness of these fabric substrates are about 300 µm and 150 µm. Poly-cotton fabrics combine the advantageous properties of cotton and polyester and it is the most popular material in the clothing industry. It also exhibits high absorbance of solutions due to its porosity, which is considered an advantage for printing and dyeing in the fabric industry.

In a capacitive device the physical distance between electrodes should be very small to achieve high capacity. In a supercapacitor, in order to prevent the top and bottom electrodes making contact with each other and short circuiting, it is necessary to use a separator between them. GF/F microfibre filter paper from VWR International was used as the separator and electrolyte holder in this work [84]. This filter paper is very dense. The SEM pictures of the thicker woven poly-cotton fabric used and the separator papers are shown in figure 4.1.

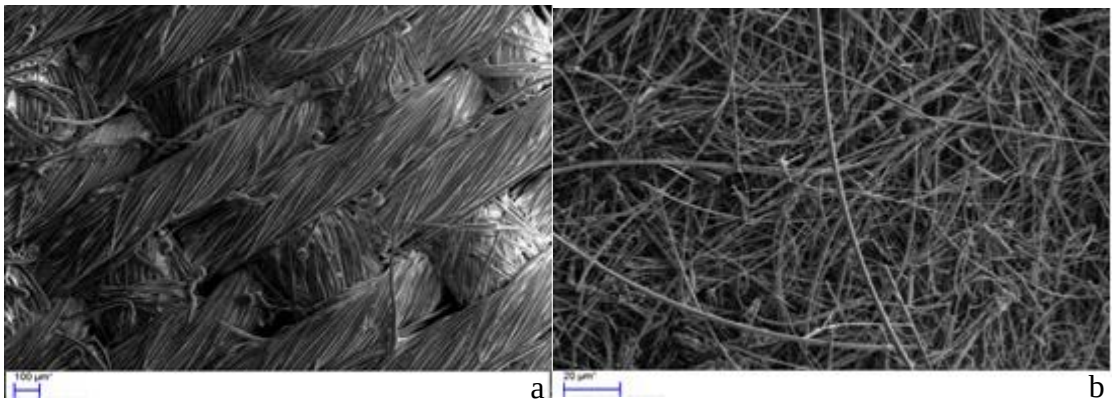

Figure 4.1: (a) SEM views of woven fabric, (b) GF/F separator paper

The electrolyte solution used throughout this chapter was 1M lithium sulphate (Li_2SO_4) solution. This solution has excellent molar conductivity and has many free ions that can form a diffusion layer in an EDLC. Theoretically, a highly concentrated acidic or alkaline solution can provide even more free ions and higher conductivity, but these may be damaging to the fibre and filter paper, resulting in the removal of carbon from the fabric which could potentially cause a short circuit between the top and bottom electrodes.

4.3 Carbon solution preparation

The carbon solution developed in this project contains two types of carbon powder. The first is activated porous carbon which is used to provide a large conductive surface area. The second is carbon black, which has a very small diameter in comparison with activated carbon and is used to fill up the gaps between each activated carbon particle and thereby improve the conductivity of the fabric electrode, reducing power loss. Detailed information of each carbon material is as follows:

The activated carbon powder is SX ULTRA which is processed from peat and supplied by Cabot Norit. It has a mean particle size of 100 µm (D90) with wide particle diameter range from 5 µm to 100 µm and an effective surface area of 1200 $m^2.g^{-1}$ [85]. According to equation 2.2, an electrode made using this powder should achieve a theoretical maximum specific double-layer capacitance of 45 $F.g^{-1}$ for the supercapacitor.

The carbon black powder is Shawinigan Black, also named acetylene black, which is a nano-scaled carbon particle. It has a mean particle size of 42 nm in diameter and an effective surface area of 75 $m^2.g^{-1}$ [86]. It has very low surface area and particle size in comparison with

activated carbon powder like SX ULTRA, so the double-layer capacitance provided by Shawinigan Black powder is neglected.

Generally carbon powders can only bond with a fabric mechanically, which means it is easily removed from the fabric. In order to create a permanently conductive carbon-coated fabric, a polymer binder is required to provide adhesion between carbon particles and the yarns of the fabric. The carbon powder is mixed with a liquid polymer binder, and mixed to form the ink. The polymer needs various properties to be suitable for use as a binder. Firstly, this polymer needs to have good adhesion to porous materials like carbon particles and fibres of cotton and polyester. Secondly, the polymer has to be impermeable and unreactive to water and aqueous electrolyte materials to prevent pseudo-capacitance occurring or carbon being removed from the electrode. Thirdly, these binders have to be soluble in appropriate solvents to provide a mixture with low viscosity solution. Finally, its adhesive property must remain even after all of the solvent has evaporated during the curing process.

In this work polystyrene (PS) was used as the binder [87]. PS is a transparent and colourless thermoplastic resin. It can be used in both solvent-solution or aqueous emulsion suspension forms for adhesive applications. It adheres well to porous materials, has good electrical insulating properties, and good water and chemical resistance [88].

In order to properly mix the carbon material and binder, the polymer binder has to be suitable to be mixed into a low viscosity solution. This is achieved by diluting the binder polymer using an appropriate solvent. The solvent will then assist the binder polymer in bonding the carbon particles and fabric once it has been dipped into the carbon solution. Finally, after curing the sample, all of the solvent is evaporated and the carbon/binder remains as a uniform coating on the fabric.

The solvent for the PS binder needs several specific properties. First, the solvent must be able to mix with the polymer without degrading the adhesive properties of the polymer at a high percentage of solvent/polymer solution. Second, the solvent needs to have a high evaporation rate at low temperature, which is necessary because a slow curing solvent would cause the carbon/binder compound in the fabric to slowly shrink and agglomerate, degrading the uniformity of the carbon fabric and its electrochemical performance. In this project ethyl acetate was used as solvent for the carbon solution.

Ethyl acetate (ethyl ethanoate) is a highly volatile, flammable, colourless liquid commonly used as a solvent in glues and in nail polish removers. The ethyl acetate used has a purity of 99.9% and was bought from Sigma Aldrich [89]. This solvent was applied to soften and dilute the PS binder.

The carbon powder used in this work was mixed with the PS dissolved by the ethyl acetate solvent. The carbon solution consisted of 100 mg of carbon powder (90 mg SXU powder and 10 mg Shawinigan Black powder) and with various weight percentages (5%-20%) of binder. Then the solution container was placed in the Hauschild engineering speed mixer for one minute with a rotating speed of 300 rpm; this process was repeated 10 times. Finally the solution container was put into a sonicator bath for 20 minutes. The sonication process ensures that the carbon black particles are dispersed uniformly in the solution and surround the larger, activated particles. This process will produce a low-viscosity smooth carbon solution ready for the dipping process.

4.4 Fabric dipping and curing process

Dip coating was conducted in a fume cabinet at room temperature. The polyester-cotton fabric samples were dipped into the carbon solution; a magnetic stirrer then mixed the solution and samples for 10 minutes. The samples, shown in figure 4.2, were removed from the solution and dried in the fume cabinet before being cured in a fan oven at 60^{o}C for 20 minutes.

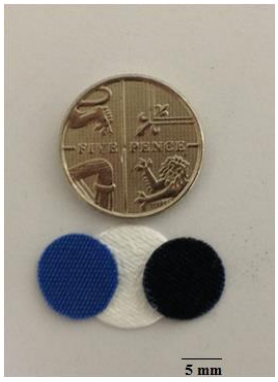

Figure 4.2: Original blue fabric substrate, paper separator and black carbon fabric electrode

The next process was to clean the surface of the cured fabric electrode. This step is essential since extra carbon will prevent the electrolyte from forming a good contact with the carbon particles bonded in the fabric yarns. This process was performed by putting the electrode into the sonicator with DI water for a few seconds until the fabric sank to the bottom of the DI water. Finally, the electrode was dried at room temperature until all of the water evaporated from the

fabric electrode. Generally, the area of each poly-cotton fabric sample is 0.785 cm^2, the weight of each piece of thick fabric electrode is 27.1 $mg.cm^{-2}$ and the weight of each piece of thin fabric electrode is 12.5 $mg.cm^{-2}$ before coating. The ability of the polyester cotton fabrics to absorb the various carbon solutions of each type of electrode according to equation 2.4 are summarised in table 4.1.

Table 4.1: Dip-coated fabric electrode.

Electrode type	Binder percentage (%)	Carbon:Fabric ratio (%wt)	Total carbon loading per electrode ($mg.cm^{-2}$)
A	5	17.3	2.99
B	10	19.2	3.32
C	15	23.5	4.05
C (thin)	15	82.4	6.41
C (20%CB)	15	23.6	4.08
D	20	34.7	5.98

Table 4.1 shows that the amount of active material loaded into the fabric increases as the binder percentage in the carbon solution increases. Six electrode types - A, B, C, C (thin), C (CB) and D - have been processed for this investigation. Type C(thin) electrode samples were made with the thin (thickness of 150 µm) poly-cotton fabrics and the same carbon solution and fabrication process of type C electrode samples. Type C (20% CB) electrode samples were made with the same fabrics for other types of electrode samples (types A to D) and the carbon solution for type C electrode samples but with more carbon black (20% of carbon black instead of 10%). In addition, type C, C(thin) and C (20%CB) electrode samples were also used to test a vacuum impregnation process after curing.

The SEM pictures of the carbon fabric samples shown in figure 4.3 are achieved with an EVO ZEISS scanning electron microscope (SEM). The electron beam voltage is 15 kV. The

electrode has also been cut to enable the cross section to be examined, as is shown in figure 4.4.

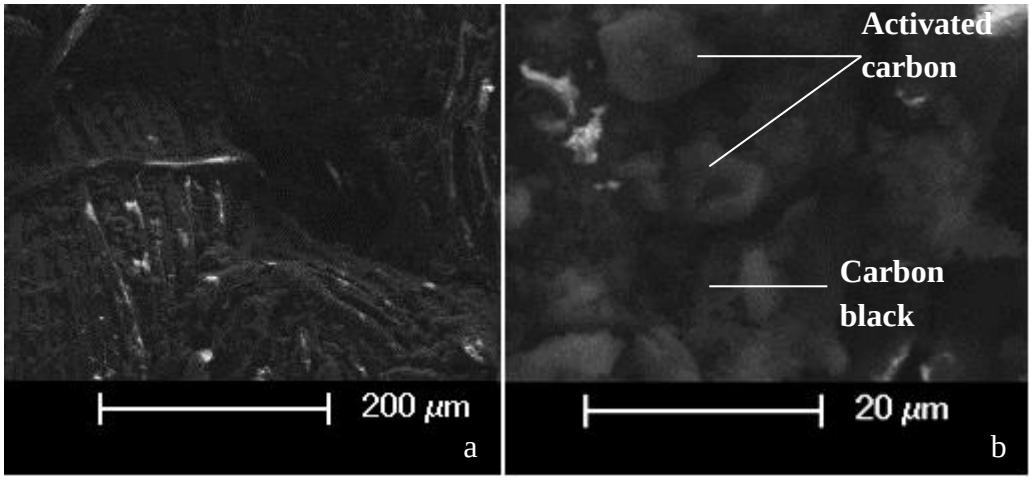

Figure 4.3: (a) SEM micrograph of carbon fabric electrode made with PS binder and both activated carbon and carbon black powders, (b) Higher magnification SEM micrograph of the carbon fabric electrode

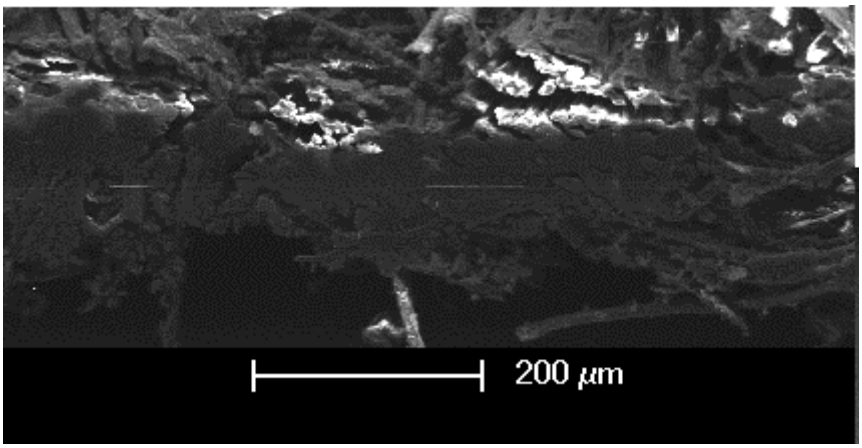

Figure 4.4: Cross-sectional view of sample made with PS binder and both activated carbon and carbon black powders

Figure 4.3 (a) is the SEM view of a fabric electrode. The darker patches on the fibre are the carbon compounds. By increasing the magnification, as shown in figure 4.3 (b) the two types of carbon (activated carbon and carbon black) are visible on the fibre. The larger particles are activated carbon particles and the smaller particles are carbon black particles. In figure 4.4 the carbon particles have penetrated through the full thickness of the fabric. Excessive carbon loading on the fabric may condense to a point that the electrode is blocked from making full contact with the electrolyte from making full contact with the carbon particles in the fabric

electrode. This would reduce the effective surface area of the carbon and prevent the fabric from reaching its full potential for storing energy.

4.5 Post treatment of fabric electrode

4.5.1 Vacuum impregnation process

Vacuum impregnation, also known as porosity sealing, is a method of replacing the air in the voids within a porous substrate with the active material. The vacuum impregnation process of fabric electrodes shown in figure 4.5 involves placing the electrode sample in a Büchi tube with the electrolyte solution 1M Li_2SO_4. The tube is then connected to a vacuum pump and air is extracted for 20 minutes leaving a vacuum of 20 mbar until no gas bubbles can be seen in the electrolyte solution. This was done to improve the distribution of the electrolyte around the carbon particles in the fabric electrodes. A magnetic stirring bar is placed in the solution and continuously stirs the electrolyte at a low rotational speed which can speed up the gas bubbles removal process and accelerate the vacuum impregnation. In this chapter, standard type C electrodes are referred to as C1 and vacuum-impregnated electrodes are denoted C2.

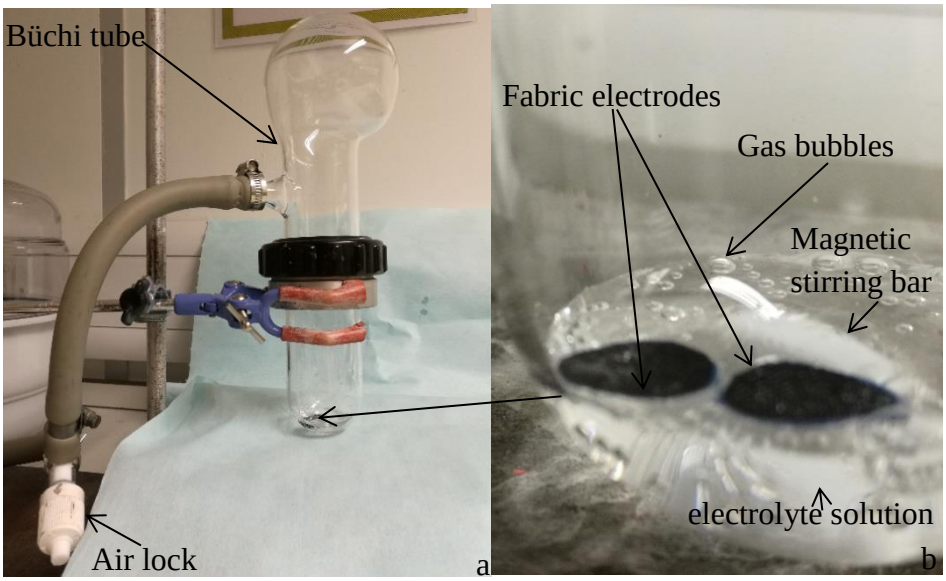

Figure 4.5: (a) Vacuum impregnation process set-up and (b) Gas bubble removal process from the fabric electrode

4.5.2 Mandrel test

The mechanical durability of the fabric supercapacitors was also investigated by the cyclical bending of type C electrode samples around a mandrel. The samples were bent around the mandrel 200 times with a radius of curvature of 1.59 mm. The electrodes were then assembled into a supercapacitor and the electrolyte was added using vacuum impregnation.

4.6 Supercapacitor test cell

The assembled supercapacitor device shown in figure 4.6 consist of two pieces of dip coated fabric electrode sandwich a separator paper, the device must be compressed to reduce the thickness of the fabric electrode and dielectric layer. This is achieved by placing the electrode and separator assembly in a PFA Tube Fitting from Swagelok. A PFA Tube Fitting is a set of thimbles made from chemically resistant plastics; this is combined with three pieces of steel rod which act as current collectors, and a spring to apply force to reduce the thickness of the fabric supercapacitor.

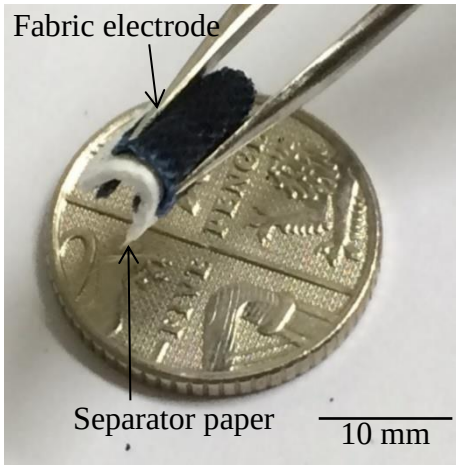

Figure 4.6: Wearable carbon fabric electrodes and white separator paper

Two of the steel rods are used as current collectors for the fabric electrodes. The four pieces of steel are used as a cap and are used with a spring to compress the supercapacitor. The components for the assembly of the supercapacitor in the test cell fitting are shown in figure 4.8 and a cross-sectional diagram of the fabric-based supercapacitor in the tube fittings can be seen in figure 4.7.

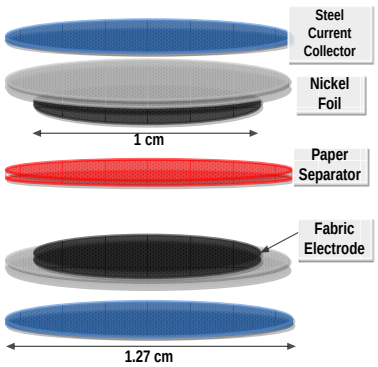

Figure 4.7: Cross-sectional diagram of a fabric-based supercapacitor

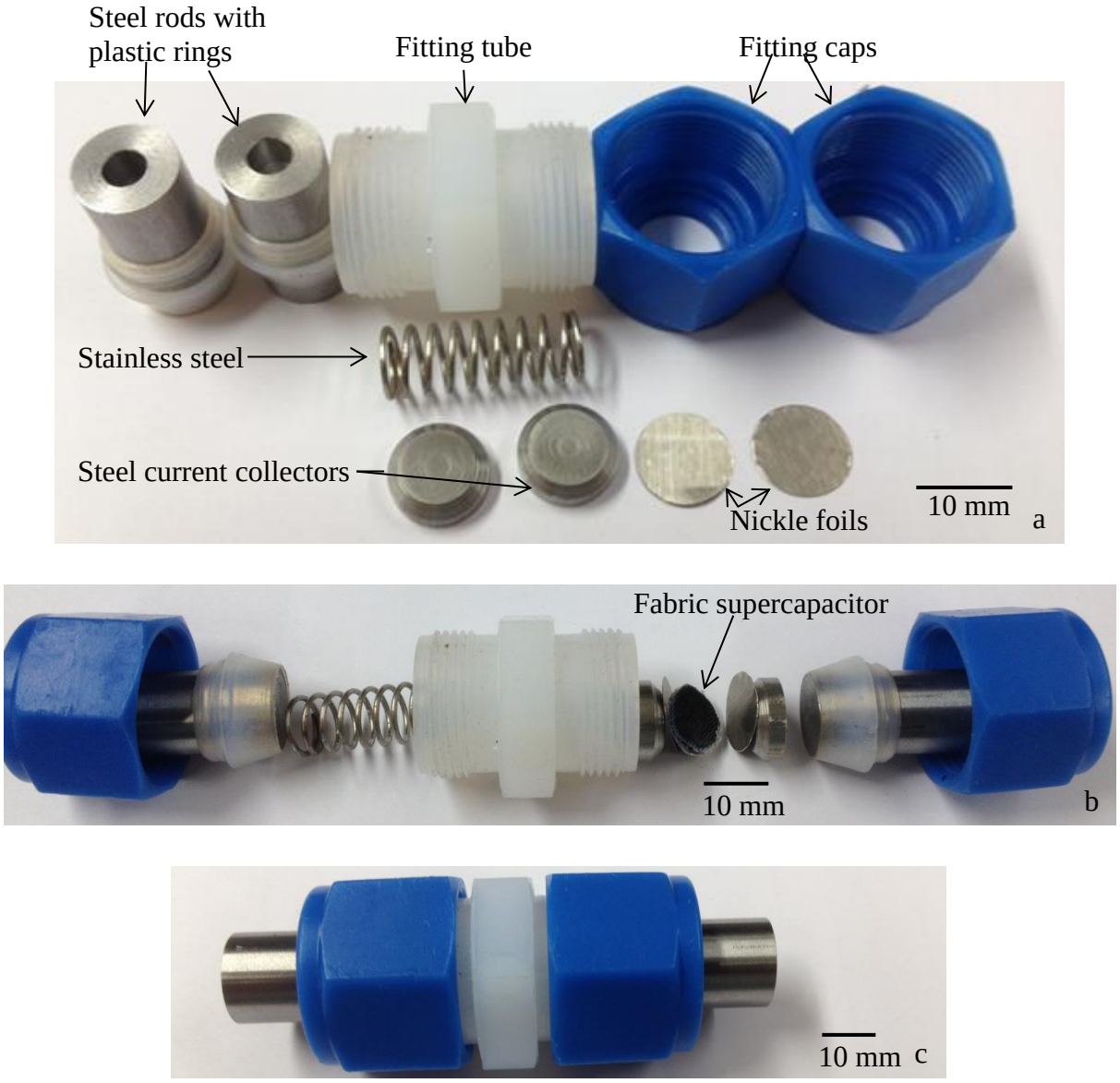

Figure 4.8: Supercapacitor assembly. (a) PFA tube fittings with steel rods, stainless steel spring, steel current collector and nickel foil, (b) Test tube fitting and fabric supercapacitor before closing the top and bottom fitting caps and (c) Complete test tube fitting

The type of current collector material will affect the performance of the electrochemical device. This is because, in an aqueous electrolyte-based device at a high applied voltage, the electrolysis of water produces H^+ ions at its anode and OH^- at its cathode [90]. The accumulation of these ions can cause the formation of a layer of oxide material between the surface of the current collector and the electrode, which will prevent further corrosion of the current collector material. This process is known as passivation. In the case of a steel current collector, the passivation of iron in water will cause a layer of iron oxide to form on its surface.

Iron oxide is a pseudo-capacitive material that will provide a large amount of temporary capacitance. If the polarity of the applied high voltage is reversed, some of the iron oxide will be reduced back to iron and conductivity will be restored. This process, called metal passivation, creates an oxide layer in a manner that depends on the scan rate during testing, device design, material and temperature. As a result of this process, the capacitance of a metallic electrode encapsulated supercapacitor will be unpredictable (see appendix A for metal passivation test examples and see appendix B for the supercapacitor test with different encapsulation materials). Therefore, a piece of nickel foil is placed between the fabric electrode and the steel collector to prevent the metal passivation between the steel collector and the electrolyte.

4.7 Analysis of results

Several methods were used to characterise the fabric-based supercapacitors using a VMP2 potentiostat/galvanostat (Biologic, France). First, the devices were tested using EIS method. EIS was performed at frequencies from 200 kHz to 20 mHz. At the open circuit condition, the peak-to-peak amplitude of the signal was 20 mV. The stability of the supercapacitor was CV method. CV results were collected at scan rates of 25, 50, 100, 150 and 200 $mV.s^{-1}$ and at voltages between + 0.8 V and -0.8 V, Finally, galvanostatic cycling (GC) was used to test the capacity, resistance and stability of the fabric supercapacitors. In the GC test the devices were cycled between 0 V and 0.8 V with a current of 0.1 A per unit gram of carbon material on the fabric electrode. In the supercapacitor with aqueous electrolyte, the typical voltage to cause water electrolysis is 1.23 V, the maximum test voltage was set to be about 66% of this value (0.8 V).

The cycling stability of supercapacitor was tested by CV method at scan rate of 200 $mV.s^{-1}$ for 15000 cycles. When apply supercapacitor in healthcare device on e-textile, assume the healthcare device requires fully charge-discharge the associate supercapacitor for 10 times per day, the whole system need to be have a lifetime for at least 3 years. It requires the supercapacitor stable (no obvious capacity lost) for more than 10950 cycles, therefore the rest cycles for the device was set at 15000 cycles.

The mechanical durability of the fabric supercapacitors was also investigated. The fabric electrodes (type C) were bent around the mandrel 100 times with a radius of curvature of 1.59 mm. The bending test number was justified by the number of accidental bending before encapsulates the fabric electrodes into the test cell, in this test this number was assumed to be 100 times. After assemble the fabric electrodes into supercapacitor and seal it in its

encapsulation design, the device's electrochemical performance is not strongly affected by bending.

The electrodes were then assembled into a supercapacitor and the electrolyte was added using vacuum impregnation. This section presents an evaluation of the performance of various fabric electrodes with different binder percentage. The different types of activated carbon used and binder material were evaluated and the results are presented in appendix C. The amount of carbon material that adheres to the fabric increases as the percentage of polymer binder increases. The specific capacitance, area capacitance, normalised and area ESR of the fabric supercapacitors with different amounts of carbon material are shown in Tables 4.2, 4.3, 4.5 and 4.6.

In the CV test, the specific capacitance of the supercapacitors was calculated via equations 3.9 and 3.5 with the ratio of the maximum current to the scan rate at 25 $mV.s^{-1}$. In the EIS test, the capacitance and ESR of the supercapacitor are determined from the bode plots extracted from the average of five repeated EIS test results based on equations 3.5 and 3.19 at 20 mHz. In the GC test, the capacitance of the supercapacitor was obtained via equations 3.9 and 3.5 with the ratio of the cycling current and the voltage discharge rate of the supercapacitor. The ESR of the proposed supercapacitors was calculated by equation 3.17 and the IR drop voltage and test current.

Table 4.2: Specific capacitance ($F.g^{-1}$) obtained by three methods.

Electrode information			Specific capacitance		
Electrode type	Vacuum treatment	Carbon:Fabric ratio(%wt)	CV (25 $mV.s^{-1}$)	GC (0.1 $A.g^{-1}$)	EIS (20 mHz)
A	No	17.3	9.24	9.29	9.23
B	No	19.2	9.33	9.36	9.28
C1	No	23.5	10.8	11.2	10.2
C2	Yes	23.5	14.3	14.1	10.3
C(20% CB)	Yes	23.6	10.4	9.01	7.8
C (thin)	Yes	82.4	9.64	10.4	7.36
D	No	34.7	5.71	7.23	5.69

Table 4.3: Area capacitance ($F.cm^{-2}$) obtained by three methods.

Electrode information			Area capacitance ($F.cm^{-2}$)			
Electrode type	Vacuum treatment	Carbon:Fabric ratio(%wt)	CV (25 $mV.s^{-1}$)	GC (0.1 $A.g^{-1}$)	EIS (20 mHz)	Theoretical maximum
A	No	17.3	0.043	0.047	0.043	0.539
B	No	19.2	0.048	0.049	0.048	0.623
C1	No	23.5	0.082	0.087	0.078	0.878
C2	Yes	23.5	0.126	0.125	0.079	0.878
C(20% CB)	Yes	23.6	0.099	0.086	0.080	0.780
C2(thin)	Yes	82.4	0.157	0.170	0.120	2.52
D	No	34.7	0.053	0.068	0.053	1.07

According to tables 4.2 and 4.3, the supercapacitor maximum specific capacitance measured using all three techniques was obtained from the supercapacitor with C2 electrodes (14.1 $F.g^{-1}$, 0.125 $F.cm^{-2}$) which have 22.1% carbon content by weight, in comparison with the results achieved by the supercapacitor with C1 electrodes (11.2 $F.g^{-1}$, 0.087 $F.cm^{-2}$). This shows that the vacuum impregnation technique did increase both specific and area capacitance of the fabric supercapacitor.

From Tables 4.2 and 4.3, it was found that the supercapacitor made with the fabric electrodes with additional carbon black C (20% CB) achieved lower specific and area capacitance (9.01 $F.g^{-1}$, 0.086 $F.cm^{-2}$) than the supercapacitor with C2 electrodes (14.1 $F.g^{-1}$, 0.125 $F.cm^{-2}$). It shows carbon black powder cannot provide high double layer capacitance than activated carbon powder due to its relative smaller surface area.

Tables 4.2 and 4.3 also show that the maximum area capacitance measured using all three techniques was obtained from supercapacitor using electrodes type C (thin) (0.17 $F.cm^{-2}$) which have 82.4% carbon content by weight. it shows the thin poly-cotton fabric electrode has high porosity and is able to retain a large percentage of carbon within the yarn's structure; however, the specific capacitance of the supercapacitor made with the C(thin) electrode was lower than that made with the C2 electrode. This indicated that there was too much carbon material in the C(thin) electrode which was blocking the carbon particle from making contact with the electrolyte.

The capacitance bode plots from the EIS test are shown in figure 4.9. From these results it can be seen that the capacitance increases with increasing carbon content up to the type C electrodes. The supercapacitors fabricated with type D electrodes, however, demonstrate the lowest specific capacitance values. This indicates that there is an optimum carbon percentage and that increasing carbon content beyond this actually reduces performance.

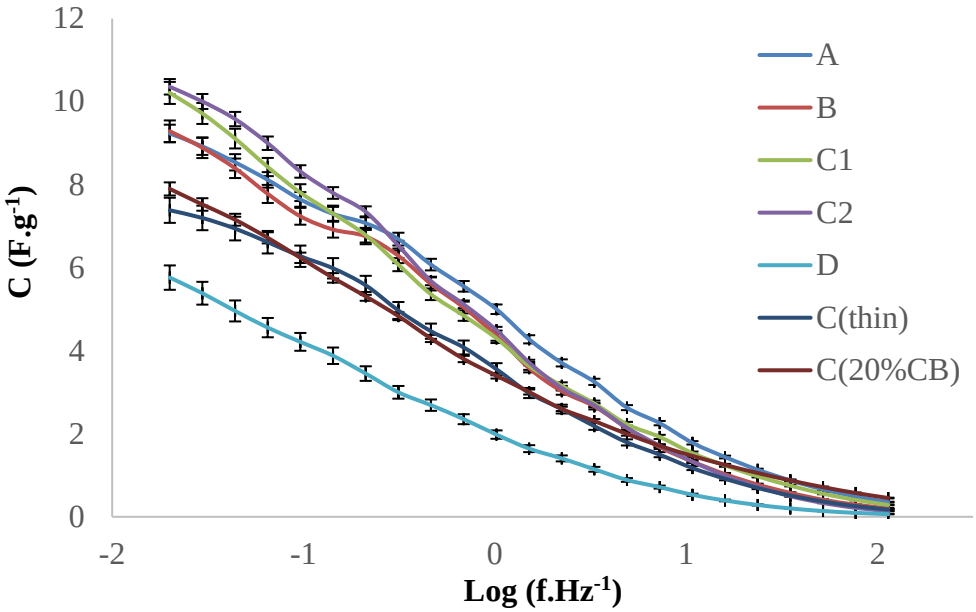

Figure 4.9: Specific capacitance of the device types A, B, C1, C2, C(thin), C(20%CB) and D from 20mHz to 112 Hz, The error bars represent the standard deviations that were calculated based on the results from 5 repeated tests

In figure 4.9, the specific capacitances of the supercapacitors using the seven different types of electrode were calculated by equations 3.19 and 3.5 from 20 mHz to 112 Hz. The supercapacitor using the type C2 electrodes achieves a higher specific capacitance than all other types at frequency below 0.5 Hz . Above 0.5 Hz, the type A electrodes achieve highest specific capacitance. From table 4.2 the specific capacitances of four types of supercapacitor were at least three times smaller than their theoretical maximum value (45 $F.g^{-1}$). Table 4.3 suggests the practical area capacitances of the supercapacitor using different dip-coated carbon fabric electrodes were about four times lower than their theoretical maximum area capacitance. It is because most of the carbon particles were not in contact with the electrolyte to form the electrical double-layer structure. The large size particles physically block the electrolyte from making contact with the other carbon particles located deeper within the fabrics. From figure 4.9, table 4.2 and 4.3 the supercapacitor made by the C(20%CB) electrode achieved lower capacitance than the result of the C2 electrode; this is because in comparison with activated carbon, carbon black has a smaller surface area. The capacitance of the electrode will be reduced if the amount of carbon black is increased. In figure 4.9 the uncertainty (error) of the EIS test results is very small (less than 5%), it is due to periodic test signal with small voltage amplitude and the fitting tube can isolate the device from the outside. The possible source of uncertainties (errors) are come from the test bench sensitivity, experiment condition and electrolyte/electrode wettability issue at different test frequency.

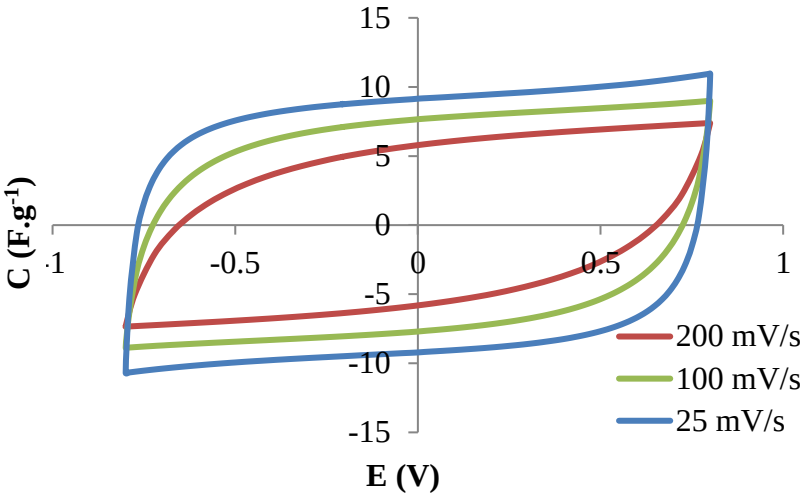

Figure 4.10: CV test of the device C1 type between +/- 0.8 V at the scan rate of 200, 100, 25 $mV.s^{-1}$.

The CV curves shown in figure 4.10 indicate that the supercapacitor demonstrates capacitive behaviour and is electrochemically stable at scan rates from 25 to 200 $mV.s^{-1}$. For the scan rate of 200 $mV.s^{-1}$, the CV curves show the supercapacitor becoming more resistive. From table 4.4 the specific capacitance varies from 7.15 $F.g^{-1}$ to 10.8 $F.g^{-1}$ according to the ratio of the maximum current to the scan rate.

Table 4. 4: CV, results for specific capacitance ($F.g^{-1}$) of the supercapacitors for types A, B and C at different scan rates.

Electrode information		CV scan rate (mV.s-1)					
Electrode type (binder percentage)	Carbon :Fabric ratio(%wt)	25	50	75	100	150	200
A	17.3	9.23	9.12	8.85	8.83	8.69	8.37
B	19.2	9.33	8.32	8.01	7.82	7.48	7.02
C1	23.5	10.8	10.1	9.53	8.96	7.81	7.15
C2	23.5	14.3	13.4	12.6	11.9	10.4	9.48
D	34.7	5.71	5.36	5.03	4.78	4.40	4.13

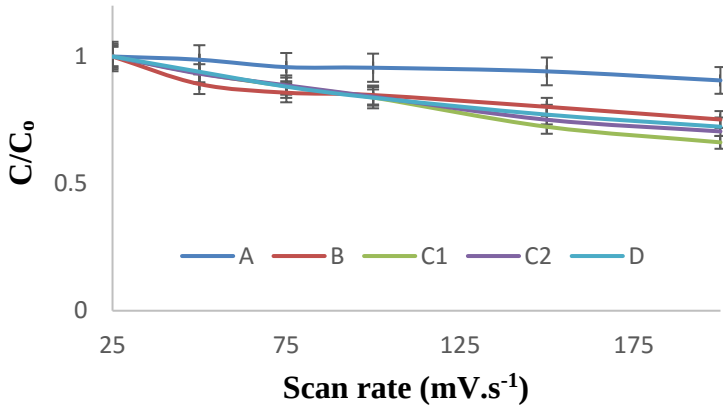

Figure 4.11: Capacitance variation of supercapacitor made from three different types of electrode at different scan rates. The error bars represent the standard deviations that were calculated based on the results from 5 repeated tests

From figure 4.11 and table 4.4, the specific capacitance of the type C1 supercapacitor tested at 25 $mV.s^{-1}$ drops from 10.8 $F.g^{-1}$ to 7.15 $F.g^{-1}$ at 200 $mV.s^{-1}$, which is about a 33% decrease in capacitance. The device using fabric electrodes C2 demonstrated lower capacitance decrease for about 30% for type B between 25 to 200 $mV.s^{-1}$. In compassion with the result with type C1 device, the result from type C2 device did indicated the vacuum impregnation did let electrolyte get in contact with the majority of carbon particles and improves the wettability issue of the active material in the fabrics. In figure 4.11 the possible source of uncertainties (errors) are come from the test bench sensitivity, experiment condition, electrolyte/electrode wettability issue at different scan rate.

The supercapacitor assembled using fabric electrodes with lower percentages of carbon material (types A and B) show a smaller drop in specific capacitance at higher scan rate (about 9.4% for type A and 24% for type B between 25 to 200 $mV.s^{-1}$). This is due to the wettability of the active material in the fabrics. When the supercapacitor contains less carbon material, the electrolyte will make contact with a greater percentage of the carbon surface area at the high scanning rate.

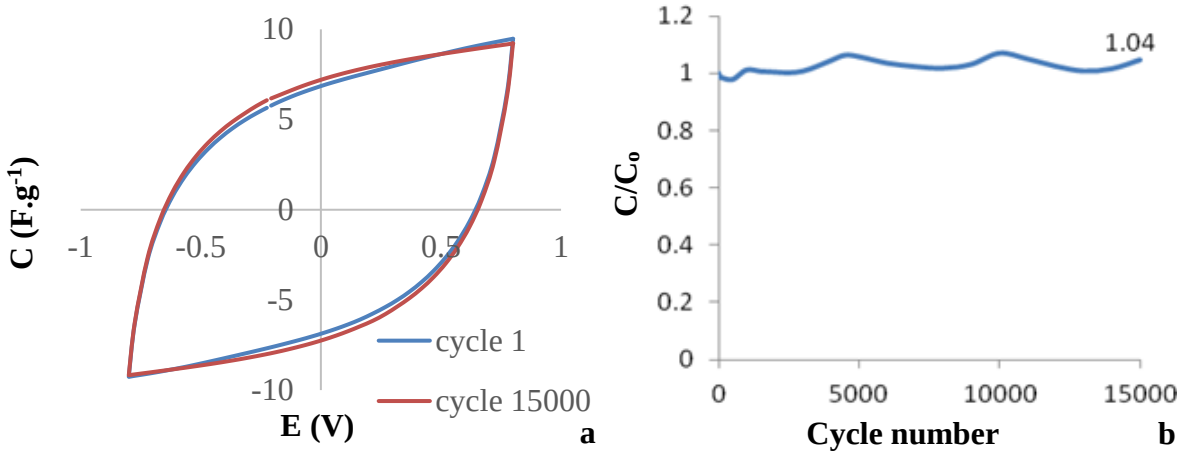

Figure 4.12: (a) CV test of the supercapacitor (electrode type C2) for 1 cycle and 15000 cycles between +/- 0.8 V at a scan rate of 200 $mV.s^{-1}$. (b) CV stability test of the supercapacitor (electrode type C2) for 15000 cycles over 66 hours.

Figure 4.12 (a) shows the CV plots for the 1st and 15000th cycles of the type C2 supercapacitor. The shape and value of the supercapacitor current density shows negligible change after 15000 cycles in comparison with its original CV curve. It indicates that the tested cells were electrochemically stable and the capacitance was not varying significantly. According to figure 4.12 (b), the overall capacitance variation is less than 5% during 15000 cycles of cycling test. The capacitance variation shown in figure 4.12 (a) and (b) is correlated to small temperature changes in the laboratory over the 66-hour test period which caused a variation in ESR which affects the capacitance measurement. This demonstrates an excellent level of adhesion of carbon material to the fabric substrate, which forms a continuous and stable conducting network.

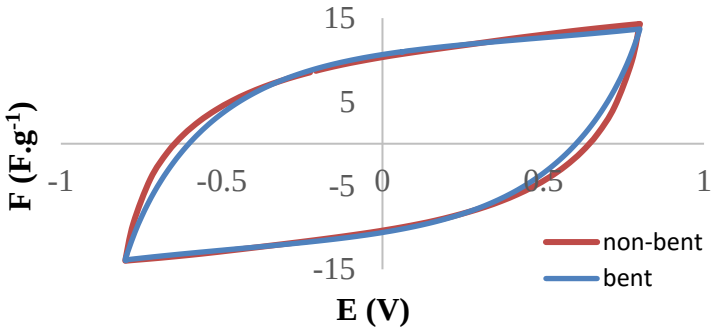

Figure 4.13: CV test of the supercapacitor (electrode type C2) with and without bending test between +/- 0.8 V at the scan rate of 200 $mV.s^{-1}$.

Figure 4.13 shows the CV plots obtained from supercapacitors fabricated with type C2 fabric electrodes (bent and non-bent). The shape and values of the supercapacitor current density plot

of the bent sample shows a small difference in comparison with the non-bent CV curve. This indicates that the electrochemical performance of C2 electrodes was not strongly affected by repeated bending.

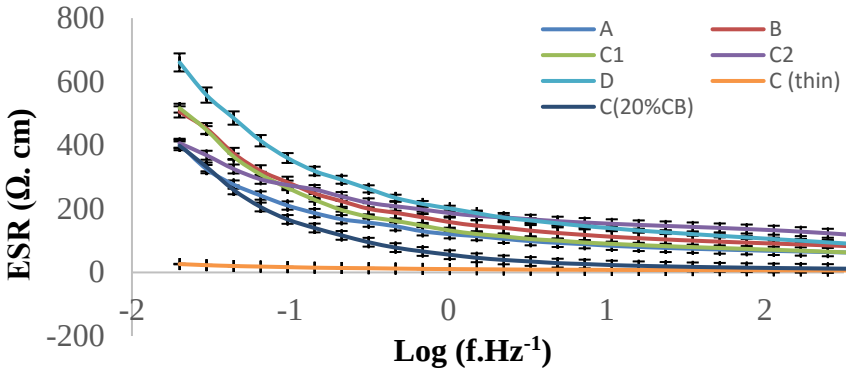

Figure 4.14: Bode plot of the normalised supercapacitor devices ESR (Ω.cm) from 20 mHz to 112 Hz, extracted from EIS test. The error bars represent the standard deviations that were calculated based on the results from 5 repeated tests

Table 4.5: Normalised ESR (Ω.cm) of the device types A, B and C at different scan rates.

Electrode information		Frequency /Log ($f.Hz^{-1}$)					
Electrode type	Carbon : Fabric ratio(%wt)	1.7 (20m Hz)	-0.67 (0.21 Hz)	0.35 (2.2 Hz)	1.37 (23 Hz)	1.72 (52 Hz)	2.05 (112 Hz)
A	17.3	404	167	106	77.2	72.1	67.8
B	19.2	505	224	140	103	96.8	90.8
C1	23.5	516	196	114	82.6	76.8	71.2
C2	23.5	406	239	172	146	140	132
C (20%CB)	23.6	398	116	39.3	19.0	16.1	14.0
C (thin)	82.4	26.3	13.9	9.43	7.58	7.18	6.78
D	34. 7	660	291	172	126	115	105

The normalised ESR results are shown in table 4.5 and figure 4.14 with the impedance result expressed according to the circuit model shown in figure 3.12. The high frequency ESR indicates a total resistance due to the electrolyte and electrode materials. At the lowest frequency, ESR will be increased significantly due to diffusion resistance. According to figure 4.15 the supercapacitors with thinner fabric electrode type C(thin) demonstrated lower normalised ESR than the other supercapacitors with electrode types. This could be because the carbon/polymer compounds fully penetrated the fabric substrate to form a much better conductive network that reduced the ESR of the device. According to table 4.5 and figure 4.15, the normalised ESR of the supercapacitor with C (20%CB) is lower than the other group of results based on the same fabrics. This shows that the additional conductive additive (carbon black) did fill the gap between the activated particles to forms a conductive network to reduce the device ESR.

Table 4.6: Normalised ESR (Ω.cm) and area ESR (Ω.cm^{-2})

Electrode information		ESR (Ω.cm-2)		ESR (Ω.cm)	
Electrode type	Carbon :Fabric ratio (%wt)	GC (0.1 A.g^{-1})	EIS (20 mHz)	GC (0.1 A.g^{-1})	EIS (20 mHz)
A	17.3	18.2	39.6	18.5	404
B	19.2	17.3	54.2	17.7	505
C1	23.5	15.8	50.4	16.1	516
C2	23.5	21.6	39.6	22	406
C(20% CB)	23.6	12.9	24.8	20.7	398
C (thin)	82.4	10.3	35.7	6.7	26.3
D	34. 7	19.1	64.6	20.6	660

Table 4.6 shows the ESR normalised to carbon mass; i.e., the value given is the product of the ESR and the carbon mass. Whilst adding more carbon actually lowers the normalised ESR (Ω.cm), the fact that the area ESR (Ω.cm^{-2}) has increased indicates a diminishing benefit, which is most notable for type D fabric electrodes. The normalised ESR (Ω.cm) becomes an important consideration when optimising the supercapacitor, comparing it with others from the literature and when considering scaling the design (altering the area and thickness). According to table 4.6 the ESR (Ω.cm^{-2} and Ω.cm) of the supercapacitor made with C (20% CB) obtained by both GC and EIS methods are lower than type C2 devices, it indicates that additional carbon black in the fabric electrodes does reduce the device resistance and it will also reduce its specific capacitance since - in comparison with activated carbon - carbon black does not have a high enough surface area to form the double-layer capacitance. The type C(thin) device demonstrated the lowest ESR (Ω.cm^{-2} and Ω.cm) values; this is because these electrodes are made with thinner fabric substrate and very high carbon mass loading. The value of ESR obtained from the EIS test is significantly larger than that obtained from the GC test, which is due to the test current used in GC being very small (~0.5 mA) in order to obtain the least biased

device capacitance. Table 4.6 also shows that the vacuum impanation process improves both normalised and area ESRs of the supercapacitor based on the type C electrode. This is because, during the vacuum impregnation process, when air bubbles are removed from the fabric electrodes, the bubbles will move the carbon powders to stick on the fabric yarns and reduce the ESR of the fabric electrode.

Table 4.7: Specific energy density ($Wh.kg^{-1}$) and power density ($kW.kg^{-1}$) determined by GC test ($0.1\ A.g^{-1}$).

Electrode information		Energy and power density	
Electrode type	Carbon :Fabric ratio(%wt)	Energy density ($Wh.kg^{-1}$)	Power density ($kW.kg^{-1}$)
A	13.6	10.7	2.38
B	15.1	10.8	2.25
C1	18.5	13.1	2.02
C2	18.5	16.4	1.48
C(20% CB)	18.6	10.7	1.46
C (thin)	64.7	11.9	2.16
D	27.3	8.32	1.13

From table 4.7, the normalised energy density according to equation 3.7 is proportional to the amount of carbon material that adhered to the fabrics, apart from the type D fabric electrode. The normalised power density according to equation 3.6 is based on the ESR of a supercapacitor from the GC test with a voltage range of 0.8 V. As shown in table 4.8, the supercapacitor with electrode type A achieves the highest normalised power density out of the non-vacuum impregnated electrodes (i.e. B, C1 and D). Table 4.8 also shows that the power density of the supercapacitor decreases with increasing carbon mass. This result reflects the increasing normalised ESR; i.e. the increasing carbon loading reduces the absolute ESR at a diminishing rate.

The supercapacitor using electrode type C(thin) contains the highest percentage of carbon materials in the fabric electrode with the third highest power density in comparison with other

electrodes (i.e. B, C1, C2 and D). This indicates that normalised power density of the supercapacitor is a trade-off between the conductive material weight and the normalised ESR achieved.

As shown in tables 4.2, 4.6 and 4.7, vacuum impregnation does increase the specific capacitance and energy density of the fabric-based supercapacitor by optimising the wettability between the electrode materials and the aqueous electrolyte. However, this process introduces extra device ESR and hence reduces its power density; this may be due to the fact that, during vacuum impregnation, some of the carbon material in the electrode will move as the air bubbles come out of the fabric electrodes.

Theoretically, the more carbon material that adheres to the fabric electrode the higher the measured supercapacitor ESR and the higher the capacitance. In order to demonstrate this theory, type D electrodes were prepared with a carbon solution containing 20% binder. As shown in table 4.6, the carbon: fabric ratio increases to 27.9% with device area ESR of 19.1 $\Omega.cm^{-2}$ obtained by GC test (0.1 $A.g^{-1}$) and 64.6 $\Omega.cm^{-2}$ from the EIS test at 20 kHz. According to table 4.2, the specific capacitance of this device is 7.23 $F.g^{-1}$ obtained from the GC test. These results were significantly worse than those using the other electrodes (A, B and C) because, as the percentage of binder in the carbon solution increases, the carbon powders are more likely to stack on top of each other, which introduces more resistance rather than capacitance to the fabric supercapacitor.

4.8 Conclusions

This chapter presents a flexible three-layer supercapacitor using a fabric substrate. The supercapacitor presented here achieves a specific capacitance of 14.1 $F.g^{-1}$ (table 4.2), area-specific capacitance of 0.125 $F.cm^{-2}$ (table 4.3), and a low normalised ESR of 22 Ω.cm (table 4.6), and achieves an excellent cycling stability over 15000 cycles (figure 4.12).

The use of the dipping technique with PS binder allows carbon powders (activated carbon and carbon black) to infiltrate the poly-cotton fabrics and fill up the fabric yarns to form a conductive network and double-layer structures. According to the bending test shown in figure 4.14 the dip coated carbon fabric electrode are resist to the mechanical stretching and bending. The weight of carbon materials in the fabrics can be roughly controlled by varying the percentage of binder used in the carbon solution. This variation will influence the electrochemical behaviour of the EDLC. However the supercapacitor made by dipping the electrode also has some disadvantages: first it is not an area-selective technique in that it is not

a printing process. Second, the results of the supercapacitor by dipping the electrode are much smaller than its theoretical maximum area capacitance and not as good as other devices demonstrated in the literature. The following chapters describe the development of a new technique to overcome these two shortages, and attempts to implement the supercapacitor in single piece of fabric substrate.

In comparison with the supercapacitor electrode implemented by Jost et al. [42], their device achieves bigger equivalent specific capacitance (20 $F.g^{-1}$), but the activated carbon (Kuraray Yp series) in their electrodes is far more expensive than the activated carbon (Norit SXU) used in this work (table 2.1). However, in comparison with traditional rigid supercapacitors, the electrodes and separator materials are potentially wearable and fully scalable. In contrast with other flexible supercapacitors that use expensive carbon materials like CNT or graphene, the use of commercial available activated carbon as electrode material significantly reduces the cost of the supercapacitor.

5 Spray-coated fabric electrodes for supercapacitor

This chapter presents the experimental fabrication of a supercapacitor with spray-coated fabric electrode. The fabrication process includes materials formulation, fabric-based electrode spraying/curing process, and device testing. The analysis and conclusions are presented at the end of the chapter.

5.1 Design motivation

Dipping is the most common method used in the dyeing industry. It is relatively easy to perform but provides no area selectivity. More importantly, this process offers little control over how much solution is absorbed into the substrate. As shown in figure 4.4, the cross section of the electrode after dipping is fully occupied by carbon particles, which could make the fabric electrode more brittle, as it adds extra carbon weight to the electrode and reduces its potential capacitance by blocking the electrolyte from reaching every activated carbon particle. A supercapacitor made with dip coated electrode cannot achieve a high specific capacitance since the carbon material fully fills up the volume of the fabric electrode.

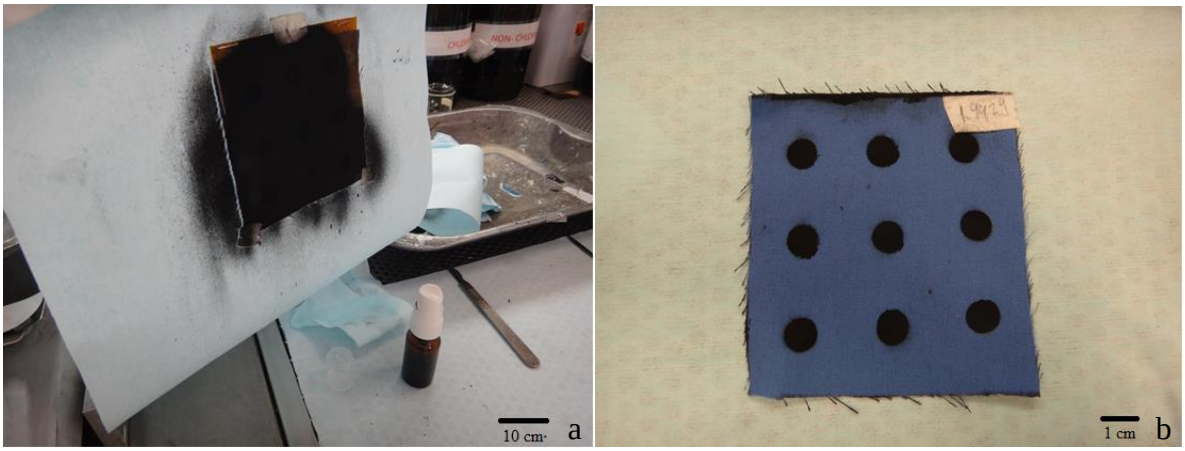

Figure 5.1: (a) Spray-printed electrode with polymer mask, (b)Spray-printed electrode.

One alternative fabrication method is spray coating. In spray coating, the carbon ink/solution is transformed into a vapour by the high pressure airflow and sprayed on to the surface of a fabric substrate as shown in figure 5.1 (a). It is possible to adjust the spray pressure and experiment set-up to let the carbon vapour penetrate the fabric substrate and adhere to the yarns uniformly. In spray coating, the amount of solution reaching the surface of the fabric substrate can be controlled by the diameter of the spray nozzle, spray pressure, the duration of spray coating and the distance of spray coating. As shown in figure 5.1 (b), spray coating can also be used to selectively coat the fabric area by using a mask or stencil to select specific areas.

5.2 Material formulation

As previously highlighted, the carbon solution is required to adhere well to the fabric, but excessive carbon can block electrolyte flow into the electrode. Beyond a certain point, more carbon powders being absorbed into the fabric results in less capacitance. The activated carbon powder used in the previous chapter has a large mean particle size (D90) of 100 µm, which can prevent the electrolyte making contact with the carbon particles to form the EDL. In the spray-coating process, powder that has a large particle size is highly likely to block the nozzle of the spray gun and terminate the coating process. Therefore, it is beneficial to find some activated carbon powder that has a smaller mean particle size while still offering a high specific area. YP-80F is a porous activated carbon produced by Kuraray Chemicals, which is processed from coconut shells and is recommended for use in supercapacitor electrodes. It has practical size of 5-25 µm, it has a PH of 7-10, and a surface area of 1900 $m^2.g^{-1}$~2200 $m^2.g^{-1}$[91]. According to equation 2.2, the supercapacitor made with this powder shall achieve a maximum specific capacitance of 87.4 $F.g^{-1}$.

In supercapacitor design, spray-coated carbon/polymer film can be used as a supercapacitor electrode, as shown in figure 5.2. The thickness, film formation and density of these electrodes can be adjusted Drobny et al. [92] demonstrate the electrochemical performance of YP-80 F carbon/polymer film by different fabrication methods. The supercapacitor made with spray-coated thin YP-80 F thin film on metal foils and organic electrolytes achieved a specific capacitance of 10.2 $F.cc^{-1}$ (21.7 $F.g^{-1}$).

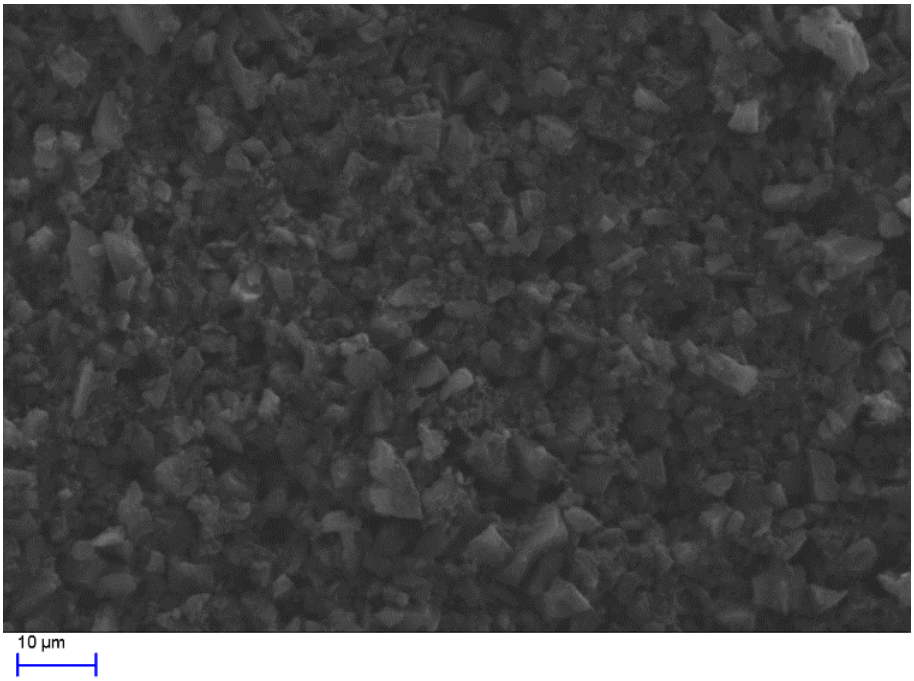

Figure 5.2: Spray-coated YP-80f activated carbon/polymer film electrode.

The manufacturer's technical information states that the typical specific capacitance of a supercapacitor made with YP-80 F activated carbon powder is 32 $F.g^{-1}$ [91]. This powder will be used in the development of the spray-coated carbon fabric electrode. In addition, activated carbon powder can be further improved using the following technique; first, the particle size of the activated carbon powder can be reduced by milling, and second the wettability of the powder can be improved by baking the activated carbon powder in air to create a thin oxide material on the surface of carbon particles.

The binder solution used also influences the performance of the electrode. PS is an acceptable binder for attaching two porous materials such as activated carbon and fabric, but this polymer is brittle and not very suitable for such a flexible application. Ethylene-co vinyl acetate (EVA) is a copolymer of ethylene and vinyl acetate; in comparison with PS, it is much less brittle but also provides good adhesion to porous materials. EVA is a solvent-soluble thermoplastic material which can be dissolved by specific solvent under heating to form liquid glue used on many materials like fabric, rubber and wood [88].

The solvent used in the carbon solution is another material that can be improved further. Generally, a high-volatility solvent will help the sample achieve good uniformity without the carbon solution shrinking excessively, but it will cause cracking since high-volatility solvent is evaporated quickly during curing process. It is disadvantageous in a carbon electrode as the

carbon particles may come off from the fabric during use. In spray coating the high volatility solvent in the carbon vapours will evaporate immediately after they have been blown away from the spray nozzle; however, it can leave the cured carbon compounds to block the spray nozzle and terminate the spray-coating process. A low-volatility solvent like 1, 2, 4-Trichlorobenzene (1, 2, 4 TCB) [93] will minimise these problems, and this will be evaluated in the spray-coated carbon fabric electrode.

5.3 Improved carbon solution preparation

The carbon powder used in this work was mixed with EVA dissolved by 1, 2, 4 TCB solvent. The carbon solution contained 100 mg of carbon powder (90 mg YP-80F powder and 10 mg Shawinigan Black powder) and a fixed percentage (15%) of EVA. Then the solution container was placed in the Hauschild engineering speed mixer for one minute with a rotating speed of 1000 rpm; this process was repeated 10 times. Finally, the carbon solution was placed in a sonicator bath for 20 minutes. The sonication process ensures that carbon black particles are dispersed uniformly in the solution and surround the larger, activated particles.

5.4 Fabric spray coating and curing process

In this work four different woven fabrics have been used for electrode substrates; these are silk fabrics (denoted as S), cotton sheet (denoted as C_{ot}), thick poly-cotton fabrics (denoted as B_{thick}) and thin poly-cotton fabrics (denoted as W_{thin}) that were used in the dip-coated electrode for the supercapacitor. The SEM images of the silk fabrics, cotton sheet and thin poly-cotton fabrics are given in appendix D. Figure 5.3 shows the photo of the spray-coated fabric electrodes based on blue thick poly-cotton fabrics and cotton sheet.

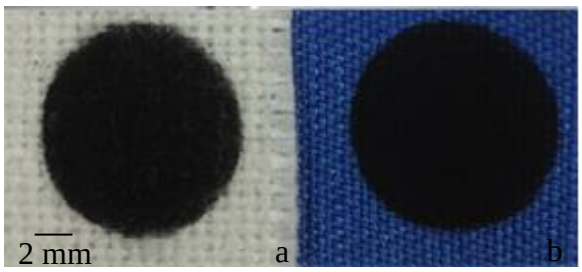

Figure 5.3: Spray-coated black carbon electrodes on (a) cotton and (b) polyester/cotton (blue) fabric substrate.

Before the spray-coating process, the carbon solution was heated to 80^{o}C. This step is required to reduce the viscosity of the carbon solution and prevent carbon solution from blocking the spray nozzle, the diameter of the spray nozzle is about 300 µm. Fabric samples were

sandwiched between metal masks to achieve the designed pattern as shown in figure 5.4 (a). The set-up of the metal masks mounted vertically on a moving belt in front of the spray nozzle shown in figure 5.4 (b).

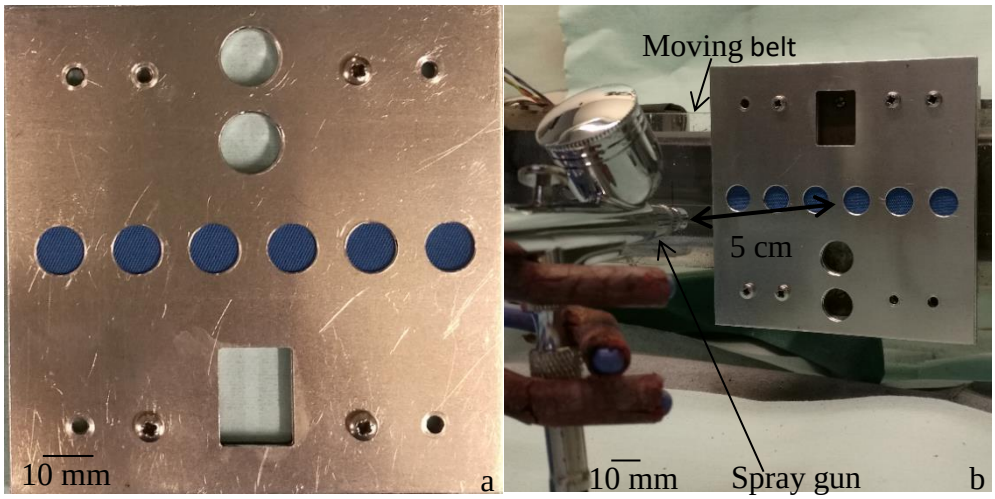

Figure 5.4: (a) Thick poly-cotton fabric in metal mask and (b) polyester/cotton (blue) fabric substrate.

When spray coating commenced, the metal masks were moving slowly through the carbon vapour area, then the spray gun was switched off and the direction of the moving belt was reversed to pull the metal mask back to its original position. These processes count for one set of the spray-coating process. The time taken for each fabric sample to pass through the carbon vapour area was approximately 0.4 seconds. The carbon solution was spray coated on both sides of the fabric samples for 4,8,12 and 16 sets of processes. The spray-coating process was conducted in a fume cabinet at room temperature. The spray nozzle was placed in front of the fabric sample at a fixed distance of 5 cm shown in figure 5.2 and a fixed air pressure of 25 psi (1.72 bars).

Then the carbon fabric electrodes were cured in the box oven for 10 minutes at 150 ^{o}C. Next, the spray-coated electrodes were processed by the surface cleaning technique state in chapter 4 then dried at room temperature overnight until all of the DI water had evaporated. This process is the same as for the dip-coated fabric electrodes presented in chapter 4.4. Finally, the fabric electrode was dried at room temperature until all of the water had evaporated from fabric electrode.

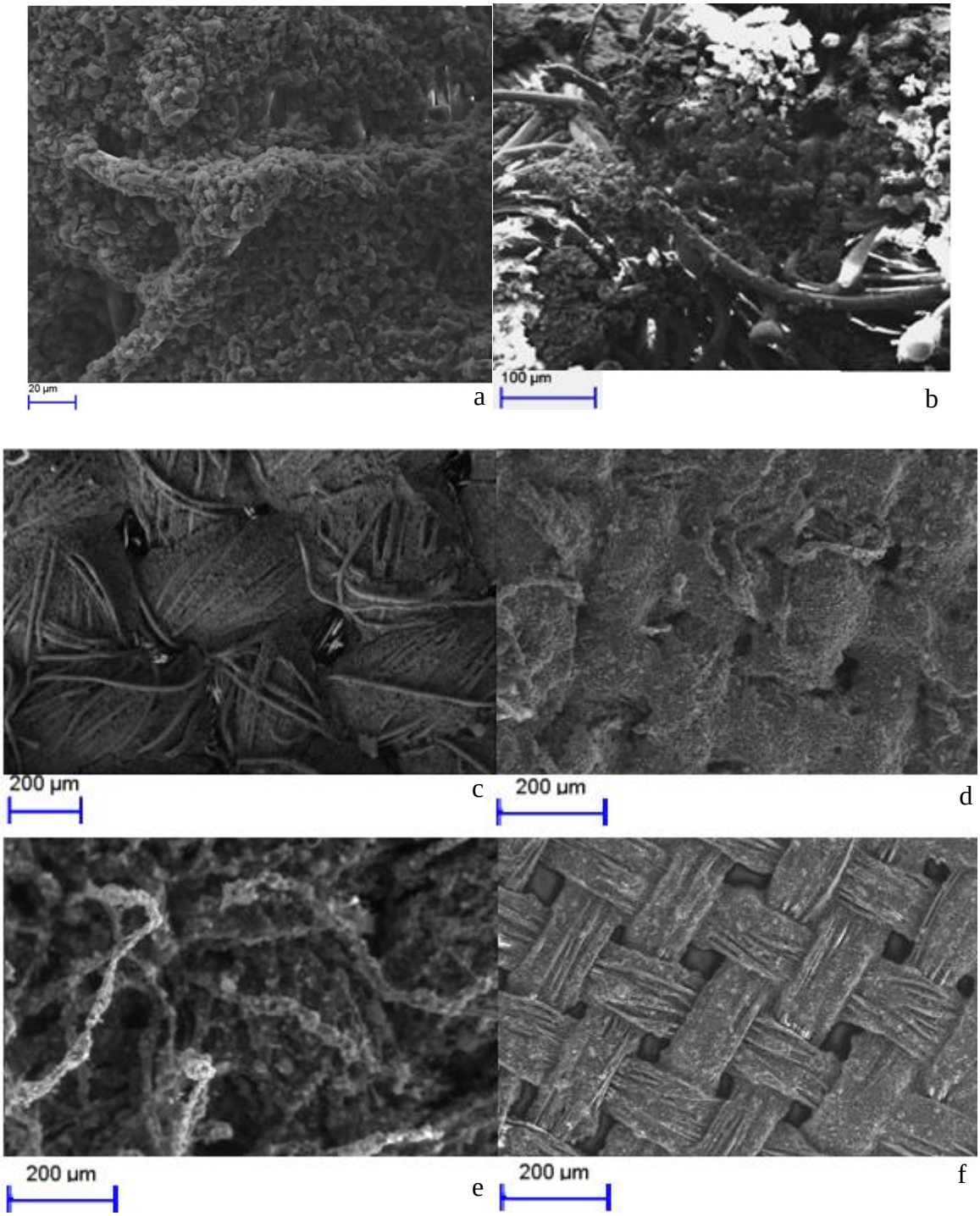

Figure 5.5: (a) SEM micrograph of spray-coated carbon fabric electrode (type B_{thick})made with EVA binder visualised from above and (b) cross-sectional view of sample(type B_{thick}). lower magnification SEM micrograph of the spray-coated carbon fabric electrode (c) :type B_{thick} (d) :type W_{thin} (e) :type C : (f) :type S

Figure 5.5 (a) to (f) shows the SEM photo of the spray-coated fabric electrodes. The carbon particles are attached in a uniform coating to most of the individual yarns but not lumped

together, which would otherwise block the electrolyte flows into the electrode. As shown in the cross-sectional view of the spray-printed electrode in figure 5.5 (b), in a spray-printed electrode, the carbon powder does not fill up the entire volume of the fabric.

5.5 Supercapacitor assembly process

The assembled supercapacitor cell shares the same structure as described in the previous chapter. The fabric electrodes were processed with vacuum impregnation with 1M Li_2SO_4 aqueous electrolyte for 20 minutes. When closing the test cell the compressed current collector bends the nickel layers and sometime causes device short circuits It is because the fabric supercapacitors are thin, compressible and smaller (in size) than the nickel layer.

An alternative way to solve this problem is to coat a layer of flexible membrane between the electrode and the current collector. The fabrication details of this membrane and its test results with dip-coated thick poly-cotton fabrics are given in appendix E.

In this chapter, the nickel layer was omitted and the old steel test rods replaced by type 303 stainless steel rods. Type 303 stainless steel has good corrosion-resistant properties due to the presence of sulphur in the steel composition.

5.6 Analysis of results

In this chapter the assembled supercapacitor is the same as the one described in the previous chapter. The supercapacitors made with various spray-coated fabric electrodes with aqueous 1M Li_2SO_4 electrolyte were tested using a VMP2 potentiostat/galvanostat (Biologic, France).

In this section the performance comparison between four different types of spray-coated fabric electrodes with different carbon mass loading percentage is presented. The area of each fabric sample is 0.785 cm^2 and each piece of fabric electrode has a different weight before coating, as shown in table 5.1. These results are presented in tables 5.2 to 5.7. The electrode is denoted by its substrate type and the number of spray-coating process - for example, the blue thick poly-cotton fabrics with undergoing four spray-coating processes denoted as B_{thick4}.

Table 5.1: Spray-coated fabric electrodes information.

	Electrode type			
	B_{thick}	W_{thin}	S	C_{ot}
Original weight ($mg.cm^{-2}$)	27.1	12.5	4.45	69.8
Thickness (μm)	300	150	50	500
Number of spray coatings	Total carbon loading per electrode ($mg.cm^{-2}$)			
4	1.04	0.92	0.255	1.14
8	1.25	2.81	0.401	1.56
12	2.38	3.94	0.701	2.56
16	3.83	5.41	1.47	3.68
Number of spray coatings	Carbon:Fabric ratio(%wt)			
4	3.84	7.3	5.21	1.63
8	4.6	22.48	9.01	2.23
12	8.78	31.52	15.7	3.67
16	14.1	43.3	33.0	5.27

According to table 5.1 the amount of active material loaded into all four different fabrics increases as the number of spray-coating processes increased. Silk fabrics cannot load with similar amounts of active material for the same spray number; in comparison with the other three fabrics, silk fabric samples are very thin and much less compact, and during the spray coating-process most of the carbon vapours pass through the silk fabrics. A similar effect has been found in thick poly-cotton (B_{thick}) and cotton (C_{ot}) fabric cases but less in the thin poly-cotton fabrics(W_{thin}). As shown in table 5.1, in comparison with other fabrics, the amount of carbon staying in the thin poly-cotton fabrics (W_{thin}) increased dramatically as more carbon solution was spray-coated on to the fabrics. This may be caused by the tight yarn structure as well as the thickness of the fabrics.

The electrode samples made with cotton fabrics and the 12 and 16 spray-coating processes did not pass the electrode surface-cleaning stage. A significant amount of carbon powders came off during the process in these two types of electrode, so these electrodes will not be used to make a supercapacitor cell for results discussion.

A similar carbon/polymer film electrode shown in figure 5.2 was prepared for result comparisons. This electrode was made with the identical fabrication process and material solution as the other fabric electrodes; carbon/polymer solution was spray-coated on top of a nickel foil for four sets of processes. The area of each nickel electrode is 0.785 cm^2 and its thickness is 55 µm before coating process. Each nickel electrode contains 1.78 $mg.cm^{-2}$ of carbon materials, and the thickness of carbon materials.is about 10 µm. These electrodes are denoted as Ni_4.

In tables 5.2, 5.3, 5.5 and 5.6 both the normalised and area ESR results, specific and area capacitances of the supercapacitors were based on GC methods. In the CV test a total potential difference of 0.8 V was applied to the tested cell; this will influence its electrochemical performance. According to tables 4.2 and 4.3, the specific and area capacitance calculated from the CV test is larger than the results from other methods which means CV tests are likely to overestimate the capacitance of the fabric supercapacitor cell. The results from the EIS test must bond to a specific circuit model; however there are many models to describe the performance of the supercapacitor at different frequency regions. The EIS capacitance results from tables 4.2 and 4.3 are based on the basic resistor-capacitor model (figure 3.12) and equations 3.9 and 3.5; it is not a universal model to describe the performance of supercapacitors at all frequency regions, at low frequency regions (i.e. below 10 Hz), the resistor-capacitor model will lead to underestimate the capacitance of the supercapacitor cell.

Table 5.2: Comparison of specific capacitance ($F.g^{-1}$) of the supercapacitors measured using all three techniques.

Electrode information			Specific capacitance		
Electrode type	Number of spray coatings	Carbon:Fabric ratio(%wt)	CV (25 $mV.s^{-1}$)	GC (0.1 $A.g^{-1}$)	EIS (20 mHz)
B_{thick}	4	3.84	18.9	15.3	9.71
	8	4.6	19.1	14.8	14.3
	12	8.78	17.3	15.5	13.3
	16	14.1	17.9	15.4	14.0
W_{thin}	4	7.3	19.5	15.2	13.8
	8	22.48	17.2	14.7	14.0
	12	31.52	14.0	13.3	11.9
	16	43.3	13.9	12.9	11.6
S	4	5.21	33.7	30.5	28.4
	8	9.01	25.9	20.8	17.2
	12	15.7	26.3	20.2	18.3
	16	13	14.1	11.7	10.7
C_{ot}	4	1.63	10.4	9.36	8.90
	8	2.23	1.14	4.76	0.60
Ni	4	1.58	12.3	10.5	9.41

Table 5.3: Comparison of area capacitance ($F.cm^{-2}$) of the supercapacitors measured using all three techniques.

Electrode information			Area capacitance			
Electrode type	Number of spray coatings	Carbon:Fabric ratio(%wt)	CV (25 $mV.s^{-1}$)	GC (0.1 $A.g^{-1}$)	EIS (20 mHz)	Theoretical maximum
B_{thick}	4	3.84	0.0395	0.0318	0.0202	0.655
	8	4.6	0.0478	0.0370	0.0357	0.787
	12	8.78	0.0825	0.0738	0.0634	1.50
	16	14.1	0.138	0.118	0.1073	2.41
W_{thin}	4	7.3	0.0359	0.0280	0.0255	0.580
	8	22.48	0.0968	0.0832	0.0789	1.77
	12	31.52	0.110	0.105	0.0934	2.48
	16	43.3	0.151	0.139	0.125	3.41
S	4	5.21	0.0181	0.0156	0.0145	0.161
	8	9.01	0.0208	0.0167	0.0138	0.253
	12	15.7	0.0369	0.0566	0.0256	0.442
	16	33	0.0216	0.0344	0.0314	0.926
C_{ot}	4	1.63	0.0238	0.0215	0.0203	1.03
	8	2.23	0.0051	0.0149	0.00167	1.40
Ni	4	1.58	0.0438	0.0475	0.0335	1.12

Table 5.2 suggests that the supercapacitor made using electrode S_4 achieves the best specific capacitance (30.4 $F.g^{-1}$) compared with the other supercapacitors made with other types of electrode in all three measurement techniques. This result is close to the typical specific capacitance (32 $F.g^{-1}$) of YP-80F activated carbon powder provided by its manufacturer. As shown in figure Figure E.5 (a) and (b) the silk fabric yarns are very thin and loose, so the spray-coated carbon materials are uniformly distributed in the silk electrode without becoming lumped together, the aqueous electrolyte can reach most of the carbon particles and arise double-layer capacitance. According to table 5.2, the specific capacitance of the supercapacitor made with spray-coated fabric electrodes ($W_{thin,}$ S and C_{ot}) is reduced significantly as the amount of carbon material added into the fabrics increased. This relation indicates that when the number of spray coatings is increased, the carbon materials cover each other and prevent the formation of the double-layer capacitance. As a result, the specific capacitance is reduced (table 5.2), both specific and area capacitances of the supercapacitor made with the cotton electrode decreased significantly as more carbon coating was applied. In type C_{ot} electrodes, the carbon materials are more likely to stack on top of the previous carbon coating layer, and the carbon vapour does not fully penetrate the cotton fabrics to form a uniform conductive network. It is also proved by the results relating to the supercapacitor made with thin film electrode Ni. In this case, carbon materials are definitely stack on each other layer by layer and supercapacitor made with thin film electrode Ni can only achieve specific capacitance of 10.5 $F.g^{-1}$which is smaller than the typical specific capacitance (32 $F.g^{-1}$) of the YP-80F carbon powder.

Table 5.2 also suggests that the specific capacitances of the supercapacitor made with four different types of B_{thick} fabric electrodes do not vary significantly (around 15 $F.g^{-1}$) regardless of the amount of carbon coated on to the fabric electrodes. This could be due to the following reasons: first, the highest carbon weight percentage in the spray-coated electrodes (B_{thick} fabrics) was 14.4% (table 5.2) which is less than the lowest carbon weight percentage (17.3%, table 4.2) in the dip-coated electrodes of the same fabrics. This shows that, in the fabric supercapacitor, the fabric electrode has an optimal material loading percentage - when below this percentage the specific capacitance is not strongly influenced by the electrode material weight. Second, spray coating can make the carbon materials distribute uniformly in the fabric electrode and not lump together. This allows most of the carbon particles to make contact with the electrolyte and hence maintains the specific capacitance when more carbon materials are added to the fabric electrodes.

Specific capacitance is an important factor to determine the electrode material efficiency in EDLC design. It has a theoretical maximum value that is determined by the material properties such as electrode material surface area, electrolyte and the current collector characteristics. Apart from the wettability issue that has been optimised by the vacuum impanation process, in fabric EDLC design the carbon particle distribution in the electrode can influence the specific capacitance. In dip-coated fabric electrodes, the amount of carbon coated into the fabrics cannot be controlled easily; it is very hard to reduce the amount of carbon loaded into the fabric to find the optimal material loading percentage. According to figure 4.3 (chapter 4) the carbon particles coated into the fabrics are lumped together due to solvent evaporation, which means that a lot of carbon particles have been physically covered by others and polymer binder, these carbon surface is not form double-layer capacitance, these carbon particles shall only increase the electrode weight percentages and reduce the device specific capacitance. Therefore, in the supercapacitor made with dip-coated fabric electrodes, specific capacitance decreased as more carbon material was loaded into the electrode by increasing the binder percentage. In the spray-coated fabric electrode, the amount of carbon loaded into the fabric can be controlled; it can be used to coat the required amount of carbon into the fabric electrodes to find the optimal carbon weight percentage. However, for different fabric samples and carbon solution combinations, this optimal weight percentage is different.

According to table 5.3 the supercapacitor made using electrode W_{thin16} achieves the best area capacitance (0.139 $F.cm^{-2}$) compared to the supercapacitors made from other types of fabric electrode in all three measurement techniques. This is because the W_{thin} fabric can retain a lot of carbon materials (table 5.1). Table 5.3 also suggests that the area capacitance of the supercapacitor made with two different poly-cotton fabrics increases as more carbon material is loaded into the fabrics. In the silk fabric, the area capacitance initially increases as carbon material increases; however, when the carbon: fabric ratio increased from 15.5% (S_{12} fabric electrode) to 30%(S_{16} fabric electrode), its area capacitance decreased from 0.0566 $F.cm^{-2}$ to 0.0344 $F.cm^{-2}$. This is because, after 12 coating processes, carbon materials are likely fill the entitle volume of silk substrate; the carbon materials cover each other and reduce the area capacitance. A similar relation appears in the supercapacitor made with the cotton electrode (C_{ot}), where its specific area capacitance decreases dramatically when more carbon materials are coated into the cotton substrate. The specific capacitance of the type C_{ot} supercapacitors drops from 9.36 $F.g^{-1}$ (C_{ot4}) to 4.76 $F.g^{-1}$ (C_{ot8}). This indicates that carbon vapour is not likely

to penetrate the cotton substrate so the carbon materials lump together and decrease its area and specific capacitances.

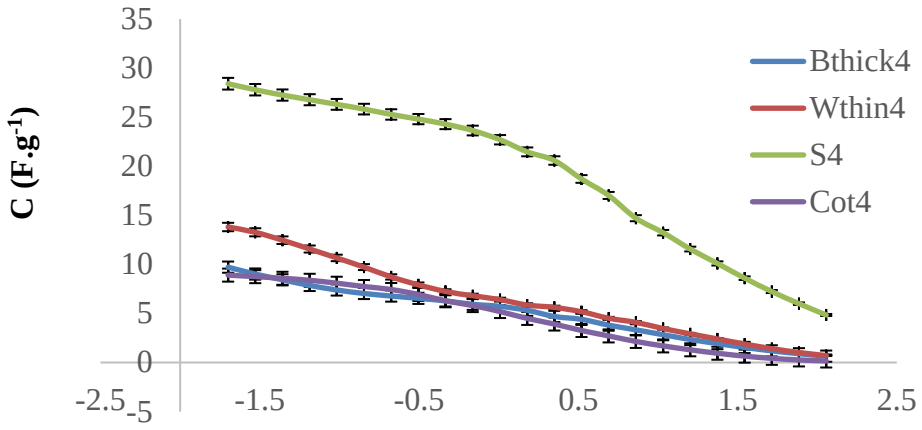

Figure 5.6: Specific capacitance ($F.g^{-1}$) of supercapacitor made using fabric electrode B_{thick4}, W_{thin4}, S_4, C_{ot4} and thin film electrode Ni_4 from 20 mHz to 112 Hz. The error bars represent the standard deviations that were calculated based on the results from 5 repeated tests.

The capacitance bode plots extracted from the EIS test are shown in figure 5.6. The supercapacitor using electrode S_4 has a higher specific capacitance on all frequencies. From figure 5.3, the specific capacitance of the supercapacitor using the silk substrate S_4 (28.4 $F.g^{-1}$) at 20 mHz was at least two times smaller than its theoretical maximum value (87.5 $F.g^{-1}$).

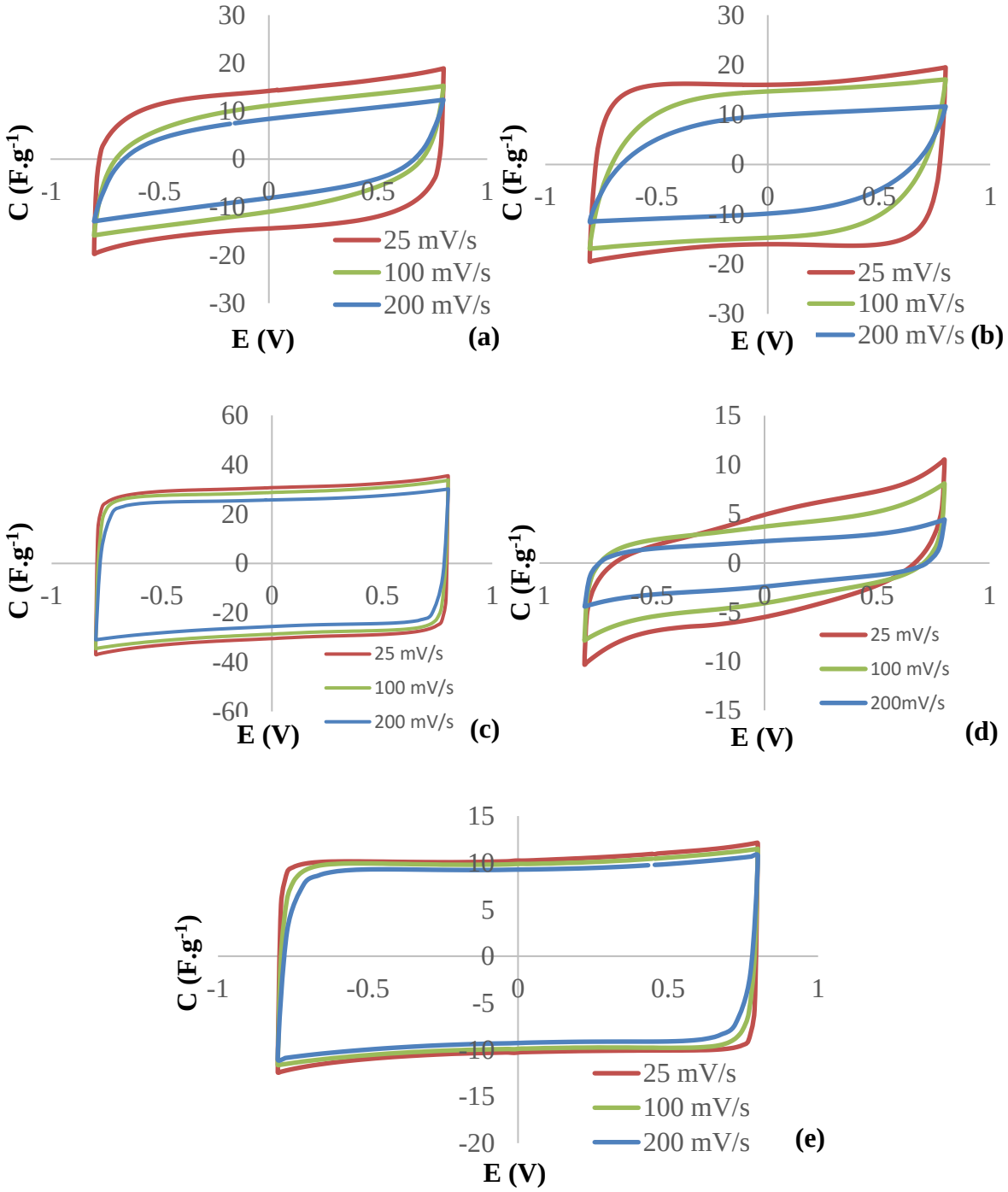

Figure 5.7: CV test of supercapacitor made using spray-coated electrodes: (a) thick poly-cotton fabrics (B_{thick4}), (b) thin poly-cotton fabrics (W_{thin4}), (c)silk fabrics (S_4), (d) cotton fabrics (C_{ot4}), and nickel foil (Ni_4) between +/- 0.8 V at the scan rate of 200, 100, 25 $mV.s^{-1}$.

The CV results shown in figure 5.7 suggest that the supercapacitor with all five types of electrode demonstrates capacitive behaviour and is electrochemically stable at scan rates from 25 to 200 $mV.s^{-1}$. For the scan rate of 200 $mV.s^{-1}$, the CV curves show the supercapacitor made

with the poly-cotton based electrodes and cotton based electrodes (figure 5.7 (a), (b) and (d)) becoming more resistive and less capacitance can be demonstrated. According to table 5.4 the specific capacitance of the supercapacitor made with B_{thick4} electrodes varies from 12.3 $F.g^{-1}$ to 18.9 $F.g^{-1}$, with the W_{thin4} electrodes it varies from 11.6 $F.g^{-1}$ to 19.5 $F.g^{-1}$ and with the C_{ot4} electrodes it varies from 4.43 $F.g^{-1}$ to 10.4 $F.g^{-1}$ according to the ratio of the maximum current to the scan rate. Figure 5.7 (c) and (e) also shows that the shape of the CV curves relating to the supercapacitor made with the silk and nickel electrodes maintains a semi-rectangular shape (a good capacitive shape) regardless of the scan rate change. This indicates that the supercapacitor made with thin electrodes achieved very good wettability with aqueous electrolyte. This supercapacitor maintains good capacitive behaviours with low ESR and low leakage current. The CV curves of the supercapacitor made with the cotton electrodes (C_{ot}) changes a great deal as the scan rate changes, with some shapes changing closed to 0.8 V at the low scan rate (25 $mV.s^{-1}$). The CV curve indicates that some reactions occur during the test. During the CV test, electrolysis occurs when the voltage increases close to 0.8 V, at which point the cotton materials may react with the ionic species in the electrolyte. In addition, the extra resistance and capacitance caused by the reaction introduces an additional shape, thereby changing about the CV curve. Figure 5.7 (d) also shows that the carbon material did not fully penetrate the cotton fabrics to form a good continuous conductive network, as the device compressed in the tube fitting is not a single fabric supercapacitor device but behaves like a fabric supercapacitor combination.

Table 5.4: Specific capacitance ($F.g^{-1}$) of B_{thick4}, W_{thin4}, S_4, C_{ot4} and thin film electrode Ni_4 at different scan rates.

Electrode information		CV scan rate ($mV.s^{-1}$)					
Electrode type	Carbon :electrode ratio(%wt)	25	50	75	100	150	200
B_{thick4}	3.84	18.9	16.5	15.6	15.2	13.0	12.3
W_{thin4}	17.3	19.5	17.8	17.6	17.1	15.5	11.6
S_4	5.21	33.7	32.8	31.1	30.6	30.5	30.3
C_{ot4}	1.63	10.4	9.14	8.61	8.06	6.55	4.43
Ni_4	1.58	12.3	11.7	11.5	11.3	10.7	10.7

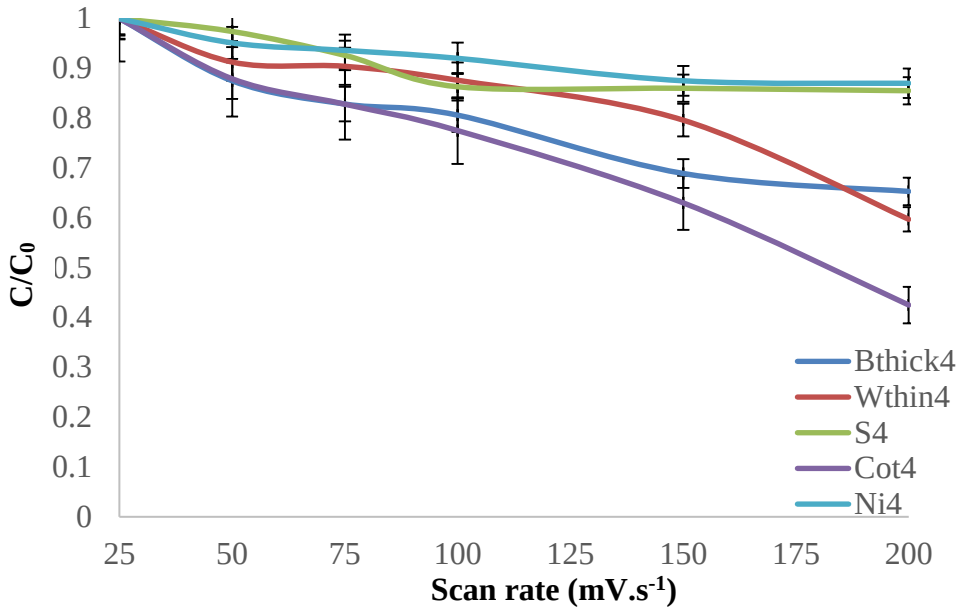

Figure 5.8: Capacitance variation of supercapacitor made using spray-coated fabric electrode B_{thick4}, W_{thin4}, S_4, C_{ot4}, and Ni_4. The error bars represent the standard deviations that were calculated based on the results from 5 repeated tests.

As shown in table 5.4 and figure 5.8, the specific capacitance of the B_{thick4} electrode supercapacitor tested at 25 $mV.s^{-1}$ drops from 18.9 $F.g^{-1}$ to 12.3 $F.g^{-1}$ at 200 $mV.s^{-1}$, which is about a 34.9% decrease in capacitance. The supercapacitor assembled using W_{thick4} electrodes shows a smaller drop in specific capacitance from 19.5 $F.g^{-1}$ at 25 $mV.s^{-1}$ to 11.6 $F.g^{-1}$ at 200 $mV.s^{-1}$, which is about a 40.5% decrease in capacitance. The supercapacitor made with very thick cotton electrode (C_{ot4}) shows a bigger drop in specific capacitance of about 57.5% at the higher scan rate. This indicates that this type of electrode has a wettability issue with the aqueous electrolyte; at a high scan rate, the electrolyte cannot make contact with the carbon material and less double-layer capacitance arises at the electrode/electrolyte interface.

The supercapacitor assembled using thinner electrodes made from silk fabric and nickel foil electrodes (Types S_4, and Ni_4) show a smaller drop in specific capacitance at a higher scan rate (about 10.1% for type S_4 and 13% for type Ni_4 between 25 to 200 $mV.s^{-1}$). This is due to the wettability of the active material in the electrode. These two types of electrode are very thin; the electrolyte can make contact with most of the carbon material after the vacuum impregnation process.

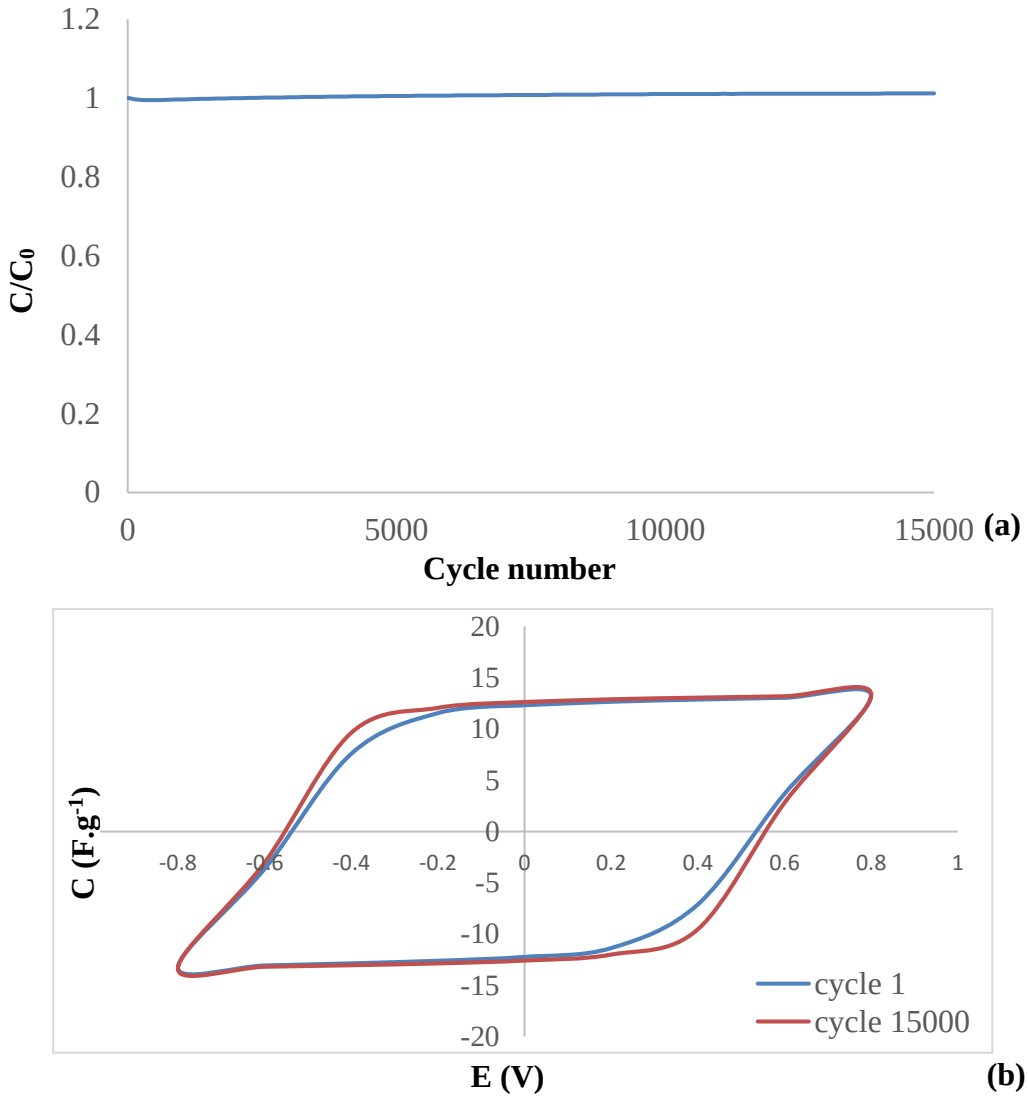

Figure 5.9: (a) CV stability test of supercapacitor (electrode type B_{thick4}) for 15000 cycles over 66 hours. (b) CV test of the supercapacitor (electrode type B_{thick4}) for 1 cycle and 15000 cycles between +/- 0.8 V at a scan rate of 200 $mV.s^{-1}$.

From figure 5.9 (a) and (b) the overall capacitance variation is less than 2% during 15000 test cycles. The small capacitance variation shown in figure 5.9 (a) is correlated to small temperature changes in the laboratory over the 66-hour test period which caused a small ESR variation that affects the effective capacitance measurement. This demonstrates an excellent level of adhesion of carbon material that distributes uniformly in the fabric substrate which forms a continuous and stable conducting network.

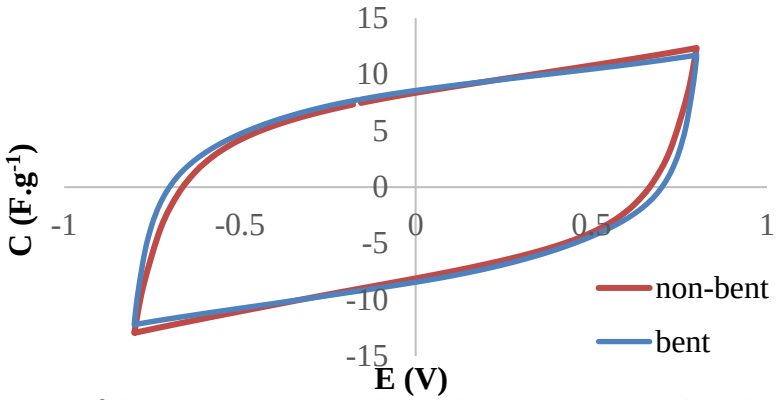

Figure 5.10: CV test of the supercapacitor (electrode type B_{thick4}) with and without the bending test between +/- 0.8 V at the scan rate of 200 $mV.s^{-1.}$

The mechanical durability of the fabric supercapacitors was also investigated by cyclical bending of type B_{thick4} electrodes samples around a mandrel. The samples were bent around the mandrel 100 times with a radius of curvature of 1.59 mm. The electrodes were then assembled into a supercapacitor and the electrolyte was added using vacuum impregnation.

Figure 5.10 shows the CV plots obtained from the supercapacitors fabricated with type B_{thick4} fabric electrodes (bent and non-bent). The shape and values of the supercapacitor current density plot of the bent sample shows a small difference in comparison with the non-bent CV curve. This indicates that the electrochemical performance of the supercapacitor with carbon spray coated fabric electrode (B_{thick4}) was not strongly affected by repeated bending.

Table 5.5: Normalised ESR (Ω.cm) of the device types B_{thick4}, W_{thin4}, S_4, C_{ot4} and thin film electrode Ni_4 at different scan rates.

Electrode information		Frequency /Log ($f.Hz^{-1}$)					
Electrode type	Carbon :Fabric ratio(%wt)	-1.7 (20 mHz)	-0.67 (0.21 Hz)	0.35 (2.2 Hz)	1.37 (23 Hz)	1.72 (52 Hz)	2.05 (112 Hz)
B_{thick4}	3.84	161.3	29.9	17.7	13.9	13.2	12.7
W_{thin4}	17.3	231.6	81.5	35.6	27.8	26.5	25.1
S_4	5.21	518.1	108.9	62.9	42.7	39.5	37.2
C_{ot4}	1.63	84.2	39.7	29.7	25.2	24.2	22.9
Ni_4	1.58	192.3	40.8	17.1	10.4	9.15	8.29

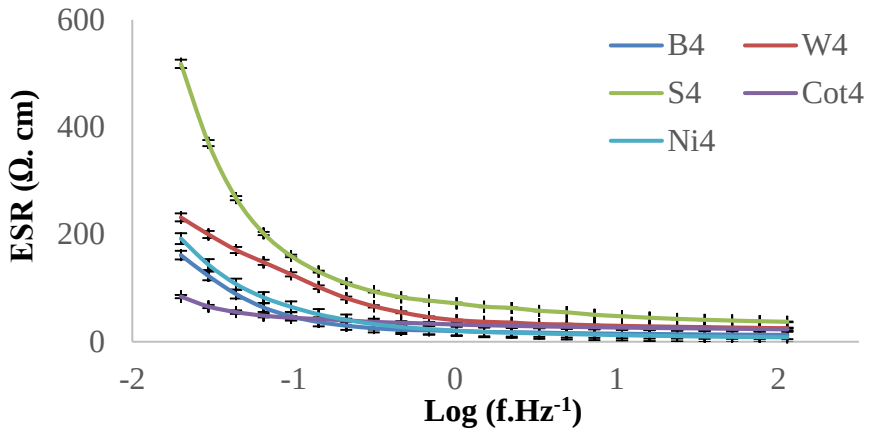

Figure 5.11: Bode plot of the normalised supercapacitors nominalised ESR (Ω.cm) from 20 mHz to 112 Hz, extracted from the EIS test. The error bars represent the standard deviations that were calculated based on the results from 5 repeated tests.

The normalised ESR results are shown in table 5.5 and figure 5.11 and the impedance result was expressed according to the circuit model shown in figure 3.12 (chapter3). The high frequency ESR indicates a total resistance due to the electrolyte and electrode materials. At the lowest frequency, ESR will be increased significantly due to diffusion resistance. According to figure 5.11 the supercapacitors with the silk fabric electrode S4 demonstrated highest normalised ESR compared with the other supercapacitors with fabric electrodes from 20 Hz to 112 Hz. This could be due to the fact that the silk substrate cannot retain more carbon materials in its loose yarn structure.

Table 5.6: Normalised ESR (Ω.cm) and area ESR (Ω.cm^{-2}).

Electrode information			ESR (Ω.cm^{-2})		ESR (Ω.cm)	
Electrode type	Number of spray coatings	Carbon :Fabric ratio(%wt)	GC (0.1 A.g^{-1})	EIS (20 mHz)	GC (0.1 A.g^{-1})	EIS (20 mHz)
B_{thick}	4	3.84	17.6	163	20.8	167
	8	4.6	23.5	130	20.1	111
	12	8.78	41.8	189	18.7	85
	16	14.1	64.7	199	18.1	55.8
W_{thin}	4	7.3	17.7	89	36.4	183
	8	22.48	51.7	160	34.8	108
	12	31.52	70.9	176	34.1	84.6
	16	43.3	97.0	161	33.7	56.3
S	4	5.21	N/A	70.6	N/A	435
	8	9.01	57.3	97.4	224	381
	12	15.7	91.3	156	205	349
	16	33	155.9	212	166	226
C_{ot}	4	1.63	45.9	135	28.3	84
	8	2.23	50.8	3972	25.2	1789
Ni	4	1.58	N/A	24.8	N/A	118

According to figure 5.10 and tables 5.5 and 5.6, the impedance result was expressed as a series of combination of the frequency-dependent capacitances and a series resistance ladder network. In the GC test the supercapacitor made with S_4 and Ni_4 achieves a very small IR voltage drop that is below the minimum detection level of test-setting, so the ESR results from the GC test are not shown in table 5.5. The supercapacitor made with spray-coated fabric electrodes shows some relations between ESR and the amount of active material (carbon) coated into the fabric substrates. The normalised ESR (Ω.cm) decreased when more carbon material was coated into the fabrics; however, the area ESR ($\Omega.cm^{-2}$) increased when more carbon material was coated into the fabrics. These relations have been shown in all four different types of fabric. Table 5.5 also shows that the supercapacitor made with silk fabric electrode exhibits much higher normalised ESR (Ω.cm) than all other types of electrode substrate; this point is also proved by the EIS results shown in figure 5.11.

Table 5.7: Energy and power density of supercapacitor made using spray-coated fabric electrode determined by GC test (0.1 $A.g^{-1}$).

Electrode information			Energy and power density	
Electrode type	Number of spray coatings	Carbon :Fabric ratio(%wt)	Energy density ($Wh.kg^{-1}$)	Power density ($kW.kg^{-1}$)
B_{thick}	4	3.84	17.6	7.08
	8	4.6	17.0	5.30
	12	8.78	17.8	2.99
	16	14.1	17.7	1.93
W_{thin}	4	7.3	17.5	7.96
	8	22.48	17.0	2.72
	12	31.52	15.3	1.99
	16	43.3	14.8	1.45
S	4	5.21	35.1	N/A
	8	9.01	23.9	8.89
	12	15.7	23.2	5.57
	16	33	13.5	3.26
C_{ot}	4	1.63	10.8	2.47
	8	2.23	5.48	2.24
Ni	4	1.58	12.1	N/A

Energy density and power density are other representations of the device's specific capacitance and ESR. As shown in tables 5.7, the supercapacitor made using electrode type S_4 achieves the best energy density (35.1 $Wh.kg^{-1}$) and S_8 achieves the best power density (8.89 $kW.kg^{-1}$) compared to the supercapacitors that use all other electrode types. This indicates that the supercapacitor made with the silk electrode can realise the full double-layer capacitance potential of carbon powders. According to table 5.6, the silk electrode contains much lower amounts of carbon material than the other types of fabrics; and the real normalised energy and power of the silk-based supercapacitor are very low. The energy density of the supercapacitors made with thick poly/cotton was maintained around 17 $Wh.kg^{-1}$ regardless of how much carbon material was loaded into the fabrics. Table 5.6 also shows that, for supercapacitors made with thin poly-cotton (W_{thin}), silk (s) and cotton (C_{ot}) fabrics, the energy density and power density decreased as more carbon was coated on to the fabric electrode. This indicates that in the fabric supercapacitor, when more carbon material is introduced into the fabrics, carbon particles are likely to accumulate as a result of solvent evaporation. The carbon particles that are covered by others will not form double-layer capacitance but will introduce extra resistance.

5.7 Conclusions

This chapter presents a group of three-layer flexible supercapacitors made using spray-coated fabric electrodes. The supercapacitor presented here based on type B_{thick4} electrodes achieves a mass specific capacitance up to 15.3 $F.g^{-1}$ (table 5.2), a low normalised ESR of 20.8 Ω.cm (table 5.6), high energy density of 17.6 $Wh.kg^{-1}$(table 5.7) and power density of 7.08 $kW.kg^{-1}$ (table 5.7), and also achieves excellent cycling stability over 15000 cycles (figure 5.9).

This chapter also demonstrated the electrochemical performance of supercapacitor with spray coated fabric electrode based on 4 different fabric substrates with different amount of electrode material. The results shown in table 5.2 to 5.7, figure 5.6, 5.7 and 5.11 shows different fabric substrates dose influence the amount and uniformity of electrode material that can be introduced into the fabric substrates, it varies the electrochemical performance of supercapacitor made by theses fabric electrodes.

The supercapacitor made by the thinnest fabric (silk) substrate achieved the highest specific capacitance (30.4 $F.g^{-1}$) than supercapacitor with other types of fabric electrode, this result is also close to the typical specific capacitance value of the carbon material (32 $F.g^{-1}$). The CV curves of the supercapacitor made by the silk substrate are similar to the CV curves of the supercapacitor made by carbon film electrodes shown in figure 5.7 (c) and (e). These results

indicate the supercapacitor with thin fabric electrode demonstrated better electrode material electrochemical efficiency than supercapacitor with thicker fabric electrodes. However, in comparison with other results in table 5.3 the area capacitance of the supercapacitor with silk fabric electrode is much lower than other results that are not appropriate with actual energy storage/buffer design in wearable electronics.

In comparison with the supercapacitor made using the dip-coated fabric electrode with low priced general purpose carbon powder, the supercapacitor made using the spray-coated fabric electrode with YP series activated carbon powder achieved better results in all important parameters. The use of the spray-coating technique allows carbon powders (activated carbon and carbon black) to infiltrate the poly-cotton fabrics uniformly, which will form a good conductive area in designed part of fabric substrate and achieve a better electrochemical performance than supercapacitor constructed with dip coated fabric electrode.

6 Two-layer and single-layer flexible solid-state fabric supercapacitor

This chapter presents details of the experimental investigation into two types of solid-state fabric supercapacitor. The first one is fabricated by two pieces of spray coated poly-cotton electrode without paper separator. The second solid-state fabric supercapacitors is made with only one layer of spray coated cotton electrode. Details of the fabrication process include electrolyte materials section, and supercapacitor setup and testing. Finally, the last section presents the results, analysis and conclusions of the chapter.

6.1 Design motivation

Traditionally, an aqueous multilayer supercapacitor presented in chapters 4 and 5 was constructed using two electrical double-layer interfaces (fabric electrodes) to sandwich a charge separator. The charge separator contains the aqueous electrolyte and also acts as a charge barrier that prevents electrical short circuits. This type of supercapacitor is relatively easy to construct but would require extra encapsulation (packaging) in practical use to retain the electrolyte.

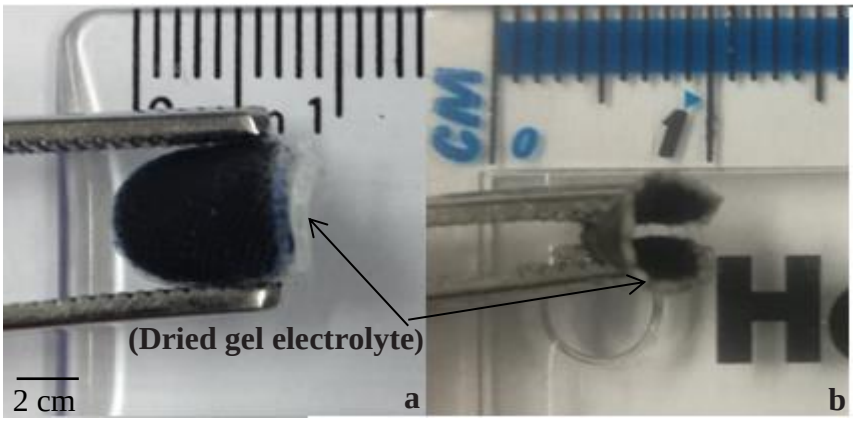

Figure 6.1: Photograph of solid-state fabric supercapacitor using (a) two pieces of poly-cotton electrode compressed together , (b) single piece of cotton electrode before testing.

One alternative way to overcome the drawback of the multilayer supercapacitor with aqueous electrolyte is to use a gel electrolyte to replace both the charge separator and aqueous electrolyte. This is known as a solid-state supercapacitor and is shown in figure 6.1. In the semi-dried gel, the dense water-polymer lattice networks prevent short circuits, and the ionic species around the lattices will provide free ions that form the double-layer interfaces with

respect to the electrode materials. In a solid-state supercapacitor it is not always necessary to place a charge separator in between the two supercapacitor electrodes. The basic structure of the two-layer solid-state fabric supercapacitor is shown in figure 6.2 (left) and is very similar to the structure used previously (see figure 4.7). Figure 6.2 (right) shows the basic structure of the single-layer solid-state fabric supercapacitor, in this type of device electrode materials are locate at the top and bottom of a single fabric layer, it leaves a gap in between and filled with the gel electrolyte.

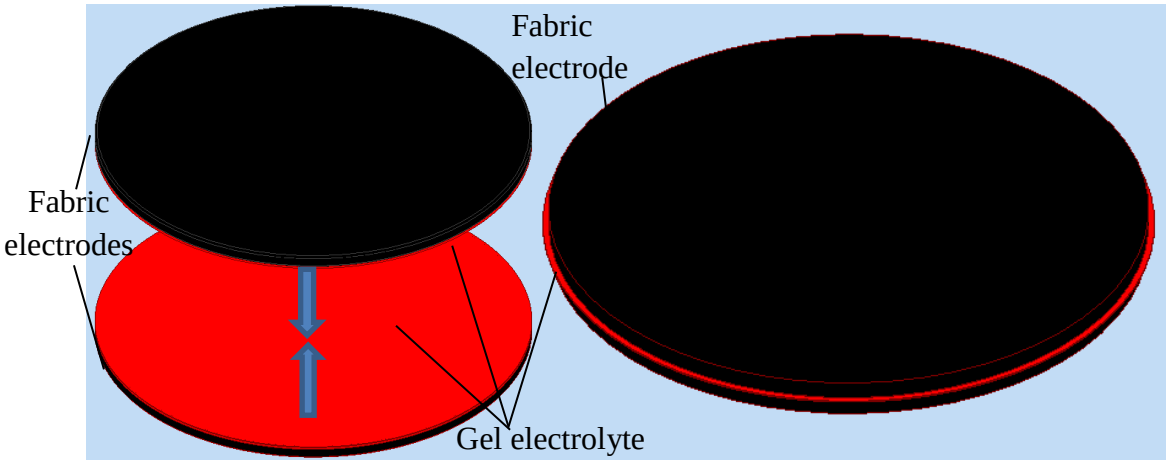

Figure 6.2: Two layer solid-state fabric supercapacitor.

This chapter demonstrates a solid-state fabric electric double-layer supercapacitor using only non-hazardous materials, which will also simplify subsequent packaging. The fabric electrodes were achieved via the spray-coating process with YP-80F carbon powders and the standard woven poly-cotton and cotton fabric substrates. The operation and stability of the solid-state supercapacitors has been evaluated using the same methods previously described.

6.2 Improved electrolyte formation

The electrolyte is an important component in supercapacitor design; it will not only define the maximum device-operating voltage but will also influence the ESR and device packaging. The viscosity of the electrolyte will also influence the wettability of the electrode materials that form the double-layer capacitance, and therefore the energy and power density.

In the previous chapters, all multilayer supercapacitors used $LiSO_4$ inorganic salt and DI water as the electrolyte. This aqueous electrolyte has very high ionic conductivity and very low viscosity that benefits the EDLC device, but it does have some drawbacks. First, the aqueous electrolyte has low maximum operating voltage of around 1V; this factor limits the device energy density. Second, the package design of a supercapacitor using aqueous electrolyte is

very hard since the package needs to seal and compress the supercapacitor cell. Third, the multilayer supercapacitor with aqueous electrolyte requires a charge separator layer to hold the electrolyte solution and prevent device short circuits. Finally, a supercapacitor using an aqueous electrolyte typically exhibits a high current leakage, which reduces the stability and life time of the supercapacitor. As a result, it is not a suitable approach to use an aqueous electrolyte in a solid-state device.

It is therefore desirable to replace the aqueous electrolyte with the gel electrolyte. The gel electrolyte will increase the operating voltage of the supercapacitor, reduce current leakage, and simplify the device packaging. Traditionally, gel electrolyte contains hazardous materials like alkalines (KOH) or acids (H_2SO_4) as the ionic conductive spices; these gel electrolytes are not suitable for wearable electronics. The gel electrolyte shown in figure 6.3 presented in this work contains inorganic salt, vinyl-alcohol polymer (PVA) and DI water. The inorganic salts tested in this work include $LiSO_4$, ammonium dihydrogen phosphate ($NH_4H_2PO_4$ or ADP) and diammonium phosphate ($(NH4)_2HPO_4$ or DAP). ADP and DAP are the stable forms of ammonium phosphate salt; they are well known for their use in fertiliser, fire retardant (DAP) and dry fire extinguisher (ADP), as they have good water solubility (57.5 g/100 mL (10 °C) for DAP and 40.4 g/100 mL for ADP). Uddin et al. [94] demonstrated the performance of ADP/PVA gel composite film; the flexible film showed a good dielectric permittivity, improved thermal stability and higher glass transition temperature than pure PVA film did.

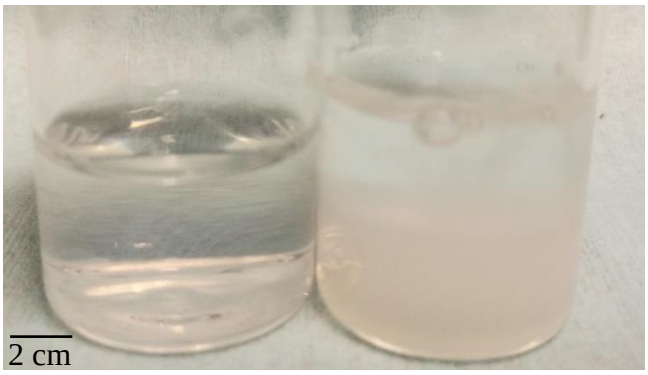

Figure 6.3: Photograph of (left) successful transparent gel electrolyte, and (right) failed gel electrolyte with PVA polymer and the salt separated from DI water and lumped together.

The gel electrolyte solution presented in this work was prepared by dissolving 0.5 g of PVA beads (Mw 146,000-186,000, 99+% hydrolyzed (Aldrich)) [95] in 5g of DI water (in the glass container) on a hot plate (80^{o}C). The mixing process was assisted with magnetic stirring (1200 rpm). After the PVA polymer had completely dissolved in the DI water and there was only

4.5g of gel solution remaining in the glass container, the heat function of the hot plate was switched off, and the magnetic stirring was continued. Then inorganic salt 0.15g Li_2SO_4 (0.25M) or 0.31g ADP (0.5 M) or 0.29 g DAP (0.4 M) were dissolved in another 1g of DI water to form a salt solution. Finally, when the gel solution had cooled down to 40^oC, the salt solution was added to the gel solution to form the gel electrolyte. For Li_2SO_4 and DAP gel electrolytes, the amounts of salt in the solutions are at their maximum value at room temperature; at this point, more salts were added into the gel solution which caused the polymer to separate from the DI water and to form lumps. This resulted in electrolyte mixing failure, as shown in figure 6.3.

6.3 Improved fabric electrode fabrication and vacuum impregnation process

The flexible electrodes used in this work are type $B_{thick10}$, $B_{thick14}$ and modified C_{ot8} fabric electrodes, presented in chapter 5. In this study the area of each fabric electrode is 0.785 cm^2; the thickness of each $B_{thick10}$ fabric electrode is about 300 µm; and each pieces of $B_{thick10}$ fabric electrode has a weight of 27.1 $mg.cm^{-2}$ before coating. In the $B_{thick10}$ electrode the carbon materials account for 6.67% (1.82 $mg.cm^{-2}$) of the final electrode weight. In the $B_{thick14}$ electrode carbon materials account for 10.3% (2.80 $mg.cm^{-2}$) of the final electrode weight.

6.3.1 Improved electrode fabrication for single-layer flexible solid-state fabric supercapacitor

The fabrication process of cotton fabric electrodes undergoes some changes. The results discussed in chapter 5 indicate that in cotton fabric electrodes design, the carbon materials are not likely to fully penetrate the cotton fabrics. This process has the potential to leave a fabric gap in between the top and bottom carbon layers. After filling this fabric gap with gel electrolyte, the fabric-gel layer can act as a charge separator that prevent top and bottom electrode short circuit. In order to maintain this fabric gap, the pressure applied in spray coating reduces to 20 psi (1.38 bars) and the spray distance increases to 7.5 cm. This set-up ensures that the carbon material slowly arrives on the cotton fabric surface but is unable to penetrate it. The spray-coating process was repeated eight times and this type of electrode is denoted as C_{ot8a}. In this study the area of each C_{ot8a} fabric electrode is 0.785 cm^2, the thickness of this type of electrode is about 500 µm, and each C_{ot8a} fabric electrode has a weight of 69.8 $mg.cm^{-2}$ before coating. The carbon materials in each piece of C_{ot8a} electrode are 1.80 $mg.cm^{-2}$ (2.58%).

6.3.2 Improved vacuum impregnation process for flexible solid-state fabric supercapacitor

In the next step two pieces of poly-cotton fabric electrodes or a single piece of C_{ot8a} type electrode were dipped into the gel electrolyte under vacuum. The aim of this step is to enhance the wettability between the fabric electrodes and the polymer electrolyte.

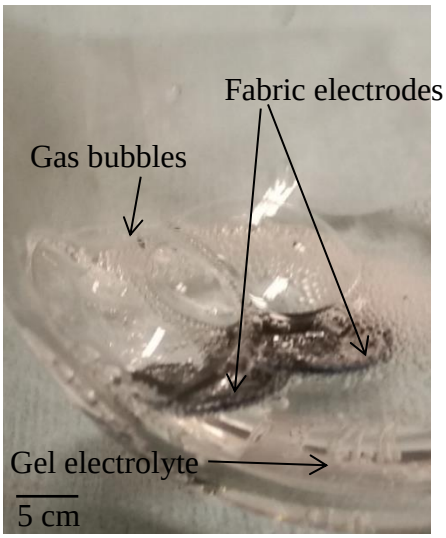

Figure 6.4: Vacuum impregnation process set-up with PVA gel electrolyte and fabric electrode.

Figure 6.4 shows the vacuum impregnation process of fabric electrodes with the gel electrolyte. In comparison with the aqueous electrolyte, the gel electrolyte contains more air inside the solution which comes from the PVA polymer dusts and heating process, the polymer gas bubbles shown in figure 6.4 prevent the air from being extracted from the solution and the fabric samples. This either requires increasing the system's vacuum level until no air bubble exist in the gel solution, process time extension, or heating up the gel electrolyte and stirring the gel solution; however these processes may alter the ingredient percentages of the gel solution, or further damage the fabric samples by removing carbon materials from the fabric electrode. Therefore, the vacuum impregnation process of fabric electrodes with the gel electrolyte is different from the process described in chapter 4.

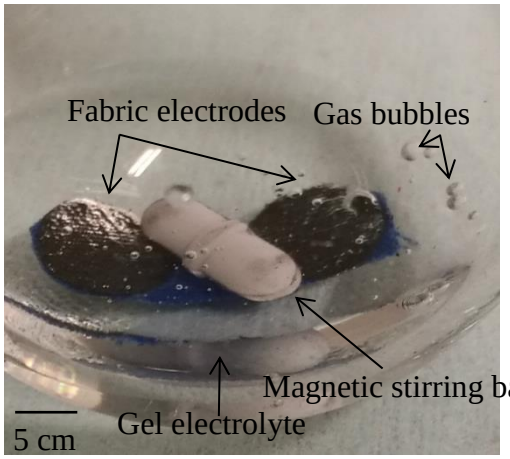

Figure 6.5: New vacuum impregnation process set-up with PVA gel electrolyte and fabric electrode before switching on the vacuum valve.

As shown in figure 6.5, a small and heavy magnetic stirring bar is placed on top of the fabric electrode where there is no carbon material coating, and the fabric electrodes are sunk at the bottom of the Büchi tube. After switching on the vacuum valve and leave a vacuum of 20 mbar for five minutes, it was switched off and the air lock was opened to force the gel electrolyte flow into the fabric electrodes. These processes were repeated five times until the fabric sample sank to the bottom of the gel electrolyte without help from the magnetic stirring bar at the existing room pressure and temperature.

6.4 Solid-state supercapacitor set-up

The assembled two-layer solid-state supercapacitor device shown in figure 6.1 consists of two spray-coated fabric electrodes processed by vacuum impregnation with gel electrolyte. After the vacuum impregnation process, two pieces of the type $B_{thick10}$ or $B_{thick14}$ fabric electrode were stacked together and sandwiched between two pieces of nickel foil, the supercapacitor cell was compressed by metal plates, and the thickness of the two fabric layers was controlled at roughly 400 µm.

For the single-layer cotton solid-state supercapacitor, a cotton electrode (contains gel electrolyte) was sandwiched in between the nickel layers and compressed to roughly 400 µm. Then the compressed supercapacitor cell was cured in the box oven at 70^{o}C for 15 minutes. After the curing process, the dried gel electrolyte at the edge, top and bottom of the fabric electrodes shown in figure 6.1 became a thermal insulating layer. This polymer layer prevents the gel electrolyte (inside the electrode) from drying out during the testing. Finally, the semi-

dried supercapacitor cell was extracted from the nickel foils and inserted into the test tube fitting which. is the same as that for the multilayer supercapacitor presented in chapter 5. During testing the steel spring was released to measure the performance of the device without compression.

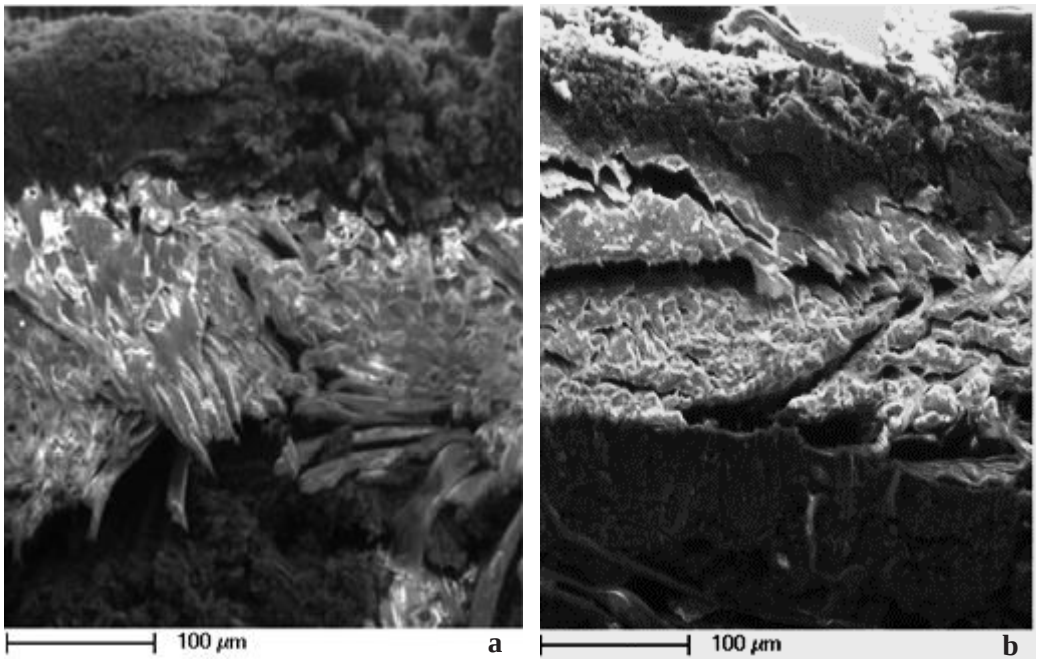

Figure 6.6(a) SEM micrograph of the cross-sectional view of the supercapacitor made with: (a) two pieces of $B_{thick10}$ type electrodes, (b) C_{ot8a} type electrode.

Figure 6.6 (a) shows the SEM image of the cross-sectional view of the supercapacitor with fabric electrode type $B_{thick10}$ and semi-dried gel electrolyte. The darker parts at the bottom and the top of the picture are the carbon material layers; the lighter part located at the centre is the inner side of the type $B_{thick10}$ electrode covered with gel electrolyte, and it is also the interface between two carbon-coated fabric electrodes. As shown in figure 6.7 (b) the improved spray-coating process prevents the carbon material from penetrating the cotton fabric, but leaves a gap inside of the fabric electrode, it forms a sandwich device whereby the top and bottom carbon materials are physically separated. When filling this gap with gel electrolyte, this device shall become a supercapacitor where the gel electrolyte-coated layer acts as the charge separator layer.

6.5 Solid-state supercapacitor test

The two-layer solid-state fabric supercapacitors with three different gel electrolytes, single layer solid-state fabric supercapacitors, and a reference multilayer fabric supercapacitor with

aqueous electrolyte were tested. This section presents an evaluation of the performance of the solid-state supercapacitor.

Table 6.1: Comparison of specific capacitance ($F.g^{-1}$) of the supercapacitors measured using all three techniques.

Electrode information			Specific capacitance		
Electrode type	Electrolyte	Carbon :Fabric ratio(%wt)	CV (25 $mV.s^{-1}$)	GC (0.1 $A.g^{-1}$)	EIS (20 mHz)
$B_{thick10}$	0.25 M Li_2SO_4 gel	6.67	15.5	11.7	9.53
	0.4 M DAP gel	6.67	16.8	15.2	9.2
	0.5 M ADP gel	6.67	20.6	15.4	11.4
	0.5 M ADP (aqueous)	6.67	20.7	17.1	15.5
$B_{thick14}$	0.5 M ADP gel	10.3	16.7	14.2	9.54
C_{ot8a}	0.5 M ADP gel	2.58	26.1	14.9	13.1

Table 6.2: Comparison of area capacitance ($F.cm^{-2}$) of the supercapacitors measured using all three techniques..

Electrode information			area capacitance		
Electrode type	Electrolyte	Carbon :Fabric ratio(%wt)	CV (25 $mV.s^{-1}$)	GC (0.1 $A.g^{-1}$)	EIS (20 mHz)
$B_{thick10}$	0.25 M Li_2SO_4 gel	6.67	0.0564	0.0425	0.0346
	0.4 M DAP gel	6.67	0.0611	0.0552	0.0334
	0.5 M ADP gel	6.67	0.0745	0.0559	0.0415
	0.5 M ADP (aqueous)	6.67	0.0744	0.0621	0.0436
$B_{thick14}$	0.5 M ADP gel	10.3	0.0945	0.0795	0.0535
C_{ot8a}	0.5 M ADP gel	2.58	0.0764	0.0434	0.0382

According to tables 6.1 and 6.2 the two-layer solid-state supercapacitors made by the $B_{thick10}$ electrode with both ADP and DAP gel electrolytes achieve similar area capacitance (around 0.055 $F.cm^{-2}$) and specific capacitance (around 15 $F.g^{-1}$) that is also close to the multilayer supercapacitor with similar electrodes and aqueous electrolyte (table 4.2). These results are higher than those recorded for the supercapacitors made by the same $B_{thick10}$ electrodes with the Li_2SO_4 gel electrolyte (11.7 $F.g^{-1}$and 0.0425 $F.cm^{-2}$). This is because the solubility of Li_2SO_4 in the water-gel solution; the Li_2SO_4 crystals separate from the gel solution and are crystallised during the curing and testing processes; and the crystallised Li_2SO_4 in the electrode cannot provide free ions but blocks the gel electrolyte from coming into contact with the

electrode material. This behaviour significantly reduces the device double-layer capacitance. Table 6 also shows that both specific and area capacitances of the supercapacitors made by the gel electrolyte are worse than those of the supercapacitor made by aqueous electrolyte that was made by the same inorganic salt and same molar concentration. Generally, the gel electrolyte has higher viscosity and resistance than aqueous electrolyte does, but it causes a wettability issue in the solid–state supercapacitor resulting in a reduced capacitance.

The single-layer solid-state supercapacitor made with the C_{ot8a} type electrode demonstrated specific capacitance (14.9 $F.g^{-1}$), which is close to the results achieved by the two-layered devices made by $B_{thick10}$ with the same gel electrolyte (0.5M ADP gel). The reason for this is because this supercapacitor contains similar amounts of carbon materials (2.85 mg in two pieces of $B_{thick10}$ type electrode and 2.30 mg in a single piece of C_{ot8a} type electrode). These carbon materials are uniformly coated into the electrode; however, the area capacitance of the single-layer solid-state supercapacitor is less than that of the two-layer solid-state supercapacitor. Tables 6.1 and 6.2 also show that the two-layer solid-state supercapacitors with 0.5M ADP gel electrolyte achieve the same properties as the multilayer supercapacitors with aqueous electrolyte: the specific capacitance decreases as carbon increases, and area capacitance increases when more carbon materials are coated on to the fabric electrode.

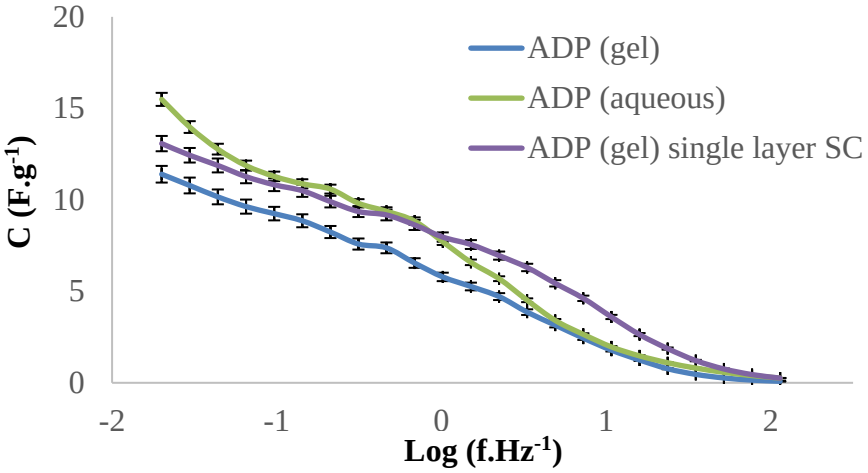

Figure 6.7: Specific capacitance ($F.g^{-1}$) of supercapacitor made using fabric electrode Bthick10, with both aqueous and gel electrolytes, and Cot8a, with from 20 mHz to 112 Hz. The error bars represent the standard deviations that were calculated based on the results from 5 repeated tests.

Figure 6.7 shows that the solid-state supercapacitors made by both $B_{thick10}$ and C_{ot8a} electrodes with ADP gel electrolyte achieve similar capacitance decrease rates at low frequency regions (from 20 mHz to 1 Hz). According to figure 6.8 the solid-state supercapacitor with gel

electrolyte exhibits a lower specific capacitance decrease rate than the multilayer aqueous supercapacitor does at the frequency region (from 1 Hz to 112 Hz).

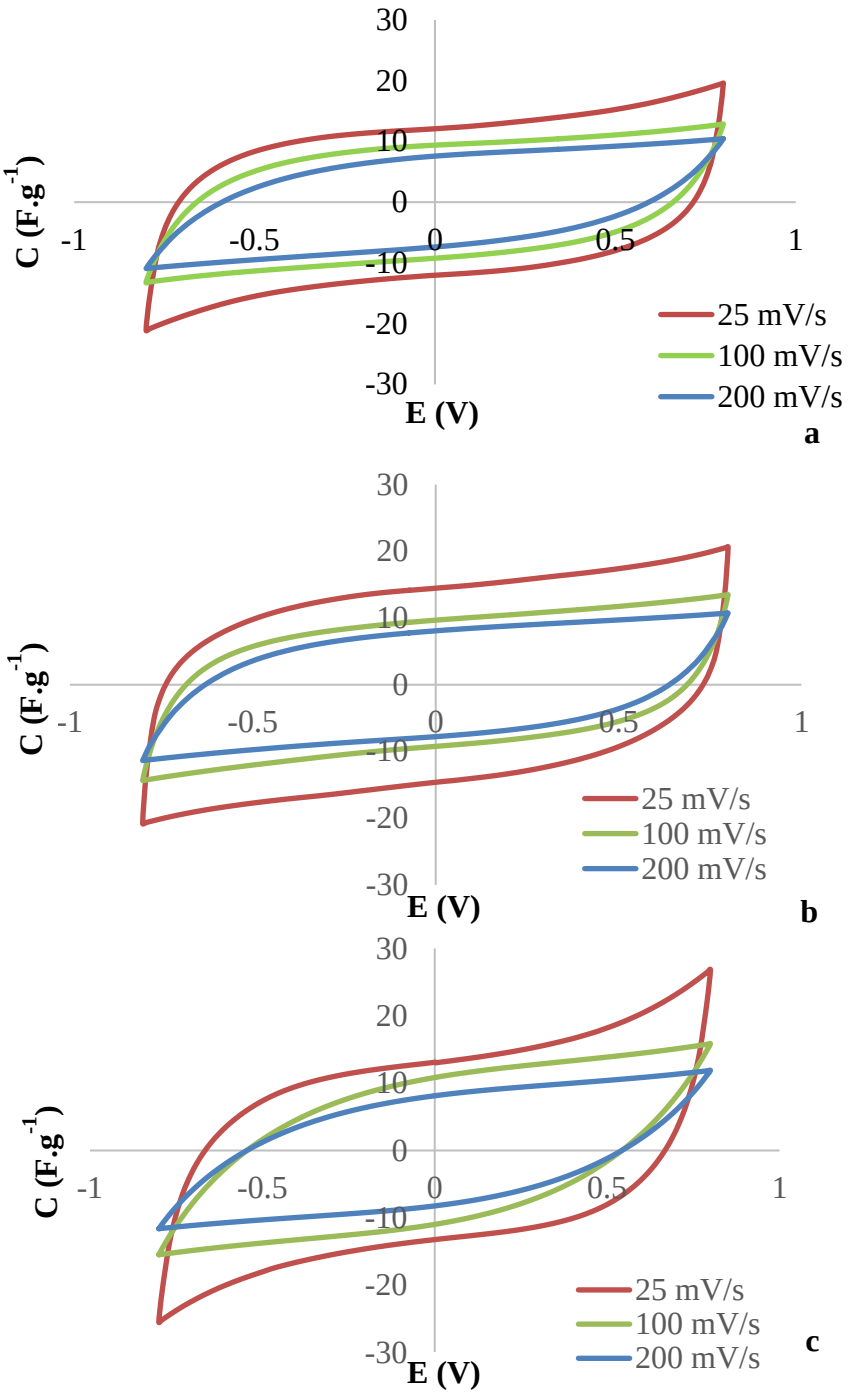

Figure 6.8: CV Test of supercapacitors between +/- 0.8 V at the scan rates of 200, 100, 25 $mV.s^{-1}$ with: (a) two pieces of $B_{thick10}$ type electrodes with ADP gel electrolyte, (b) two piece of $B_{thick10}$ type electrodes with ADP aqueous electrolyte, (c) single-piece C_{ot8a} type electrode with ADP gel electrolyte.

As shown in figure 6.8, electrochemical reactions or device short circuits did not occur in the CV test, which proves that the three types of fabric supercapacitor are electrochemically stable at scan rates from 25 to 200 $mV.s^{-1}$. The CV curves (test at 25 $mV.s^{-1}$) of solid-state fabric supercapacitor made by the ADP gel electrolyte (figure 6.4 (a) and (c)) are more curved (resistive) than the CV result of the multilayer fabric supercapacitor made by the ADP aqueous electrolyte (figure 6.4 (b)). This shows that the supercapacitor made with the ADP gel electrolyte exhibits higher resistance than the supercapacitor made with the ADP aqueous electrolyte. According to figure 6.8 (c), the current/voltage rate of the CV curve of the supercapacitor with a single piece of cotton fabric electrode changes from between 0.5 to 0.8 volts. Similar electrochemical behaviours occur in the supercapacitor with the cotton electrode and aqueous electrolyte (figure 5.7 (d)). This is due to the electrolysis of water at high voltage which corrodes the fabric electrode and introduces extra conductance and capacitance.

Table 6.3: Specific capacitance ($F.g^{-1}$) of supercapacitor using $B_{thick10}$ type electrodes with ADP gel and aqueous electrolyte and C_{ot8a} (gel electrolyte) at different scan rates.

Electrode information			CV scan rate ($mV.s^{-1}$)					
Electrode type	25	25	25	50	75	100	150	200
$B_{thick10}$	0.5 M ADP gel	6.67	20.6	17.5	14.8	13.2	11.8	10.2
	0.5 M ADP (aqueous)	6.67	20.7	16.2	14.7	13.4	12.1	12
C_{ot8a}	0.5 M ADP gel	2.58	26.1	20.4	19.6	19.2	17.5	16.8

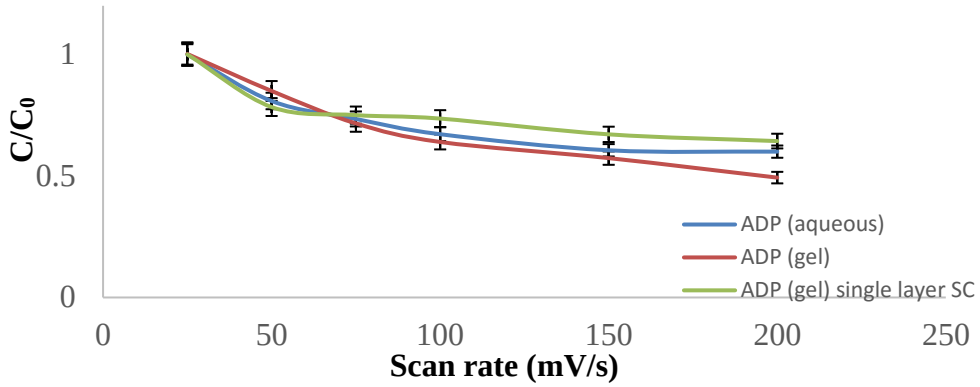

Figure 6.9: Specific capacitance ($F.g^{-1}$) of supercapacitor using $B_{thick10}$ type electrodes with ADP gel and aqueous electrolyte and C_{ot8a} (gel electrolyte) at different scan rates. The error bars represent the standard deviations that were calculated based on the results from 5 repeated tests.

As shown in table 6.3 and figure 6.9, the specific capacitance of the $B_{thick10}$ electrode two-layer solid-state supercapacitor with the ADP aqueous electrolyte tested at 25 $mV.s^{-1}$ drops from 20.7 $F.g^{-1}$ to 12 $F.g^{-1}$ at 200 $mV.s^{-1}$, which is about a 40.6% decrease in capacitance. The supercapacitor assembled using the same $B_{thick10}$ electrodes with the ADP gel electrolyte shows a much bigger specific capacitance decrease from 20.6 $F.g^{-1}$ at 25 $mV.s^{-1}$ to 10.2 $F.g^{-1}$ at 200 $mV.s^{-1}$, (50.6%). The single-layer solid-state supercapacitor made with very thick cotton electrode (C_{ot8a}) shows a drop of specific capacitance of about 35.6% at the higher scan rate. These results indicate the solid-state fabric supercapacitor with the gel electrolyte has a wettability issue; the gel electrolyte cannot make contact with all of the carbon material. At a high scan rate less double-layer capacitance arises at the electrode/electrolyte interface.

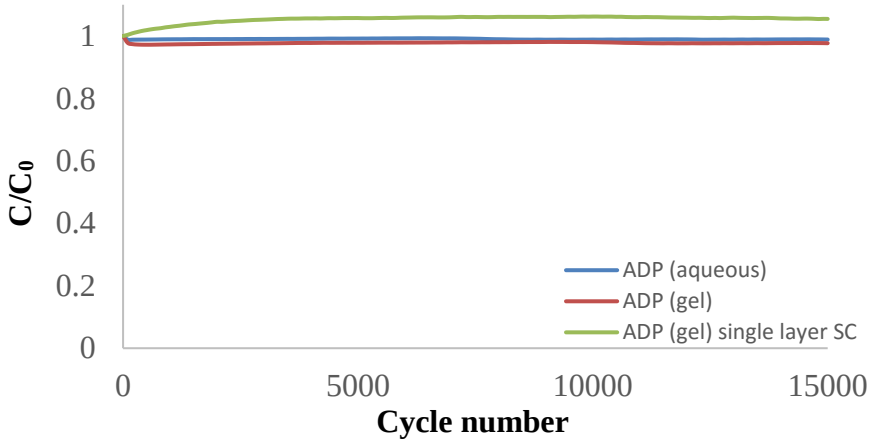

Figure 6.10: Stability test of supercapacitor using $B_{thick10}$ type electrodes with ADP gel and aqueous electrolyte and C_{ot8a} (gel electrolyte) over 15000 cycles. Co is the initial area

capacitance of the device measured from cycle 1 of the CV test between +/- 0.8 V at the scan rate of 200 mV.s^{-1}.

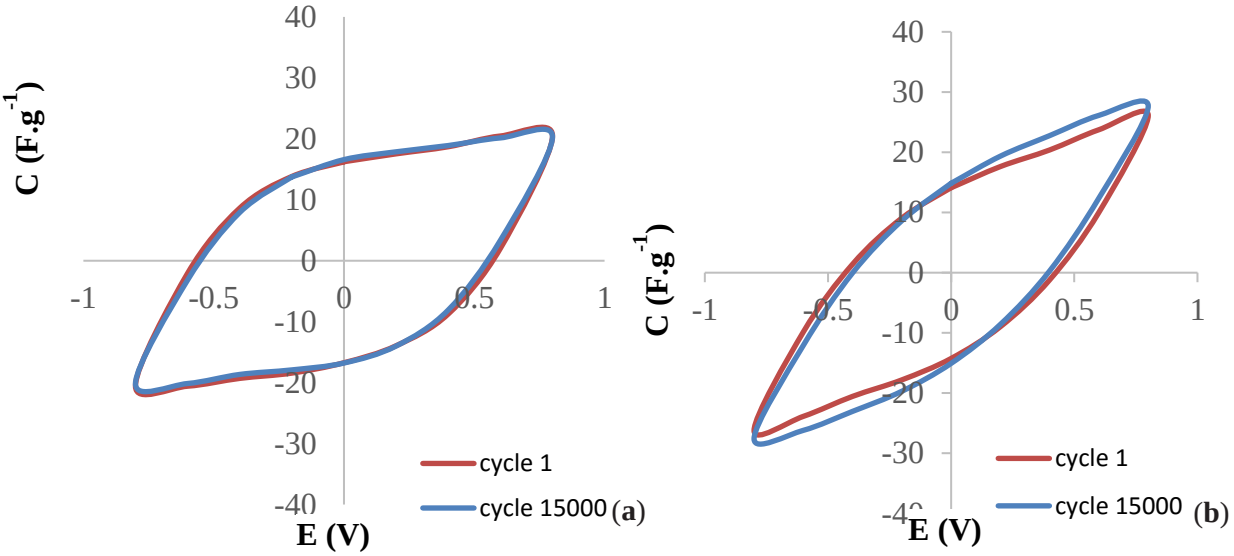

Figure 6.11: CV test of the solid-state supercapacitor for 1 and 15000 cycles between +/- 0.8 V at a scan rate of 200 mV.s^{-1} with (a) two pieces of $B_{thick10}$ type electrode, (b) single piece of C_{ot8a} type electrode.

Figures 6.10 and 6.11 show the device stability with CV responses. The overall capacitance variation of the two-layer solid-state supercapacitor with the gel electrolyte has less than 5% correlation with the small temperature changes in the test lab. The high device stability indicates excellent adhesion of the carbon powders forming a continuous conducting network, which is due to the use of the spray-coating technique and vacuum impregnation process with the polymer binder and gel electrolyte. The spray-coating process results in the blend of activated carbon and carbon black powder being spread uniformly over the fabric samples; it then infiltrates the poly-cotton fabrics and fills up the fabric yarns to form a conductive network. The vacuum impregnation process ensures that the gel electrolyte makes contact with the maximum amount of the electrode materials to form an effective double-layer interface during characterisation.

The device stability results shown in figures 6.10 and 6.11 indicate that the overall capacitance of the single-layer supercapacitor with gel electrolyte increases more than 5% over 15000 cycles, which contributes to the wettability issue. Initially after the vacuum impregnation process, not all of the electrode materials make contact with the electrolyte. During the CV test, the gel electrolyte slowly diffuses to cover the entire electrode material surface forming

double-layer capacitance. This is the reason why the capacitance steadily increases during the 3000 cycles.

Table 6.4: Normalised ESR (Ω.cm) of the supercapacitors at different scan rates.

Electrode information			Frequency /Log (f.Hz^{-1})					
Electrode type	Electrolyte	Carbon :Fabric ratio(%wt)	-1.7 (20 mHz)	-0.67 (0.21 Hz)	0.35 (2.2 Hz)	1.37 (23 Hz)	1.72 (52 Hz)	2.05 (112 Hz)
$B_{thick10}$	0.5 M ADP gel	6.67	257	117	96.4	87.0	82.3	74.5
	0.5 M ADP (aqueous)	6.67	99.3	50.5	41.5	35.3	32.9	30.1
C_{ot8a}	0.5 M ADP gel	2.58	248	122	110	106	105	104

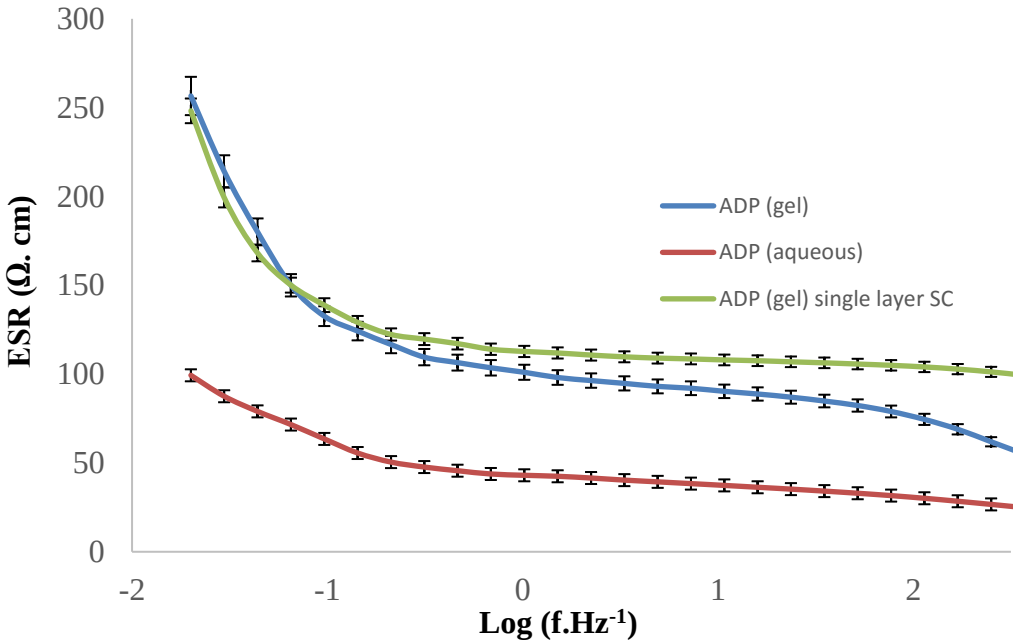

Figure 6.12: Bode plot of the specific supercapacitors ESR (Ω.cm^{-2}) from 100 Hz to 20 mHz, extracted from EIS test. The error bars represent the standard deviations that were calculated based on the results from 5 repeated tests.

According to figure 6.12, both the single-layer and double-layer supercapacitors with the ADP gel electrolyte demonstrate higher normalised ESR - from 20 Hz to 100 Hz - than the multilayer fabric supercapacitor with aqueous electrolyte. This is because gel electrolyte exhibits higher ESR than aqueous electrolyte.

Table 6.5: Normalised ESR (Ω.cm) and area ESR (ESR) (Ω.cm^{-2}).

Electrode information			ESR (Ω.cm^{-2})		ESR (Ω.cm)	
Electrode type	Electrolyte	Carbon :Fabric ratio(%wt)	GC (0.1 A.g^{-1})	EIS (20 mHz)	GC (0.1 A.g^{-1})	EIS (20 mHz)
$B_{thick10}$	0.25 M Li_2SO_4 gel	6.67	118	155.5	182	241
	0.4 M DAP gel	6.67	35.6	170.3	55.0	263
	0.5 M ADP gel	6.67	39.7	166.3	61.2	257
	0.5 M ADP (aqueous)	6.67	24.1	138.6	24.6	142
$B_{thick14}$	0.5 M ADP gel	10.3	69.5	164.8	107	253.4
C_{ot8a}	0.5 M ADP gel	2.58	96.9	162.7	183	248

According to the results from the GC tests shown in table 6.5, the two-layer solid-state fabric supercapacitors with ADP and DAP gel electrolytes achieve similar normalised ESR (55 Ω.cm for DAP devices and 61.2 Ω.cm for ADP devices) and area ESR (35.6 Ω.cm^{-2} for DAP devices and 39.7 Ω.cm^{-2} for ADP devices). These results show that fabric electrodes are fully impregnated with the gel electrolyte which forms a gel barrier that acts as the paper separator

to prevent the short circuits. The normalised ESR (182 Ω.cm) and area ESR (35.6 $\Omega.cm^{-2}$) of two-layer solid-state fabric supercapacitors with Li_2SO_4 gel electrolyte are higher than those the others (ADP and DAP devices); this is due to the fact that some Li_2SO_4 crystals separate from the gel electrolyte during the curing process, which increases its resistance. Table 6.6 also indicates the normalised and area ESR (107 Ω.cm, 69.5 $\Omega.cm^{-2}$) of two-layer solid-state fabric supercapacitors (ADP gel electrolyte) with type $B_{thick16}$ electrode are higher than for the same device made with $B_{thick10}$. This shows that extra material coating leads to a wettability issue that increases the electrode resistance. A similar issue is also found in the GC test results of the single-layer solid-state supercapacitor made with the C_{ot8a} type cotton electrode. In this type of electrode, a fabric gap filled with gel electrolyte occurs between the top and bottom electrodes, and it introduces high resistance that increases the normalised and area ESR of both devices.

Table 6.6: Energy and power density of supercapacitor made using a spray-coated fabric electrode determined by GC test (0.1 $A.g^{-1}$)

Electrode information			Energy and power density	
Electrode type	Electrolyte	Carbon:Fabric ratio(%wt)	Energy density ($Wh.kg^{-1}$)	Power density ($kW.kg^{-1}$)
$B_{thick10}$	0.25 M Li_2SO_4 gel	6.67	13.4	0.603
	0.4 M DAP gel	6.67	17.5	2.0
	0.5 M ADP gel	6.67	17.7	1.80
	0.5 M ADP (aqueous)	6.67	19.7	2.96
$B_{thick14}$	0.5 M ADP gel	10.3	16.3	0.667
C_{ot8a}	0.5 M ADP gel	2.58	17.2	0.744

Table 6.6 shows that the energy densities of two-layer solid-state supercapacitors made by $B_{thick10}$ type electrodes with ADP and DAP gel electrolytes are 17.7 and 17.5 $Wh.kg^{-1}$; these densities are similar to that of the single-layer device made by the C_{ot8a} type electrode (17.2 $Wh.kg^{-1}$). The two-layer solid-state supercapacitors with Li_2SO_4 gel electrolyte demonstrates lower energy density and power density than all other devices (13.4 $Wh.kg^{-1}$ and 0.603 $kW.kg^{-}$

[1]). However, both the energy density and power density of the supercapacitors with gel electrolytes are lower than the supercapacitors with aqueous electrolytes which contain the same salt and molar concentration (19.7 $Wh.kg^{-1}$ and 2.96 $kW.kg^{-1}$). The gel electrolyte has much higher viscosity than the aqueous electrolyte; the fabric yarns are not fully in contact with the gel electrolyte, which causes the wettability issue.

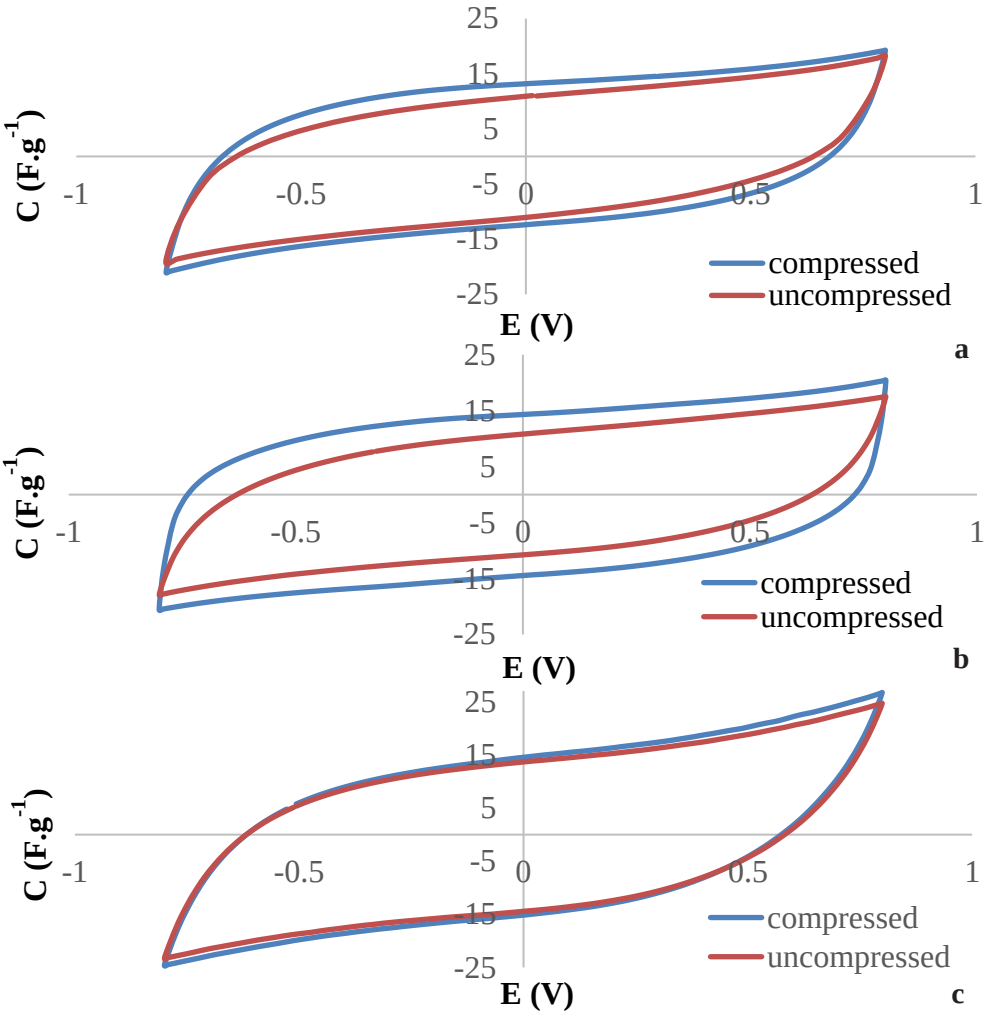

Figure 6.13: Compression test of supercapacitor with CV method with: (a) two pieces of $B_{thick10}$ type electrodes with ADP gel electrolyte, (b) two pieces of $B_{thick10}$ type electrodes with ADP aqueous electrolyte, (c) single-piece C_{ot8a} type electrode with ADP gel electrolyte between +/- 0.8 V at the scan rate of 25 $mV.s^{-1}$.

Figure 6.13 shows the CV performance of fabric supercapacitor with three sets of electrode and electrolyte combinations, and the compression pressure (by stainless steel spring) applied previously was about 25 $N.cm^{-2}$. After releasing the spring in the test cell, the specific capacitance of the supercapacitor made with two piece $B_{thick10}$ type electrodes with the ADP aqueous electrolyte reduces to 15.6 % from 20.5 $F.g^{-1}$ is drops to 17.3 $F.g^{-1}$, As shown in figure

6.14 both two-layer and single-layer solid-state supercapacitors with gel electrolytes achieve less specific capacitance decrease after removing the compression spring. In the two-layer solid-state supercapacitor, specific capacitance drops to 7.46% from 20.6 $F.g^{-1}$ drops to 19.1 $F.g^{-1}$. The specific capacitance decrease of the single-layer solid-state supercapacitor is 8.04% from 26.1 $F.g^{-1}$ drops to 24.0 $F.g^{-1}$.

Table 6.7: Test results of fabric supercapacitors with and without compression determined by GC test (0.1 $A.g^{-1}$).

	Electrode information			Capacitance	ESR	
Electrode type	Electrolyte	Carbon:Fabric ratio(%wt)	Compression	Specific capacitance ($F.g^{-1}$)	ESR ($\Omega.cm^{-2}$)	ESR (Ω.cm)
$B_{thick10}$	0.5 M ADP gel	6.67	Yes	15.4	39.6	61.2
	0.5 M ADP gel	6.67	No	14.5	41.6	63.9
	0.5 M ADP (aqueous)	6.67	Yes	17.1	24.0	37.1
	0.5 M ADP (aqueous)	6.67	No	14.4	35.6	55.0
C_{ot8a}	0.5 M ADP gel	2.58	Yes	14.9	62.3	183
	0.5 M ADP gel	2.58	No	13.7	102.7	194

According to table 6.7 the ESR of the multilayer supercapacitor made by $B_{thick10}$ and ADP aqueous electrolyte increases by 32.7% (from 0.054 Ω.cm-2 (37.1 Ω.cm) and increases to 0.08 Ω.cm-2 (55 Ω.cm). . This is because the fabric electrodes are soft and compressible. After reducing the pressure applied on the multilayer device, fabric electrodes will restore its original thickness by taking apart the carbon conductive network which results in a large increase in device resistance. Two types of solid-state supercapacitor cell show less than 10% increase in both ESRs (Ω.cm and $\Omega.cm^{-2}$) because, in solid-state supercapacitors, the cured gel electrolyte

can maintain the designed thickness of the fabric electrode regardless of the pressure applied on the supercapacitor cell.

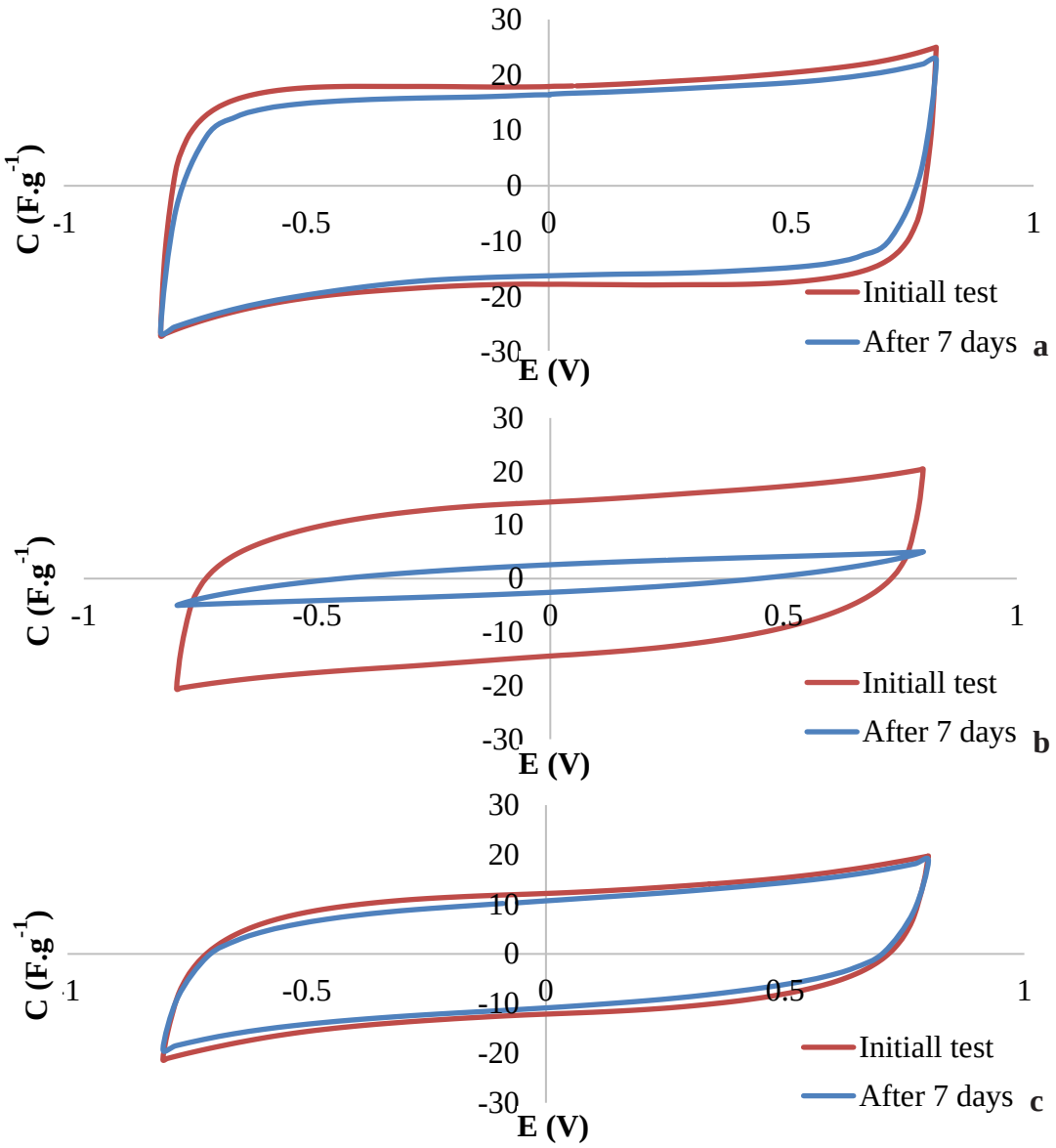

Figure 6.14: Supercapacitor test over seven days with: (a) two piece of $B_{thick10}$ type electrodes with ADP gel electrolyte, (b) two piece of $B_{thick10}$ type electrodes with ADP aqueous electrolyte, (c) single-piece C_{ot8a} type electrode with ADP gel electrolyte between +/- 0.8 V at the scan rate of 25 $mV.s^{-1}$.

Figure 6.14 shows the CV test results of fabric supercapacitors with three sets of electrode and electrolyte combinations over seven days. As shown in figure 6.14 (a) after keeping the fabric supercapacitor (with ADP aqueous electrolyte) in the test cell for seven days without any testing procedures, its CV results indicate that this type of device becomes much more resistive and very small capacitance can be found. This is probably because most of the solvent (DI

water) in the aqueous electrolyte evaporated, and the ADP crystal separated out from the electrolyte, thus preventing the formation of a double-layer capacitance.

As shown in Figure 6.16 (a) and (c) the CV results of two kinds of fabric supercapacitor with ADP gel electrolyte do not have significant difference after being kept in the test cell for seven days. This could be because the dried polymer covers the edge of the supercapacitor cell preventing the solvent evaporating from the gel electrolyte, which in turn extends the device life time.

6.6 Conclusions

This chapter presents a two-layer supercapacitor on a fabric substrate. The two-layer solid-state fabric supercapacitor based on $B_{thick10}$ type electrodes with ADP gel electrolyte achieves a mass-specific capacitance of 15.4 $F.g^{-1}$, area-specific capacitance of 0.0559 $F.cm^{-2}$, a low normalised ESR of 61.2 Ω.cm, and good cycling stability of less than 3% capacitance variation over 15000 cycles. Another achievement from the work in this chapter is the single-layer solid-state fabric supercapacitor based on C_{ot8a} type electrodes with ADP gel electrolyte. This device achieves a mass-specific capacitance of 14.9 $F.g^{-1}$, area-specific capacitance of 0.0434 $F.cm^{-2}$, a normalised ESR of 183 Ω.cm, and good cycling stability of less than 5% capacitance variation over 15000 cycles.

In comparison with other works, these are not as good as the aqueous supercapacitor; however, the individual carbon electrode can be sprayed on to selected areas of the fabrics, and the proposed supercapacitor is fully wearable, scalable, inexpensive, and made without an individual charge separator. This work offers a practical approach for achieving low-cost and reliable energy storage supercapacitors in fabrics for wearable applications. The final device could see use applications in a wide range of wearable electronic systems like energy harvesters, medical sensors, and a wide range of personal wearable electronics.

7 Conclusions and further improvements

This thesis presents the past 48 months' progress on the implementation of a supercapacitor based on fabric substrates. This chapter summaries the thesis by concluding the outcome from this work, discussing its importance from wider aspect of wearable electronics and figure out the further recommendations of the research in area.

7.1 Literature review

This report reviews all the literature on making flexible supercapacitors, including a comprehensive literature review about the capacitive device from capacitor to supercapacitor, a detailed review of the supercapacitor theories, discussion about supercapacitor structure, material selection for flexible supercapacitors and implementation of a fabric supercapacitor.

The literature review in this thesis also examined the advantages and disadvantages of existing fabric supercapacitors. Most of these devices were based on expansive carbon materials (i.e. CNT, graphene and graphene oxide) and pseudo-capacitive materials, their electrodes generally implemented with either non area selective method like dipping or low throughput method like electrochemical deposition, in addition significant amount of the works were build supercapacitor using conductive fabric substrates that are much expansive than normal fabrics. Normally dialy use wearable electronics require a highly stable easy and fast fabricated fabric supercapacitor, therefore these devices are not the best options. However, there were some example devices build up on general proposes electrode materials like activated carbon and calligraphic ink, the supercapacitors presented in these works also achieved competitive electrochemical performance and provide some good features like high stability, high reliability and are not expansive than those devices made by expansive carbon materials. The literature reviews also showed that the post-treatment of fabric electrode shall improves the device electrochemical performance.

7.2 The characterisation of supercapacitor

This chapter summarises the basic mathematical representation of capacitor/supercapacitor in both DC and AC condition. In AC circuits supercapacitor is behave different with capacitor, at low frequency operation region diffusion capacitance dominates the behaviours of supercapacitor, its circuit model turns into an infinite resistor-capacitor ladder network called Warburg element. This chapter also illustrates three electrochemical test procedures: impedance spectroscopy, cyclic voltammetry and galvanostatic cycling, and explains the

methods, circuit model and assumptions about extracting the important value like capacitance and resistance from these three procedures

7.3 Dip-coated fabric electrode for supercapacitors

Seven types of dip-coated fabric electrode were fabricated to assemble three-layer supercapacitors with aqueous electrolyte, these electrodes include two different poly-cotton fabrics. For poly-cotton fabric with 300 μm thickness, five different types of material ink were prepared to load carbon material into the electrode.

It was found that increase the amount of carbon dip coated into the fabric electrode does increase both the specific and area capacitance of the supercapacitor up to certain limit. The additional conductive additive species (carbon black) in the fabrics electrode dose reduce the device ESR but reduce both the device specific and area capacitance. Vacuum impregnation process did increase the specific and area capacitance of the supercapacitor made with dip-coated fabric electrode, and maintain the high device stability and physical robust against The mechanical durability test (mandrel test), however it will slightly increase the device ESR.

The supercapacitor with electrode type C2 achieved the best electrochemical performance than other supercapacitor tested in this chapter. The supercapacitor with electrode type C2 achieves a specific capacitance of 14.1 $F.g^{-1}$ (table 4.2), area-specific capacitance of 0.125 $F.cm^{-2}$ (table 4.3), and a low normalised ESR of 22 Ω.cm (table 4.6), and achieves an excellent cycling stability over 15000 cycles (figure 4.11).

7.4 Spray-coated fabric electrode for supercapacitors

The fabricated supercapacitor in this chapter meets the expectation of the initial aims: The improved ink formation and the use of spray coating technique allows a low cost and fast way to fabricates area selective carbon inserted fabric electrode for supercapacitor design. In spray-coated fabrics the material coated into the fabric electrode can be controlled to obtain the optimal electrochemical performance.

In this chapter four different fabric substrates and a metal substrate were examined to make the electrode for supercapacitor. It was found that cotton fabric cannot hold as much carbon materials as the poly-cotton fabrics. For silk electrode they cannot hold as much carbon material as other fabric electrode, however in comparison with all other results, the multilayer supercapacitors with aqueous electrolyte and silk electrode achieves the highest specific

capacitance of 30.4 $F.g^{-1}$. This result is useful for the future electrode substrate selection of the fabric supercapacitor to optimise the electrochemical performance efficiency of carbon materials.

The supercapacitor with electrode type B_{thick} achieved the most stable specific capacitance among all other electrodes, its specific capacitance (around 15 $F.g^{-1}$,table 5.2) is not varying significantly with respect of the carbon weight in the fabric electrode. However, its area capacitance is increases as more carbon spray-coated into the fabric electrode (table 5.2), this type of supercapacitor also demonstrated a good cycling stability and mechanical durability.

7.5 Flexible solid-state fabric-based supercapacitor

This chapter presents four types of two-layer fabric solid-state supercapacitor, these were based B_{thick} fabric electrodes with three different types of gel electrolyte, and a single layer fabric solid-state supercapacitor based on the modified cotton carbon electrode was fabricated. These fabric solid-state supercapacitors demonstrated a good level of electrochemical stability (figure 6.8 and figure 6.9) with respect of CV scan rate and EIS test frequency.

The performance of two-layer and single layer fabric solid-state supercapacitor was tested. The two-layer device with $B_{thick14}$ fabric electrode and ADP gel electrolyte achieved of 15.4 $F.g^{-1}$ (table 6.1), area-specific capacitance of 0.0559 $F.cm^{-2}$ (table 6.2), and a normalised ESR of 61.2 Ω.cm(table 6.6), The single layer device with C_{ot8a} fabric electrode and ADP gel electrolyte achieved of 14.9 $F.g^{-1}$ (table 6.1), area-specific capacitance of 0.0434 $F.cm^{-2}$ (table 6.2), and a normalised ESR of 183 Ω.cm (table 6.6). These two types of supercapacitor are electrochemically stable with no more than 5% capacitance variation over 15000 cycles.

Although The solid-state fabric supercapacitor proposed in this chapter achieves worse results (i e. lower capacitance and higher ESR) than the three layer aqueous supercapacitor with the same fabric electrodes. However, these devices demonstrated lower performance decrease when remove the compression spring (figure 6.14), in addition after not test the supercapacitor for seven days, the solid-state supercapacitor suffer much less performance lost than the supercapacitor with aqueous electrolyte.

The proposed solid-state fabric supercapacitor points the potential to actual integrate fabric supercapacitor onto the e-textile without complicated packaging set up or suffer a big electrochemical performance lost.

7.6 Future work

The novelties and publications arising in this thesis will have a positive influence on the development of fabric supercapacitor for wearable electronic applications. This final part of thesis discusses for the future work to improve the prototype discrete fabric supercapacitors for improved performance and integration capability into wearable electronic system.

Firstly, the fabric electrode designs should be further improved. This applies to both spray printable inks and fabric substrate. The carbon ink developed in this work are very basic contains carbon, binder, surfactant and solvent, other ink ingredients for the supercapacitor like carbon nanotube, graphene and its relative, redox materials, conductive polymer, hardener, toughening agent, coupling agent and other functional additives are necessary for the carbon ink design. An exclusive evaluation of the completed carbon ink would be necessary to obtain maximum electrochemical performance and compatibility with the fabric substrate. The fabric substrates are critical for the fabric supercapacitor electrode design, as shown in the chapter five electrode based on different fabric substrate shows a big difference in term of their electrochemical performance. In the future fabric supercapacitor electrode design the selection of fabric substrates and its compatibility of the carbon ink are responsible for the electrochemical performances and mechanical durability.

Secondly, the spray-coating process applied in this thesis is optimised for the existing device and material combinations, but there were some significant shortages that limit the electrochemical performance of spray-coated electrode. Firstly, the spray-coating process of this thesis use the normal room gas and performed in non-enclosed fume cabinet, the gas may be reacting with the ink and degrade the quality of the material ink. Secondly the spray-coating kits used in this thesis only allows a roughly control about the spray-coating quantity, it is not ideal for optimise the gravimetric value of supercapacitor. Further optimisation of the spray-coating process includes move the entire process into the sealed fume cabinet and use inert gas for spray coating process, and try different spray coating system to exactly control the amount of material that spray-coated into the fabric electrode.

Thirdly, the gel-electrolyte of the fabric supercapacitor need to be optimised. The gel-electrolyte presented in this thesis is based on water with water soluble polymer and salt, it is non-corrosive and capable for wearable electronic designs, however water based gel-electrolyte suffer from evaporation problem that reduce its device life time. This problem also limits the choice of the device packaging selection, the fitting tube used in this thesis is not suitable with

the wearable electronics. These problems can be mends by modify the gel electrolyte with some non-hazardous material, polymer and solvent that has low evaporation rate, also the final device requires a suitable packaging process to seal the device in a fine polymer film that can be integrated into wearable electronic system.

Fourthly, the device encapsulation and current collector of the fabric supercapacitor need to be improved. A complete fabric supercapacitor for wearable electronics cannot be hold in the large, bulky and heavy test cell like PFA tube or a metal coin cell, it requires several flexible material layer to connect fabric supercapacitor to the wearable system and provide environmental protection to extend the life time of the supercapacitor. These improvements can be done by fabricate different material layers on top of the fabric supercapacitor to provide electrical connectivity and protection against the environment.

Finally, the structure of the single fabric layer supercapacitor need to be modified. The single layer device presented in chapter 6 use the fabric yarns as the charge separator that physically separate the top and bottom carbon electrode. It is not a universal solution that may not applied for other type of fabrics. This problem can be solved by coated a very flexible, dense and lightweight polymer layer into the fabric before electrode coating process, theoretically this polymer layer can act as charge separator that prevent the top and bottom electrode short circuit each other, and hold the gel electrolyte to provide ionic conductivity for double layer capacitor.

Appendix A Metal passivation test

A test was performed to examine the effect of passivation on the supercapacitor performance. Table 1 is a summary of the pseudo-capacitance produced by 4 different metal materials. The test cell used in this test is identical to the configuration of an encapsulated supercapacitor shown in figure 2.6, with a 1M Li_2SO_4 aqueous Electrolyte. But the fabric electrode is replaced with the selected metal. The pseudo-capacitance generated from the oxide material is measured using an EIS test with a 10mV sine wave input. A capacitance variation test is also performed, with applied potential differences within +/- 0.8V and a scan rate of 200 $mV.s^{-1}$. This test will show the percentage change of capacitance after scan the cell for 200 cycles.

Table A.1: Pseudo-capacitance of different encapsulation material due to passivation effects

Test material	Steel(iron)	Copper	Aluminium	Nickel
Capacitance per unit area ($mF.cm^{-2}$)	28.53	20.2	22.52	20.1
Capacitance variation (%)	-19.1%	-76%	-73.9	-40%

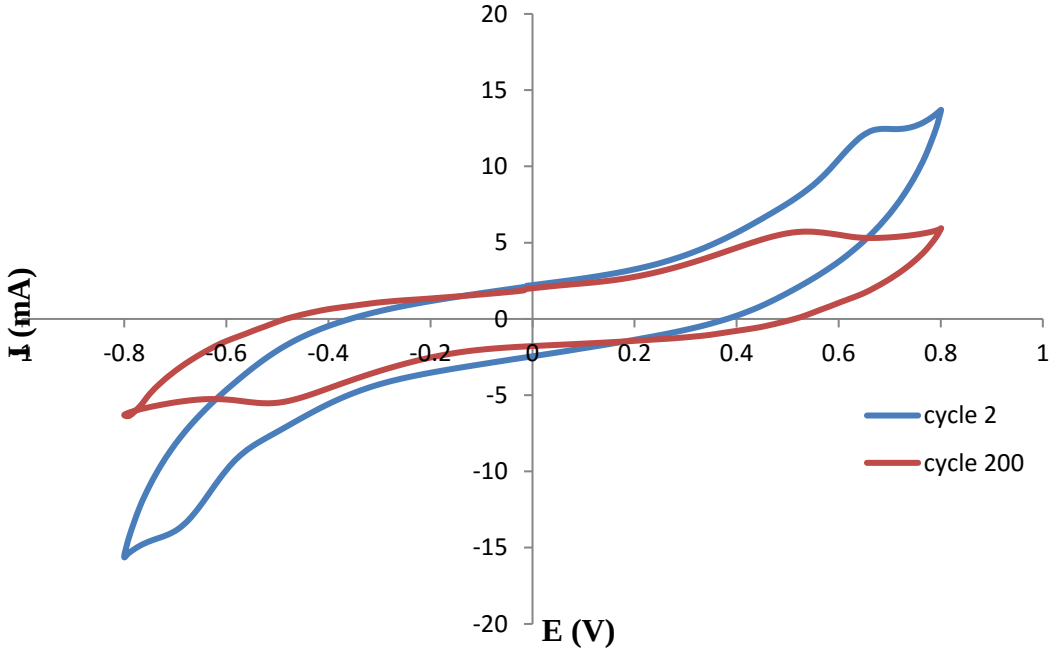

Figure A.1 Current/voltage relationship of steel at 2 and 200 cycles.

Figure A.1 is shows the current/voltage relationship of steel in the 2nd and 200th cycle of the CV test. After scanning the cell for 200 cycles, the potential difference between top and bottom electrode is in between 0.3 V and 0.5 V, the current is increasing due to the corrosion of steel immersed in the electrolyte, and is consequently denoted as faradaic current. Simultaneously, passivation of nickel material occurs and slows the corrosion, consequently the current reaches a peak value then falls to a steady state value. The capacitance generated by this process is pseudo-capacitance that should be minimised to fabricate pure electrical double layer supercapacitor

According to table A.1, steel (iron) will produce the most capacitance due to its passivation process, and this extra capacitance will vary randomly due to environmental and test conditions. For copper and aluminium, the capacitance caused by their passivation process varies significantly at a higher number of test cycles increasing. Copper and aluminium are thermally sensitive materials and so it is more likely that their passivation capacitance will be affected by the surrounding temperature. Nickel produces less capacitance due to its passivation in comparison with iron has a lower level of capacitance variation after 200 cycles in comparison with copper and aluminium. In summary, by encapsulating the supercapacitor with nickel the performance of the encapsulated supercapacitor will have the potential to achieve high stability.

Appendix B supercapacitor using different device packaging material

The stability of the encapsulated supercapacitor is tested by cyclic voltammetry for 200 cycles. In this section the corresponding CV graph of the devices in Figure B.1 and Figure B.2 will discussed. The device is tested with an input voltage range of +/- 0.8 V at scan rate of 200 $mV.s^{-1}$.

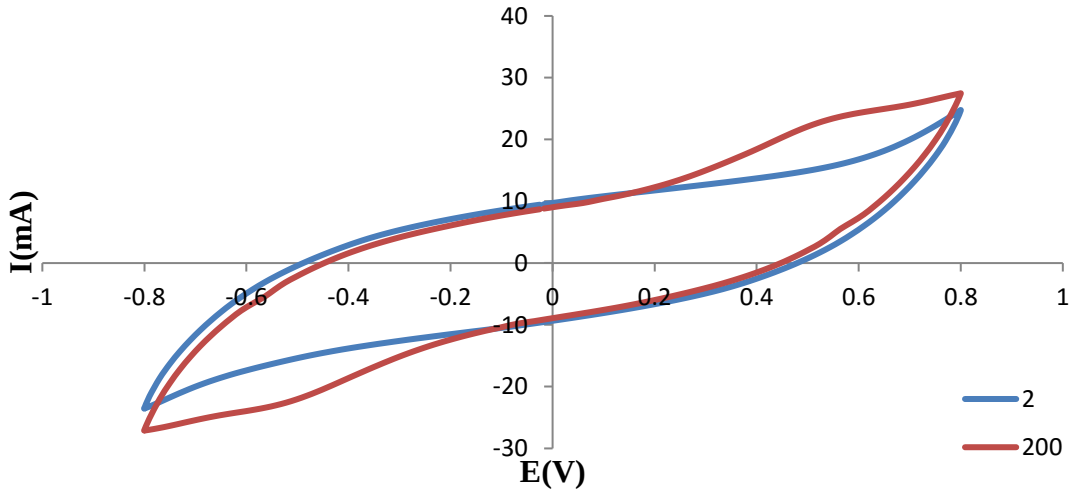

Figure B.1: CV graph of steel encapsulated supercapacitor at cycle 2 and cycle 200.

According to figure B.1 the CV characteristic of a steel encapsulated supercapacitor at cycle 2 is different from the characteristic at cycle 200. At high voltage (above 0.5 V or below -0.5 V at opposite direction) metal corrosion and passivation occurs that will change the shape of the CV characteristic. If these reactions did not occur, the shape of the CV characteristic for a pure double layer supercapacitor would take the form of a rectangular box as shown in Figure B.2 and will not have significant change as the cycling number increases.

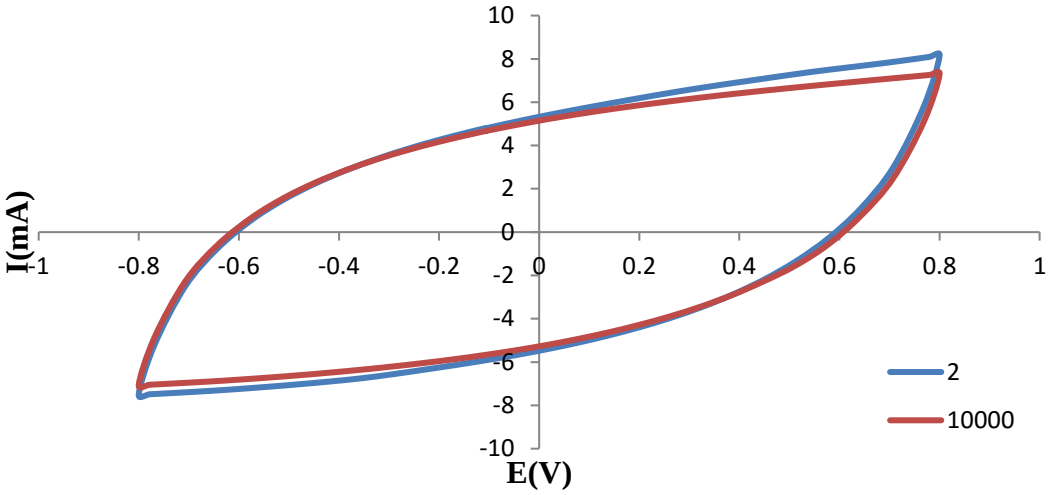

Figure B.2: CV graph of nickel encapsulated supercapacitor at cycle 2 and cycle 10000.

Figure B.2 is the CV graph of the nickel encapsulated fabric supercapacitor. After testing the device for 10000 cycles the graph does not have any significant change from its initial CV response. This is because in comparison with iron it is relatively difficult for the electrolyte to react with nickel and most of the potential will be taken by the device rather than the nickel cap. Therefore the electrochemical performance of the nickel encapsulated fabric supercapacitor is not changed after a cycling test of 10000 cycles, this shows that the device is stable.

Appendix C supercapacitor using different activated carbon powders and binders

In this section various fabric electrodes will be tested. The parameters investigated are different binder/solvent compositions and activated carbon powders. These compositions have some unique properties that will influence the properties of fabric sample:

PVDF/NMP: The carbon paste using PVDF as a binder and NMP as a solvent is very viscous because the viscosity of NMP is very high and consequently a larger proportion of NMP solvent is required to maintain the viscosity of the mixture at the low level required for the dipping process [88]. As a result the carbon fabric made using this paste contains less carbon than other mixtures, resulting in reduced conductivity. The biggest disadvantage of this composition is due to the fact that NMP is a low evaporation rate solvent, so it takes a long time to cure the sample electrode even at high temperature (80^{o}C) [96]. As a result, the carbon/PVDF compounds will shrink together randomly in the cured sample and this greatly degrades the uniformity of carbon coating on the fabric.

Matt medium/water: This composition has two clear advantages. Firstly, it is very easy to make since the matt medium is already in an emulsion form that will dissolve quickly in water. Secondly, it is very safe to use, since water is used as the solvent and matt is non-toxic. However, the biggest disadvantage of this composition was its wettability. It is very hard to mix carbon powder with water and it is unlikely that carbon particles will mix well with PMMA binder uniformly in the paste.

Epoxy/ethanol: R2218 epoxy resin can be thinned by ethanol, but as the solvent percentage rises the adhesion of this binder composition reduces significantly. Ethanol is also a very highly volatile chemical, so the paste cracks after curing. As a result, most of the carbon powder is easily removed from the fabric.

PS/cyclohexane: The solvent cementing of PS is the most effective solution for bonding carbon to poly-cotton by dipping. PS resin has good water resistance and can be dissolved in many organic solvents. However, the PS resin has some disadvantages. Firstly, PS resin has a low heat-distortion temperature at about 77 ^{o}C [88]. This limits the working temperature of final device. Secondly, PS resin is brittle. Together with the high evaporation rate of cyclohexane, cracking can occur on the electrode [96].

Detailed information of each carbon material is provided here:

Norit GSX: This powder is bought from VWR international and produced by Cabot Norit. It has a specific effective surface area of 950 $m^2.g^{-1}$, and an average pore size of 3 nm. [97]

SX ULTRA: This it is activated carbon processed from peat by Cabot Norit. It has high purity and is used in this work for the testing of carbon-coated fabric electrodes. It has mean practical size of 100µm in diameter, a neutral PH balance and an effective surface area of 1200 $m^2.g^{-1}$[85]

CA1: This is activated carbon processed from wood by Cabot Norit, this powdered carbon material will be used for testing of carbon fabric electrode. It has mean practical size of 75 µm in diameter, a PH of 2.0-3.5 and an effective surface area of 1400 $m^2.g^{-1}$[98]

Shawinigan Black: This powder, also named acetylene black, is a nano-scaled carbon particle which is used as additive material to fill the gaps between activated carbon particles and increase the electrical conductivity of electrodes. It has a mean practical size of 42nm in diameter and an effective surface area of 75 $m^2.g^{-1}$[86]

The fabric electrode contains a fixed amount of carbon powder and only the binder is varied. For most cases the carbon powders is comprised of 80% of various activated carbon powder and 20% carbon black powder. 85% of the carbon is solvent.

In electrochemical impedance spectroscopy, the capacitance of the tested cell is calculated using equation 3.18 with the imaginary impedance at the lowest testable frequency, 20 mHz. The ESR is found where the imaginary impedance is close to zero on the impedance curve. Each supercapacitor has an electrode area of 0.19 cm^2. The EIS plot of these electrodes is shown in figure C.1 and the extracted area capacitance and ESR values are given in table C.1.

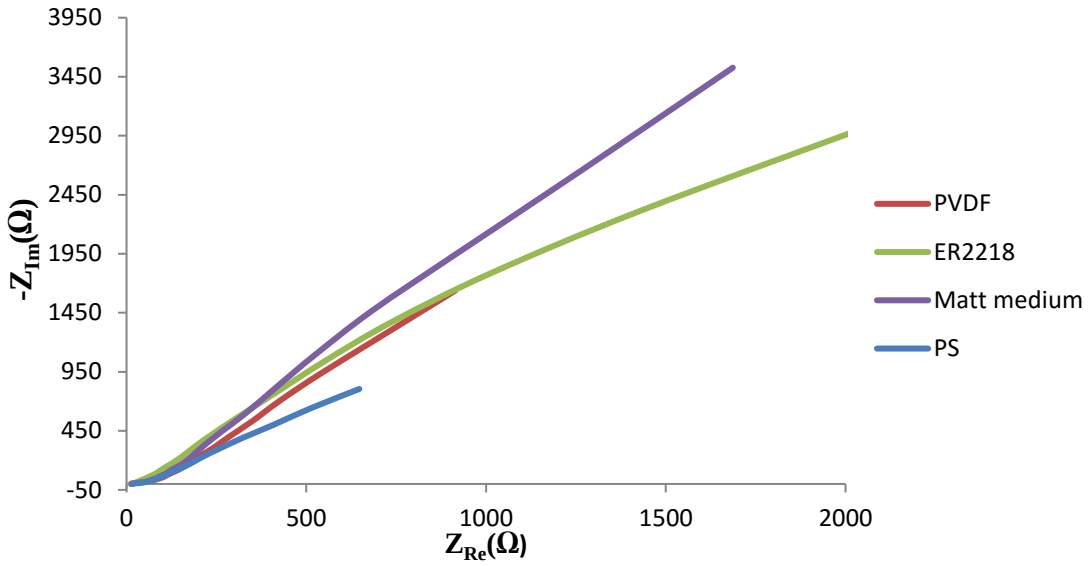

Figure C.1: EIS plot of devices with fabric electrodes using different polymer binders.

Table C.1: Test result of fabric supercapacitors with different binder ingredients.

Test No	Activated carbon type	Binder type	Binder percentage (%)	Electrolyte	Area ESR ($\Omega.cm^{-2}$)	Area Capacitance ($mF.cm^{-2}$)
A	Norit GSX	PVDF	50%	1M Na_2SO_4	5.41	88.67
B	Norit GSX	ER2218 (Epoxy)	40%	1M Na_2SO_4	7.55	93.23
C	Norit GSX	Matt medium(PMMA)	10%	1M Na_2SO_4	6.4	54.8
D	Norit GSX	PS	20%	1M Na_2SO_4	3.16	101

The binder percentage given in table C.1 is the near optimized value. Figure C.1 shows that the supercapacitor made using PS as a binder has the lowest imaginary impedance as well as the lowest real impedance at low frequencies, which indicates that this device is the least likely to convert an input electrical signal into waste energy like heat and has a relatively large capacity to capture energy in comparison with devices fabricated with electrodes using other binders.

The sample made with the PS binder has the highest value of capacitance with the lowest ESR, The ESR has to be minimized to further reduce the amount of energy wasted.

In the next step the activated carbon material will be varied. The electrolyte used is 1M sodium chloride. The binder will be 20% PS for all three tests. In addition to the parameters extracted in the previous test, the specific capacitance will also be calculated. The test results are shown in Figure C.2 and the extracted parameters are given in Table B.2.

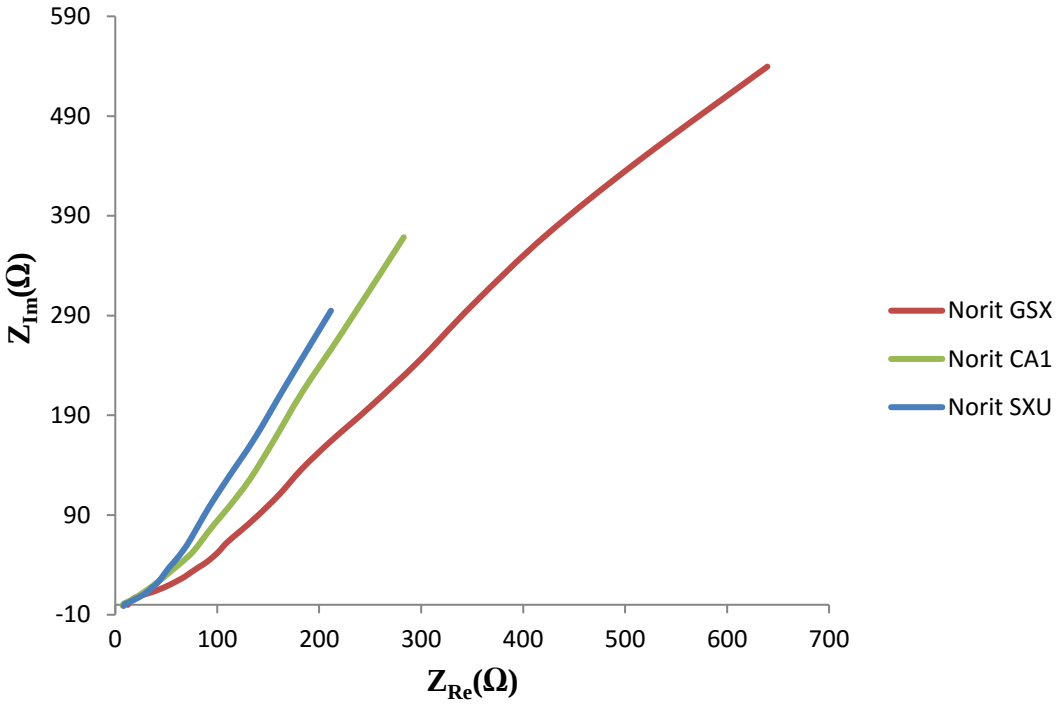

Figure C.2: EIS plot of supercapacitor with a PS binder and different activated carbon powders.

Table C.2: EIS test result of supercapacitor with different activated carbon powder.

Test No	Activated carbon type	Area Carbon loaded ($g.cm^{-2}$)	Electrolyte	Area ESR ($\Omega.cm^{-2)}$	Specific Capacitance ($F.g^{-1}$)	Area Capacitance ($mF.cm^{-2}$)
1	Norit GSX	6.225	1M NaCl	2.458	8.66	52
2	Norit CA1	5.02	1M NaCl	1.452	12.41	105
3	Norit SXU	11.25	1M NaCl	1.84	10.69	120

According to figure C.2 the supercapacitor made with Norit SXU activated carbon has the best electrochemical performance in comparison with the other two devices. From table C.2 the fabric electrode pair made with Norit SXU powder is able to adhere more material to the fabric than the other two samples, which resulted in this device having lower specific capacitance (farad/gram) than the device made with Norit CA1 activated carbon, despite the fact that has larger area capacitance. The sample that used Norit CA1 activated carbon achieves high specific capacitance and area capacitance with the lowest amount of carbon paste impregnating the fabric electrodes. In comparison with other types of carbon powder, it has a larger specific surface area and a smaller particle size. However, Norit CA1 activated carbon has a disadvantage in that this powder is an acidic material and has an average PH level of 2.5-3, which may be damaging to the fabric. This could explain why the polyester cotton fabric used in this does not hold as much of an ink formulated with this kind of carbon. The supercapacitor made with Norit GSX powder has the worst performance because it has the carbon particles have the lowest specific area.

There are some critical issues exist in this test; firstly the encapsulated material is steel that will react with aqueous electrolyte, in this case metal corrosion and passivation will occur for sure, secondly the electrode area is small, the additive impedance variation cause by metal corrosion and passivation will take a big part of the EIS result for iron encapsulated fabric supercapacitor. The corroded metal come from iron contract with Li_2SO_4electrolyte this material will be more resistive than original iron, and the passivated material iron oxide will provide additional

Pseudo-capacitance. In order to demonstrate this process EIS test will be performed twice on same supercapacitor with electrode of 0.785 cm^2 at the beginning and end of test series that has a time gap of 48 hours.

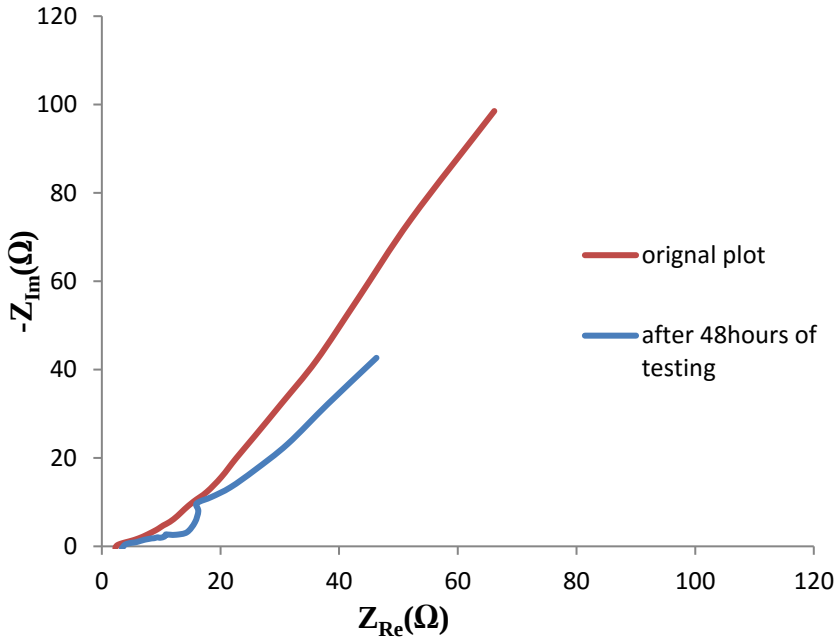

Table C.3: EIS plot of steel encapsulated supercapacitor immediately after fabrication and after 48 hours.

Figure C.3 shows the two EIS plots, which are clearly dissimilar. In the test performed after 48 hours, the cell behaves more capacitive than in its original EIS plot due to corroded iron. After the scan speed drops to a certain frequency the impedance curve is malformed due to metal passivation. The overall capacitance is larger in the later test but most of the added capacitance arises from metal corrosion and passivation. As a result the information in figure C.3 and table1contain the impedance responds from both fabric supercapacitor and corroded iron.

The next stage of this project is to find ways to limit the metal corrosion and passivation, to achieve a more stable capacitor. This is achieved by introducing a nickel foil to physically separate the electrolyte in the fabric electrode from the steel current collector. Another device was fabricated with same ingredient and process above, using the nickel foil technique. The electrolyte used is 1M Li_2SO_4 and the electrode area is increased to 0.785 cm^2.

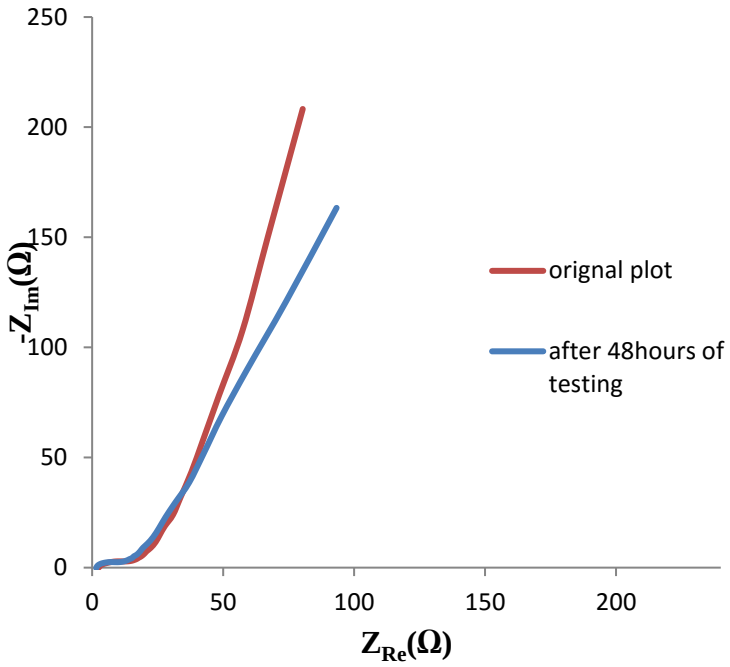

Table C.4: EIS plot of nickel encapsulated supercapacitor immediately after fabrication and after 48 hours.

Figure C.4 shows that the impedance behaviour of a nickel encapsulated supercapacitor changes less significantly compared with its performance 48 hours earlier. The capacitance is increased because the electrode is continuously infiltrated by the electrolyte electrode and the characteristic of electrode is not significantly changed. By comparing the two plots of devices encapsulated with steel and nickel from figure C.3 and figure C.4, the nickel was more resistive and less capacitive due to the internal loss of the two nickel capacitors and this is a compromise necessary to limit the level of metal corrosion and passivation. The nickel encapsulated supercapacitor finally achieved a specific capacitance 9.01 $F.g^{-1}$, area ESR of 1.24 $\Omega.cm^2$ and area capacitance 95 $mF.cm^{-2}$

Appendix D SEM pictures of fabric electrodes

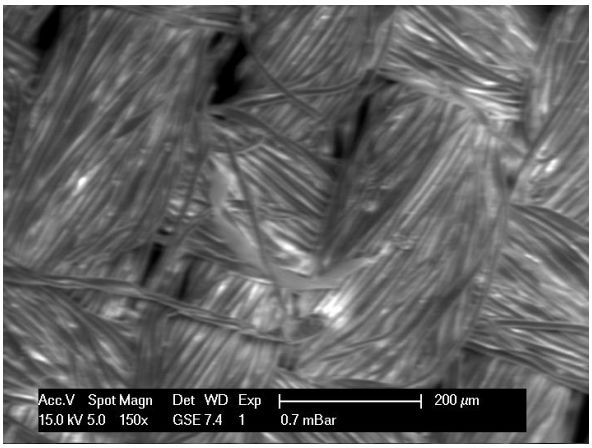

Figure D.1: SEM micrograph of thinner poly-cotton fabrics (W_{thin4}).

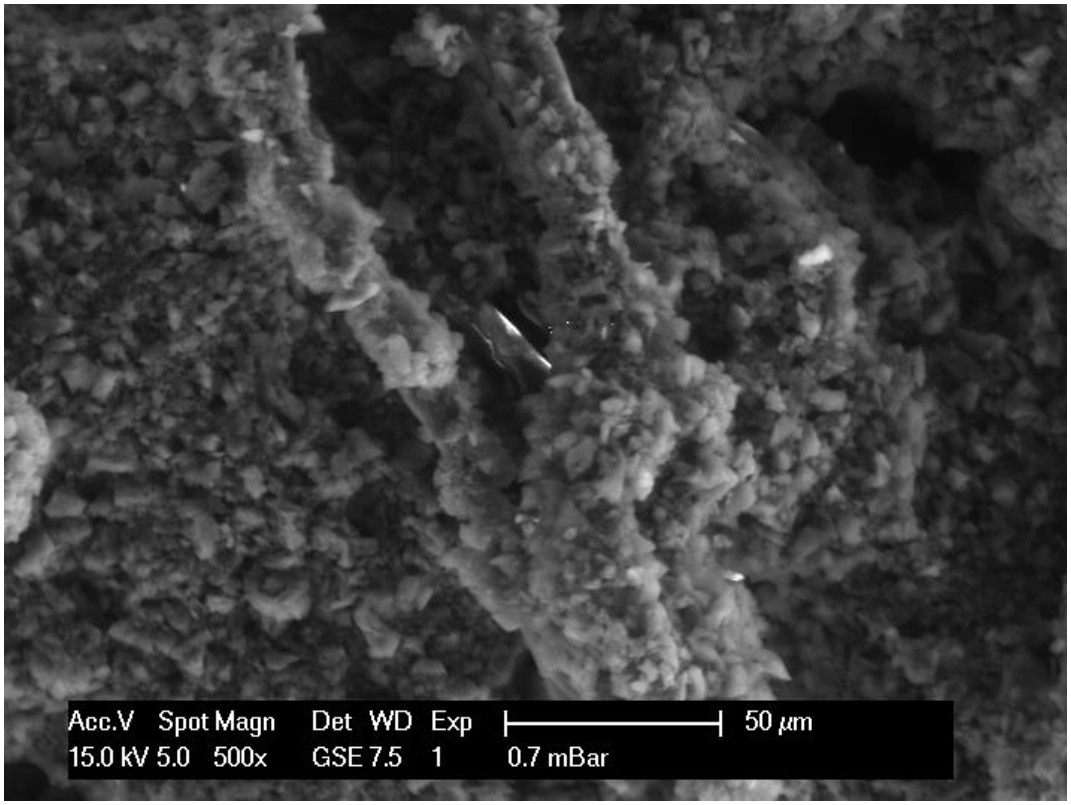

Figure D. 2: Higher magnification SEM micrograph of thinner poly-cotton fabrics (W_{thin4}) after spray-coating.

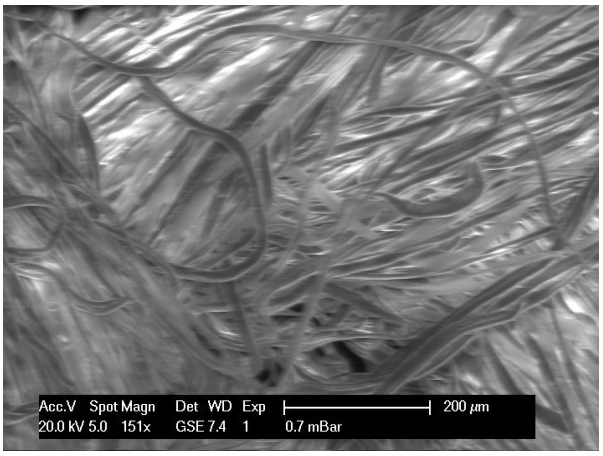

Figure D.3: SEM micrograph of cotton fabrics (C_{ot4}).

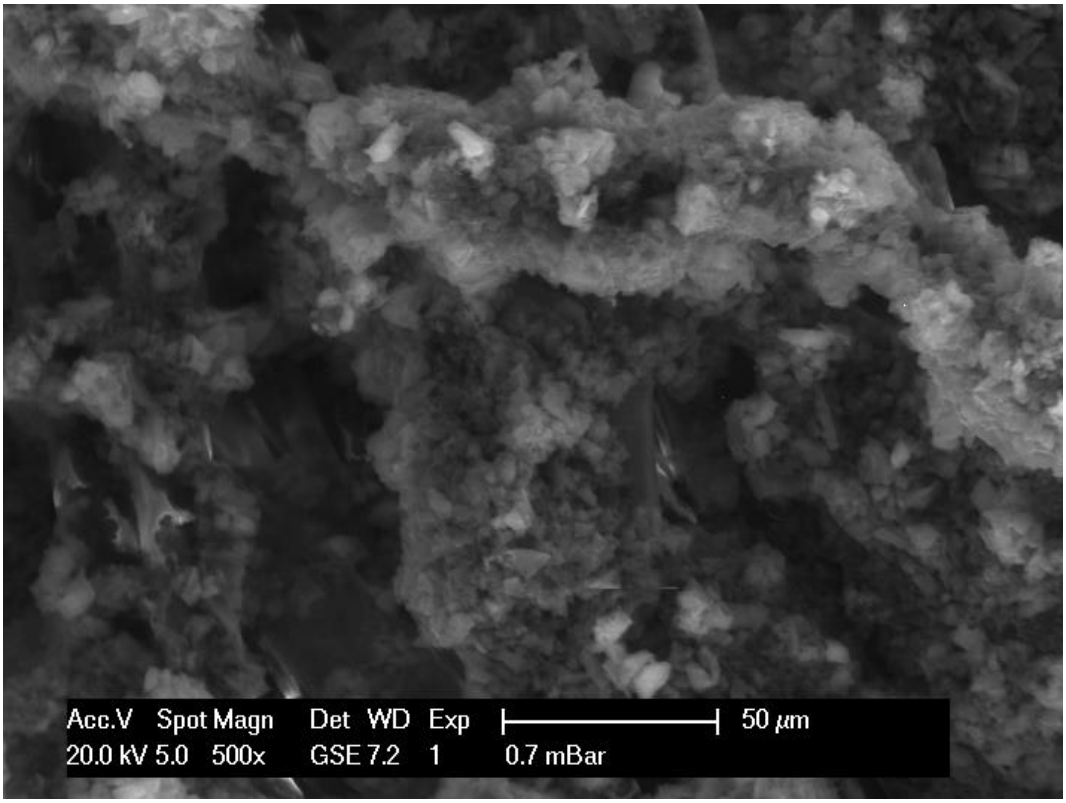

Figure D.4: Higher magnification SEM micrograph of cotton fabrics (C_{ot4}) after spray-coating

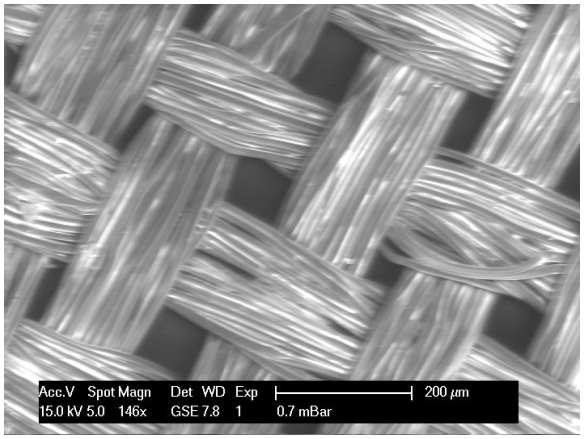

Figure D.5: (a) SEM micrograph of silk fabrics (S_4).

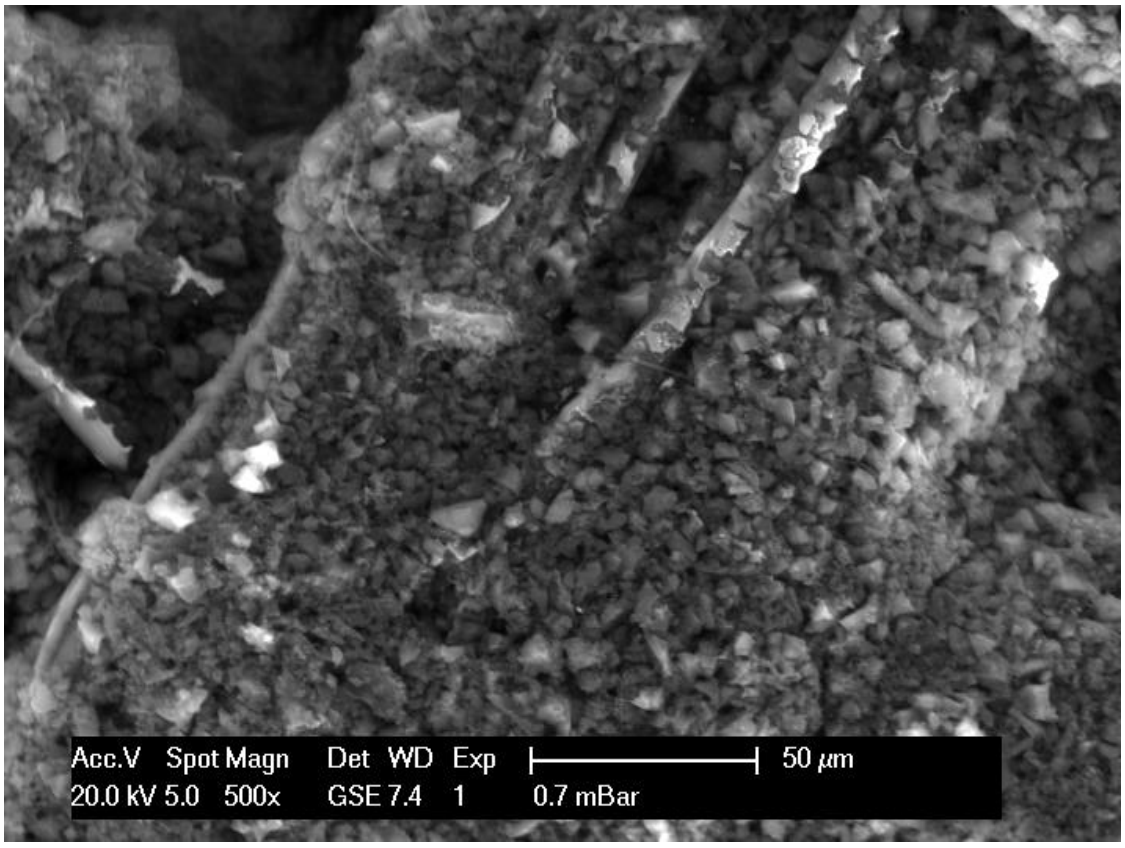

Figure D.6: Higher magnification SEM micrograph of silk fabrics (S_4) after spray-coating

Appendix E Fabrication and device testing of glassy carbon membrane

As described previously, the test cell can influence the performance of the supercapacitor. The previous method of using nickel foil to sandwich the device does prevent reactions like metal preservation and corrosion occurring in the cell. However, the downside of this method are that the nickel foil assemble may add resistance, which reduces the measured specific power density and the edge of metal foil is very sharp, which is not suitable in wearable electronic design. Also if the electrolyte is changed from an aqueous solution to an organic electrolyte to increase the operating voltage later in the project, the nickel foil may react with the organic electrolyte introducing more resistance and extra pseudo-capacitance into the cell.

The simplest way to solve this issue is to replace the medium between the electrolyte and the current collector with a more inert metal like gold or platinum. These metals are, however, expensive. Therefore glassy carbon was investigated as another possible current collector material. This has good resistance to most chemicals, impermeability to gases and liquids, excellent electrical conductivity and it has been widely used as an electrode material in electrochemistry [99]. Glassy carbon is brittle and so cannot be used in an flexible device. However this material is available in powder form and was mixed with the flexible polymer binder EVA with a low vinyl acetate percentage to form a carbon membrane that is flexible, has low in electrical resistance and excellent chemical resistivity.

The fabrication of glassy carbon membrane begins by mixing the glassy carbon powder and carbon black powder with EVA binder in 1, 2, 4 TCB solvent. The mixing process is similar with the activated carbon solution but with less solvent percentage.

Then spray coating process of glassy carbon solution is different from the spray coating process of fabric electrode. This carbon membrane needs to be thin (<20μm), uniform and process good adhesion to the stick on top of the steel collector. Therefore the carbon solution will be sprayed on to the steel current collector at a fixed distance of 15 cm and fixed air pressure of 15 psi (1.72 bars). After the spray coating process, the carbon membrane together with steel collector will be put in the vacuum chamber for 30 minutes. This step is essential since it will extract any air bubbles in the carbon membrane and prevent the electrolyte reacting with the steel current collector

Finally glassy carbon membrane is cured on a hot plate for 25 minutes at 100 ^{o}C. Then, the electrode was left at room temperature over night until any remaining of the solvent is evaporated,

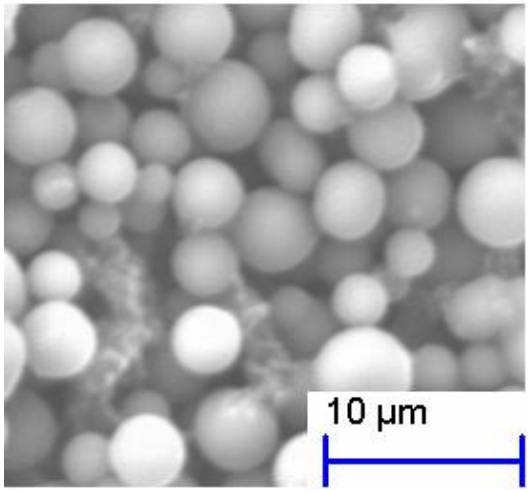

Figure E. 1: SEM micrograph of spray coated glassy carbon membrane made with EVA binder

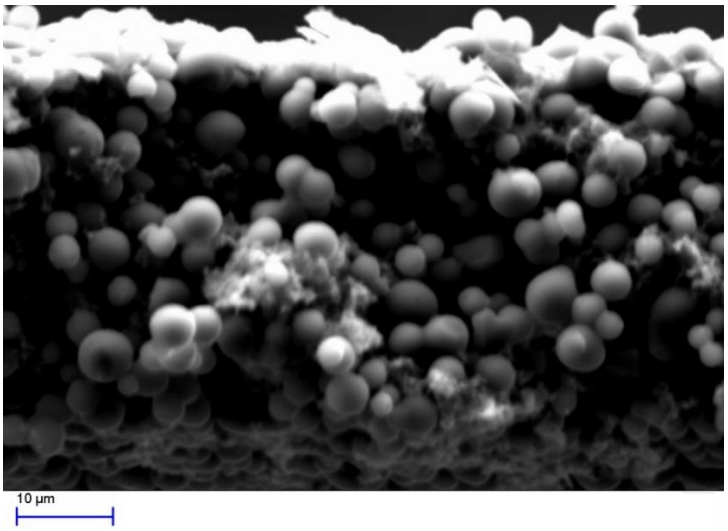

Figure E.2: cross section SEM micrograph of spray coated glassy carbon membrane made with EVA binder

According to figure E.1, the SEM view of a carbon membrane suggests that there are two kinds of carbon (glassy carbon and carbon black) and polymer binders. The big spherical particles are the glassy carbon particles and the smaller particles are carbon black particles together with polymer binder. Figure E.2, suggest that the thickness of carbon film is about 20 µm.

Table E.1: Electrochemical performance (GC method) comparison of nickel film and carbon membrane encapsulated supercapacitor using dip coated fabric electrode C1 and 1M Li2SO2 aqueous electrolyte

	nickel film encapsulated supercapacitor	carbon membrane encapsulated supercapacitor
Specific capacitance ($F.g^{-1}$)	11.2	9.69
Normalised ESR ($\Omega.cm^{-2}$)	0.079	0.102
Area capacitance ($F.cm^{-2}$)	0.087	0.074
Normalised ESR ($\Omega.cm$)	16.1	20.7
Energy density ($Wh.kg^{-1}$)	13.1	11.3
Power density ($kW.kg^{-1}$)	2.02	1.56

Table D.1 shows the carbon membrane encapsulated supercapacitor (electrode C1) demonstrated a specific capacitance of 9.69 $F.g^{-1}$ and an area capacitance of 0.074 $F.cm^{-2}$, it is about 86% of the results achieved by the same device with nickel film encapsulated set up. The carbon membrane encapsulated supercapacitor (electrode C1) also shows higher resistance (0.102 $\Omega.cm^{-2}$ and 20.7 $\Omega.cm$) than nickel film encapsulated device. It is because the carbon layer introduces extra resistance, it reduces the measured capacitance and increase the device ESR.

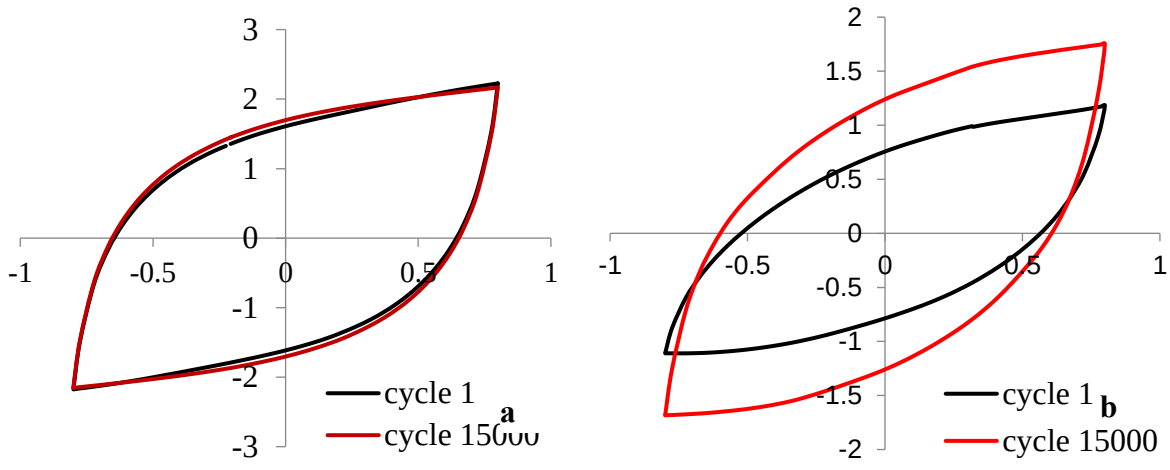

Figure E.3:CV test of the device for 15000 cycles between +/- 0.8 V at the scan rate of 200 $mV.s^{-1}$ (a) nickel encapsulated supercapacitor, (b) carbon membrane encapsulated supercapacitor

As shown in figure D.3 both types of fabric supercapacitor achieves a high device stability with no discernable chemical reaction. Capacitance variation is correlated with temperature changes to the variation of the diffusion coefficients. This shows an excellent level of adhesion of carbon material which form a continues conducting network

Reference

1 M S Halper and J C Ellenbogen, Supercapacitor: A Brief Overview, Mar. 2006, [Online]. Available: www.mitre.org/sites/default/files/pdf/06_0667.pdf

2 B E Conway, Electrochemical Supercapacitor Scientific Fundamentals and Technological Application, Kluwer Academic /Plenum Publishers, New York, ISBN: 0-306-45736-9

3 Illinois Capacitor, inc, supercapacitor, [Online] Available: http://www.illinoiscapacitor.com/pdf/papers/supercapacitors.pdf (last access on 01/07/2016)

4 Z S Nakad, "Architectures for e-Textiles". PhD thesis, Bradley Department of Electrical and Computing Engineering, Virginia Tech, 2003.

5 L Buechley and M Eisenberg, Fabric PCBs "Techniques for e-textile craft", Personal and Ubiquitous Computing, 2007

6 L B Hu; M Pasta; F L Mantia; L Cui; S Jeong; H D Deshazer; J W Choi; S M Han and Y Cui, Aqueous supercapacitors on conductive cotton, Nano Lett, 10 708, 2010,

7 K Sahay and B Dwidevi, Supercapacitors Energy Storage System for Power Quality Improvement: An Overview, J. Elec. Systems, 5, P8 , 2009.

8 M A Everett, overview: Ultracapacitor and Ultracapacitor Application, Kilofarad International, 31 March 2009

9 S Holmberg; A Perebikovsky; L Kulinsky and M Madou, 3-D Micro and Nano Technologies for Improvements in Electrochemical Power Devices, Micromachines, 5(2), 171-203, 2014

10 J M Boyea; R E Camacho; S P Turano and W J. Ready, Carbon nanotube-based supercapacitors: technologies and markets, Nanotechnology Law & Business, 2007

11 M Jayalakshmi and K Balasubramanian, Simple Capacitors to Supercapacitors - An Overview Int. J. Electrochem. Sci. 3 1196, 2008

12 Nichicon Corporation, General description of aluminium electrolytic capacitor, TECHNICAL NOTES CAT.8101E

13 P J Hall; M Mirzaeian; S I Fletcher; F B Sillars ; A J R. Rennie; G O Shitta-Bey; G Wilson , A Cruden and R Carter, Energy storage in electrochemical capacitors: designing functional materials to improve performance site, Energy Environ. Sci, 3, 1238-1251, 2010

14 Z L Li; X S Zhao, Carbon-based materials as supercapacitor electrodes, Chem. Soc. Rev. 38, 2520–2531, 2009

15 A Davies and Y A ping, Material advancements in supercapacitors: From activated carbon to carbon nanotube and grapheme, Can. J. Chem. Eng. 89(6), 1342. 2011

16 A J Bard; L R Faulkner, Electrochemical Methods Fundamentals and Applications, second edition, John Wiley & Sons, Inc, ISBN: 0-471-04372-9, 2009

17 Z L Li and X S Zhao, Carbon-based materials as supercapacitor electrodes, Chem. Soc. Rev, 38, 2520–2531 2009.

18 M Kaempgen; C K Chan; J Ma; Y Cui and G Gruner, Printable Thin Film Supercapacitors Using Single-Walled Carbon Nanotubes, Nano Lett, 9 (5), 1872–1876, 2009.

19 P C Chen; H T Chen; J Qiu and C Zhou, Inkjet printing of single-walled carbon nanotube/RuO2 nanowire supercapacitors on cloth fabrics and flexible substrates, Nano Res, 3,594–603, 2010

20 C Lekakou; O Moudam; F Markoulidis; T Andrews; J.F Watts and G. T. Reed, Carbon-based Fibrous EDLC Capacitors and Supercapacitors, Journal of Nanotechnology, Article ID 409382(8), 2011

21 H Y Jin; Z H Peng; W M Tang and H L W Chan, Controllable functionalized carbon fabric for high performance all-carbon-based supercapacitors, RSC Adv, 4, 33022, 2014

22 D V Lam; K Jo; C H Kim; S Won; Y H BO; J H Kim; H J Lee and S M Lee, Calligraphic ink enabling washable conductive textile electrodes for supercapacitors, J. Mater. Chem. A, 4, 4082, 2016

23 L B Liu; Y Yu; C Yan; K Li; Z Zheng, Wearable energy-dense and power-dense supercapacitor yarns enabled by scalable graphene–metallic textile composite electrodes, Nature communications, 6, 7260, 2015

24 X F Wang; B Liu; R Liu; Q F Wang; X J Hou; D Chen; R M Wang and G Z Shen, Fiber Based Flexible All-Solid-State Asymmetric Supercapacitors forIntegrated Photodetecting System, Angew. Chem. Int. Ed, 53, 1849 –1853, 2014

25 Y N Meng; Y Zhao; C G Hu; H H Cheng; Y Hu; Z P Zhang; G Q Shi and L T Qu, All-Graphene Core-Sheath Microfi bers for All-Solid-State, Stretchable Fibriform Supercapacitors and Wearable Electronic Textiles Adv. Mater, 25, 2326–2331, 2013

26 L Kou; T Q Huang; B N Zheng; Y Han; X L Zhao; K Gopalsamy; H Y Sun and C Gao: Coaxial wet-spun yarn supercapacitors for high- energy density and safe wearable electronics, Nature communications, 10,1038, 2014

27 Fiber Interface Coatings, online picture, last access: 12-01-2016, available at http://www.ultramet.com/fiber_interface_scanning.html

28 DS Yu et al. “Emergence of fiber supercapacitors” Chem. Soc. Rev,44, 647, 2015

29 E G Gagnon, The Triangular Voltage Sweep Method for Determining Double Layer Capacity of Porous Electrodes: IV. Porous Carbon in Potassium Hydroxide, J Electrochem soc 122 521, 1975

30 B Kastening; W Schiel and M Henschel, Electrochemical polarization of activated carbon and graphite powder suspensions: Part I. Capacity of suspensions and polarization dynamics, J Electrochemistry ,191 311, 1985

31 T Inoue; S Mori and S Kawasaki, Electric Double Layer Capacitance of Graphene-Like Materials Derived from Single-Walled Carbon Nanotubes, Japanese Journal of Applied Physics, 50, 2011

32 Timcal ENSACO 350G, [online] available: http://en.myitrade.com/xianyuanshi188/offerdetail/555739/TIMCAL-ENSACO-Conductive-Carbon-Black-350G.html (last access on 01/07/2016)

33 Norit SXU, [online] available: http://www.sigmaaldrich.com/materials-science/material-science-products.html?TablePage=101273089 (last access on 01/07/2016)

34 Yp – 50F Activated carbon, [online] available: http://www.kuraraychemical.com/products/sc/capacitor.htm (last access on 01/07/2016)

35 GS-2299 nano-Graphite Powder,[online] available: http://www.graphitestore.com/items_list.asp/action/prod/prd_id/511/cat_id/28 (last access on 01/07/2016)

36 HiPco carbon nanotube, [online] available: http://www.nanointegris.com/en/hipco (last access on 01/07/2016)

37 A J Bard and L R Faulkner, Electrochemical Methods Fundamentals and Applications, second edition, John Wiley & Sons Inc, ISBN: 0-471-04372-9, 2011

38 J A Kim; I S Park; and J H Seo, A Development of High Power Activated Carbon Using the KOH Activation of Soft Carbon Series Cokes, TRANSACTIONS ON ELECTRICAL AND ELECTRONIC MATERIALS, 15(2), 81-86, 2014

39 L B Hu; M Pasta; F La Mantia; L F Cui; S Jeong; H D. Deshazer; J W. Choi; S D M Han and Y Cui, NANO ENERGY, Nano Lett, 10 (2), 708–714, 2010.

40 Z S Zhang; T Zhai; X H Lu; M H Yu; Y X Tong and K.C Mai, Conductive membranes of EVA filled with carbon black and carbon nanotubes for flexible energy-storage devices, J. Mater. Chem. A, 1, 505-509, 2013

41 V Subramanian; C Luo; A. M Stephan; K S Nahm; S Thomas and B Wei, Supercapacitors from activated carbon derived from banana fibers, J Phys Chem C, 111:7527–31, 2007

42 K Jost; C R. Perez; J K McDonough; V Presser; M Heon; G Dion and Y Gogotsi, Carbon coated textiles for flexible energy storage, Energy Environ. Sci. 4(12), 5060–5067, 2011.
43 A G Pandolfo and A F Hollenkamp, Carbon properties and their role in supercapacitors. J. Power Sources 157, 11–27, 2006
44 K Wang; P Zhao; X. Zhou; H. Wu and Z. Wei, Flexible supercapacitors based on cloth-supported electrodes of conducting polymer nanowire array/SWCNT composites, J. Mater. Chem 21, 16373, 2011
45 X B Zang; X Li; M Zhu; X Li; Z Zhen; Y He; K Wang; J Wei; F Kang and H Zhu, Graphene/polyaniline woven fabric composite films as flexible supercapacitor electrodes, Nanoscale, 7, 7318, 2015
46 P H Yang; X Xiao; Y Li; Y Ding; P Qiang; X Tan; W Mai; Z Lin; W Wu; T Li; H Jin; P Liu; J Zhou; C Wong and Z Wang, Hydrogenated ZnO Core_Shell Nanocables for Flexible Supercapacitors and Self-Powered Systems, ACS Nano, 7 (3), 2617–2626, 2013
47 Y Wang; Z Q Shi; Y Huang; Y F Ma; C Y Wang; M M Chen and Y S Chen, supercapacitor Devices based on Graphene Materials, J.Phys. Chem C, 113, 13103-13107, 2009
48 V Conedera; F Mesnilgrente; M Brunt and N Fabre, Fabrication of activated carbon electrode by inject/inkjet? deposition, Processing of ICQNM conference, Cancun, 2009
49 Z S Zhang; T Zhai; X H Lu; M H Yu; Y X Tong and K.C Mai, Conductive membranes of EVA filled with carbon black and carbon nanotubes for flexible energy-storage devices, J. Mater, Chem, A 1, 505-509, 2013
50 M Pasta; F L Mantia; L B Hu and H D Deshazer, Aqueous supercapacitors on conductive cotton, Nano Res, 3, 452, 2010
51 W W Liu; X B Yan; J W Lang; C Pen and Q J Xue. Flexible and conductive nanocomposite electrode based on graphene sheets and cotton cloth for supercapacitor. J Mater Chem, 22: 17245–17253, 2012
52 R Yuksel and H E Unalan, Textile supercapacitors-based on MnO2/SWNT/ conducting polymer ternary composites, Int. J. Energy Res, 39,2042–2052, 2015
53 Woven carbon fabric, [online]: http://3dwovens.com/
54 P H Yang et al, Hydrogenated ZnO Core Shell Nanocables for Flexible Supercapacitors and Self-Powered Systems, *ACS Nano*, 7 (3), 2617–2626, 2013
55 X Zang; R Xu; Y Zhang; X Li; L Zhang; J Wei; K Wang and H Zhu, all carbon coaxial supercapacitors based on hollow carbon nanotube sleeve structure, Nanotechnology, 26 ,045401 2014

56 L Dong; C Xu; Q Yang; J Fang; Y Li and F Kang' High-performance compressible supercapacitors based on functionally synergic multiscale carbon composite textiles, Mater. Chem. A, 3, 4729, 2015
57 L B Dong; C J Xu; Q Yang; J Fang; Y Li and F Kang, High-performance compressible supercapacitors based on functionally synergic multiscale carbon composite textiles, J. Mater. Chem. A, 3,4729, 2015

58 P J Hall; M Mirzaeian; S I Fletcher; F B Sillars ; A J R. Rennie; G O Shitta-Bey; G Wilson , A Cruden and R Carter, Energy storage in electrochemical capacitors: designing functional materials to improve performance site, Energy Environ. Sci, 3, 1238-1251, 2010

59 C Zhao; K W Shu; C Y Wang; S Gambhir and G G Wallace, Reduced graphene oxide and polypyrrole/reduced graphene oxide composite coated stretchable fabric electrodes for supercapacitor application, Electrochimica Acta, 172, 12–19, 2015
60 Z Gao; N N Song; Y Y Zhang and X D Li, Cotton textile enbled, all-solid-state flexible supercapacitor, RSC Adv, 5, 15438, 2015

61 X B Zang; Q Chen; P X Li; Y J He; X Li; M Zhu; X M Li; K L Wang; M L Zhong; D H Wu and H W Zhu, Highly flexible and adaptable, all-solid-state supercapacitors based on graphene woven-fabric film electrodes, small, 10, 13, 2583–2588, 2014
62 F H Su and M H Miao, Asymmetric carbon nanotube–MnO2 two-ply yarn supercapacitors for wearable electronics, Nanotechnology, 25, 135401, 2014
63 S T Senthilkumar; R K Selvan; J S Melo and C Sanjeeviraja, High performance solid-state ele Chen ctric double layer capacitor from redox mediated gel polymer electrolyte and renewable tamarind fruit shell derived porous carbon, ACS Appl Mater Interfaces, 2013
64 Z L Li; X S Zhao, Carbon-based materials as supercapacitor electrodes, Chem. Soc. Rev. 38, 2520–2531, 2009
65 L Wang; X Feng L T Ren Q H Piao; J Q Zhong; Y B Wang; H W Li; Y F Chen and B Wang, Flexible solid-state supercapacitor based on a metal−organic framework interwoven by electrochemically-deposited PANI, *J. Am. Chem. Soc.*, 137 (15), 4920–4923, 2015
66 M Kaempgen; C K Chan; J Ma; Y Cui and G Gruner, Printable Thin Film Supercapacitors Using Single-Walled Carbon Nanotubes, Nano Lett. 9 (5), 1872–1876, 2009
67 Z Gao; N N Song; Y Y Zhang and X D Li, Cotton textile enabled, all-solid-state flexible supercapacitors, RSC Adv, 5, 15438, 2015

68 L Kou; T Q Huang; B N Zheng; Y Han; X L Zhao; K Gopalsamy; H Y Sun and C Gao, Coaxial wet-spun yarn supercapacitors for high-energy density and safe wearable electronics, NATURE COMMUNICATIONS, 5, 3754, 2014

69 P R Chandran and T V Arjunan, A review of materials used for solid oxide fuel cell. International Journal of ChemTech 1 489-498. 2014

70 G G Federico and L Y Noor LY 2015 new insights into the dynamics of vacuum impregnation of plant tissues and its metabolic consequences. Journal of the Science of Food and Agriculture 95: 1127-1130, 2015

71 T He; X Ren; K Cai; Y Wei and S Sun, Electrochemical performance of activated carbon treated by vacuum impregnation using fluorinated surfactant. Materials Technology 28:364-369, 2013

72 Y Hu; H H Cheng; F Zhao; N Chen; L Jiang; Z H Feng and L T Qu, All-in-one graphene fiber supercapacitor, Nanoscale, 6, 6448, 2014

73 X B Zhang; R Q Xu; Y Y Zhang; X M Li; L Zhang; J Q Wei; K L Wang and H W Zhu, All carbon coaxial supercapacitors based on hollow carbon nanotube sleeve structure, Nanotechnology, 26, 045401, 2015

74 C Choi; S H Kim; H J Sim; J A Lee; A Y Choi; Y T Kim; X Lepro; G M Spinks; R H Baughman and S J Kim, Stretchable, weavable coiled carbon nanotube/MnO2/polymer fiber Solid-State Supercapacitors, SCIENTIFIC REPORTS, 5, 9387, 2015

75 H Sun; S L Xie; Y M Li; Y S Jiang; X M Sun; B J Wang and H S Peng, large-area supercapacitor textile with novel hierarchical conducting structures, Adv. Mater, 10.1002, 2016

76 J F Zhang; M J Cheng; Y W Ge and Q Liu, Manganese Oxide on Carbon Fabric for Flexible Supercapacitors, Journal of Nanomaterials, Article ID: 2870761, 2016

77 Q Y Huang; L Liu; D Wang; J Liu; Z Huang and Z Zheng, One-step electrospinning of carbon nanowebs on metallic textiles for high-capacitance supercapacitor fabrics, J. Mater. Chem. A, **4**, 6802-6808, 2016

78 J H Yu; J Wu; H Wang; A Zhou; C Huang; H Bai and L Li, Metallic fabrics as the current collector for high-performance graphene-based flexible solid-state supercapacitor, ACS Appl. Mater. Interfaces, 8, 4724−4729, 2016

79 X Pu; L Li; M Liu; C Jiang; C Du; Z ;Zhao; W Hu and Z L Wang, Wearable self-charging power textile based on flexible yarn supercapacitors and fabric nanogenerators, Adv. Mater. 28, 98–105, 2016

80 EC-Lab Software: Techniques and Applications Version 10.1x – February 2011,[online] (last access on 01/07/2016)
available: http://www.egr.msu.edu/~scb-group-web/blog/wp-content/uploads/2012/07/EC-Lab-software-Techniques-and-Applications-manual.pdf
81 Autolab Application Note EC08, Basic overview of the working principle of a potentiostat/galvanostat (PGSTAT) – Electrochemical cell setup [online] available:
http://www.ecochemie.nl/download/Applicationnotes/Autolab_Application_Note_EC08.pdf
82 M D Stoller and R S Ruoff, Best Practice Methods for Determining an Electrode Material's Performance for Ultracapacitors, Energy Environ, Sci, 2010, 3, 1294–1301
83 C H Hamann; A Hamnet and W Vielstich, Electrochemistry, Wiley-Vch Verlag, GmbH & Co.KGaA, Weinheim, ISBN: 978-3-122-07045-6
84 Class G/F Glass microfiber filter, datasheet, [online] available:
https://uk.vwr.com/app/catalog/Productarticle_number=513-5248 (last access on 01/07/2016)
85 Norit SX ULTRA activated carbon powder, datasheet, [online] available:
http://norit-test.com/files/documents/eapa_files/SXU_Catalyst_English.pdf (last access on 01/07/2016)
86 Shawinigan Black carbon black powder, datasheet, [online] available:
http://www.trademarkia.com/shawinigan-black-71603464.html (last access on 01/07/2016)
87 Polystyrene, [online] available:
http://www.sigmaaldrich.com/catalog/product/aldrich/331651?lang=en&region=GB (last access on 01/07/2016)
88 S Ebnesajjad, Adhesives Technology Handbook, second edition, William Andrew Inc, ISBN 978-0-8155-1533-3
89 Ethyl acetate, [online] available:
http://www.sigmaaldrich.com/catalog/product/sial/270989?lang=en&region=GB
90 C H Hamann; A Hamnett and A Vielstich, Electrochemistry, WILEY-VCH Verlag GmbH & Co. KGaA, Weinheim.ISBN 978-3-527-31069-2
91 Yp – 80F Activated carbon, [online] available:
http://www.kuraraychemical.com/products/sc/capacitor.htm (last access on 01/07/2016)
92 D M Drobny; S A Tychyna; Y A Maletin; N G Stryzhakova and S A Zelinsky, Method for Manufacturing carbon electrodes for supercapacitor; pros and cons, Proceedings of the international conference nanomaterials; applications and properties, 2, 4, 4, 2013
93 1,2,4-Trichlorobenzene, [online] available:

http://www.sigmaaldrich.com/catalog/product/sial/296104?lang=en&region=GB (last access on 01/07/2016)

94 M J Uddin1; M G. Masud; A Ghosh; T. R. Middya and B. K. Chaudhuri, Ammonium Dihydrogen Phosphate/PVA Composite Films with High Dielectric Permittivity and Enhanced Thermal Stability, Advanced Science, Engineering and Medicine , 5,126–132, 2013

95 Poly(vinyl alcohol) Mw 146,000-186,000, 99+% hydrolyzed, datasheet, [online] available: http://www.sigmaaldrich.com/catalog/product/aldrich/363065?lang=en&region=GB (last access on 01/07/2016)

96 V Horie, Materials for Conservation, second edition, Elservier Ltd, ISBN-13: 978-0-75-066905-4

97 P Harris; Z Liu and K Suenaga; Imaging the Atomic Structure of Activated Carbon. J. Phys, Condens. Matter 20, 2008.

98 Norit CA1 activated carbon powder, datasheet, [online] available: http://www.norit.com/files/documents/CA1_rev7.pdf, (last access on 01/07/2016)

99 Glassy carbon, [online] available: http://www.sigmaaldrich.com/catalog/product/aldrich/484164?lang=en&region=GB, (last access on 01/07/2016)